HANDLE VIA BYEMAN
CONTROL SYSTEM ONLY

NRO APPROVED FOR RELEASE
DECLASSIFIED BY: C/IART
DECLASSIFIED ON: 9 JULY 2012

Quill

RADAR

# KP-II
## PROGRAM REPORT

☐ RT DATA ENTERED
DATE ______

☐ MICROFICHED
DATE ______

AKP-II-596 /Vol I

1 APRIL 1965

HANDLE VIA BYEMAN
CONTROL SYSTEM ONLY

SSF-II-1018-1

~~SECRET~~
SPECIAL HANDLING

HANDLE VIA BYEMAN
CONTROL SYSTEM ONLY

NRO APPROVED FOR RELEASE
DECLASSIFIED BY: C/IART
DECLASSIFIED ON: 9 JULY 2012

COPY NO. 17

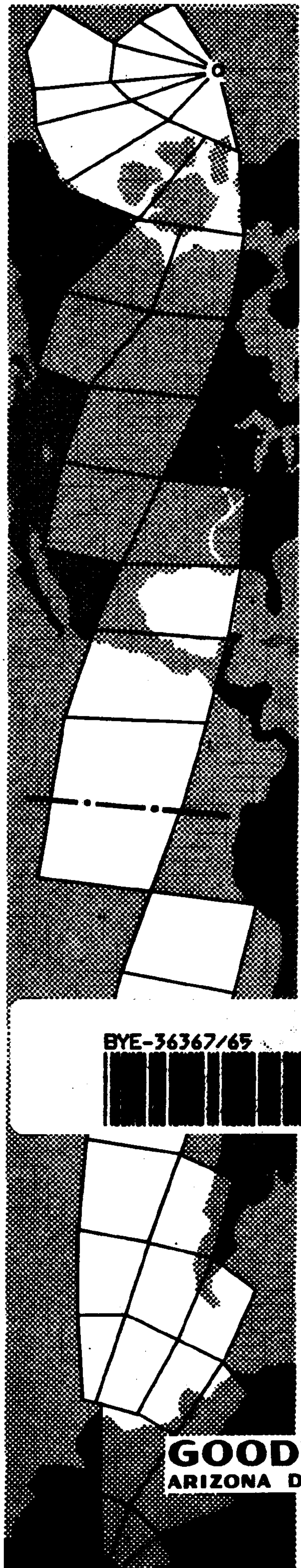

# KP-II
## PROGRAM REPORT

# KP-II ORBITAL DOPPLER RADAR
## THOR/AGENA SATELLITE PROGRAM

## VOLUME I - DESIGN AND DEVELOPMENT

AKP-II-596

1 APRIL 1965

S

BYE-36367/65 17VOL1Y

This document contains 186 pages classified as SECRET: SPECIAL HANDLING

EXCLUDED FROM AUTOMATIC REGRADING
DOD DIR 5200.10 DOES NOT APPLY

SAFSS By 36367-65



HANDLE VIA BYEMAN
CONTROL SYSTEM ONLY

**GOODYEAR AEROSPACE CORPORATION**
ARIZONA DIVISION LITCHFIELD PARK, ARIZONA

SPECIAL HANDLING
~~SECRET~~

This page intentionally left blank.

## FOREWORD

This report is submitted in response to the requirements of Air Force Contract [redacted]. Documented herein is the design, development, and testing phases of the KP-II Orbital Doppler Radar produced by Goodyear Aerospace Corporation, Litchfield Park, Arizona. The period covered is from 15 January 1963 to 1 April 1965.

Prepared by:

[redacted]
Project Engineer

Approved:

David D. Bradburn
Lt. Col., USAF
SAFSP

This page intentionally left blank.

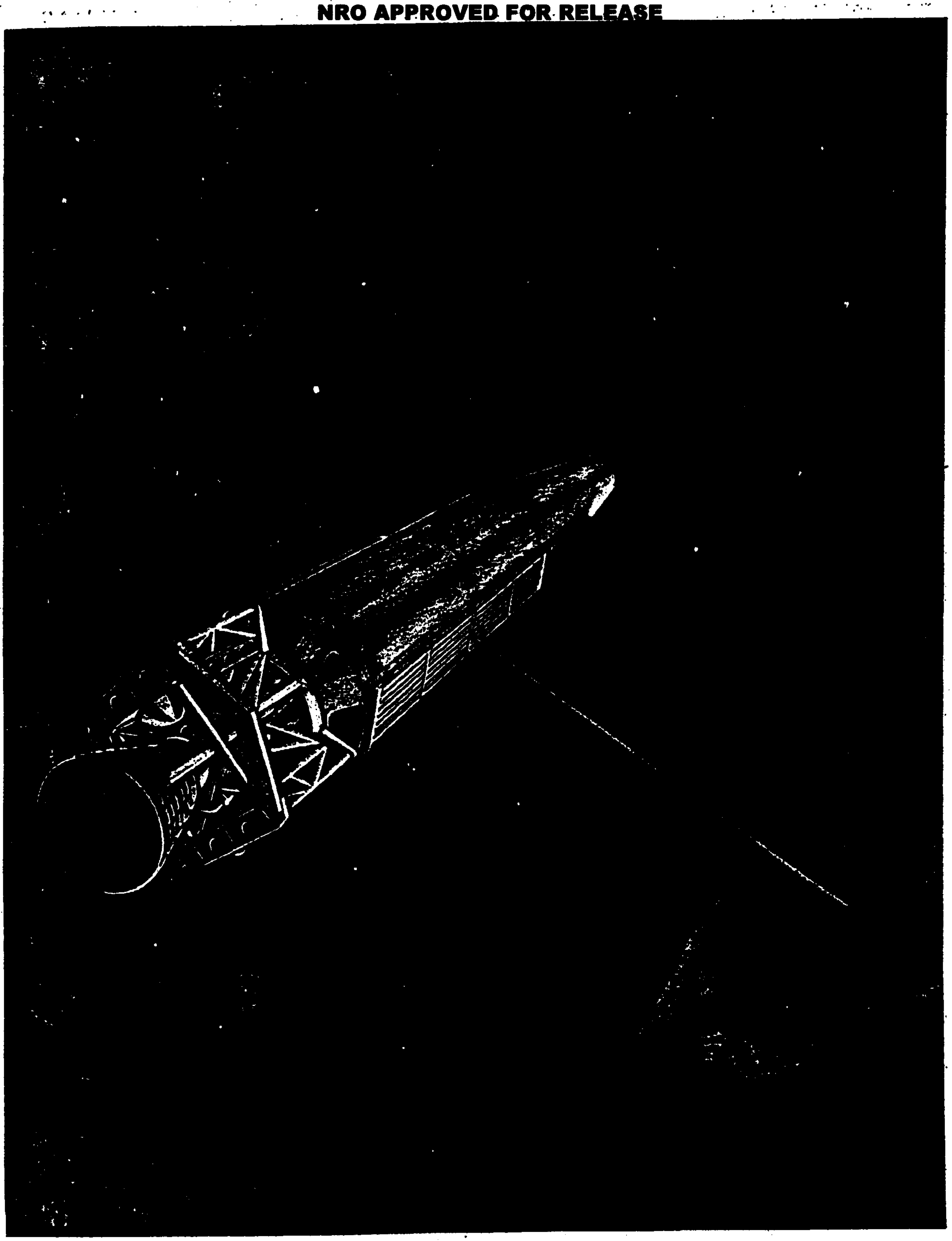

This page intentionally left blank.

## TABLE OF CONTENTS

## LIST OF ILLUSTRATIONS

## LIST OF TABLES

## SECTION I - INTRODUCTION

### 1. GENERAL

In January, 1963, Goodyear Aerospace Corporation, Arizona Division, was contracted by the Secretary of the Air Force Special Projects Office (SAFSP) to participate in an Agena Vehicle Satellite Program. The primary objective of the program was to demonstrate the feasibility of obtaining doppler high-resolution radar imagery of the earth's terrain from an orbiting satellite. To accomplish this objective, it was proposed to base the radar system, wherever practical, upon the existing designs of the Goodyear-produced AN/UPQ-102 side-looking doppler radar.

Initial studies and proposal efforts on this program had previously begun in the latter part of 1962 when a number of meetings were held between Goodyear Aerospace, Lockheed Missile and Space Company (LMSC), and the [redacted] to discuss system parameters, design concepts, and vehicle configuration. Actual work on the radar portion of the program began at Goodyear Aerospace on January 15, 1963. Twenty-three months later on December 21, 1964, successful completion of the first orbital radar test was achieved.

This program report is divided into two volumes. This volume – Volume I – documents the initial system analysis, design, and development of the Goodyear KP-II side-looking doppler radar system. Volume II describes the ground tests to which the system was subjected, and presents the results of the orbital flight test.

### 2. DESIGN PHILOSOPHY

To accomplish the program objective, extensive changes were required to the existing designs of the AN/UPQ-102 doppler radar. The KP-II radar was required to operate at 20 times the ground speed and 16 times the altitude of the AN/UPQ-102 radar. The KP-II radar was required to scan one side only; the AN/UPQ-102 radar scanned on both sides and used two receiving and recording channels. In the AN/UPQ-102 radar, the film speed and prf were slaved to ground speed; in the KP-II radar they would be constant. Additionally, the AN/UPQ-102 radar incorporated many modes of operation, such as moving target indication and variable mapping intervals, which were not included in the requirements for the KP-II radar. Finally, the more difficult vibration and pressure requirements of the satellite environment would necessitate an extensive repackaging of the radar units.

It was decided that specialized parts, such as klystrons, traveling wave tubes, cathode ray tubes, and frequency multipliers, would be procured from previously established vendors wherever possible. To ensure that these specialized parts would meet all requirements, new specification control drawings were made and the components procured to these specifications.

It was also decided that the payload would be instrumented in such a manner that flight performance and failure mode data could be obtained from narrow band telemetry information.

## 3. CONFIGURATION

The KP-II radar payload equipment which was designed and built by Goodyear Aerospace consists of the following units: Transmitter, RF-IF, Reference Computer, Control, and Recorder. The equipment, with the exception of the recorder, is installed in the forward barrel section of a standard Agena D vehicle. The recorder is installed in the conical nose section directly behind the film recovery capsule. The radar antenna, built by LMSC, is attached to the side of the Agena vehicle and is a two-dimensional slotted wave guide array. The antenna is 15 feet long, 1.8 feet in height, and is uniformly illuminated in both directions.

## 4. SYSTEM PARAMETERS

The radar payload is designed to operate at an altitude of 130 ±13 nautical miles. The orbital inclination angle is 70 degrees. A fixed radar depression angle of 55 degrees is used. The radar maps a slant range interval of 5.95 nautical miles which is independent of altitude variation. This slant range interval corresponds to a ground range interval of approximately 10 miles.

The design value for peak transmitter power is 30 kilowatts and the average transmitter power is 262 watts. The length of the transmitter pulse is 1.0 microsecond. By the use of pulse compression techniques this is reduced to an effective pulse width of 0.06 microsecond. The minimum acceptable resolution for the system is 50 feet slant range resolution and 50 feet azimuth resolution. Actual system performance was found to be better than these minimum acceptable values.

The pulse repetition frequency (prf) has a 16-step variable range from 8215 to 8735. Changes in prf are accomplished via the payload command system. A grey code is used to allow a one-step change in prf to be accomplished by a single command. During flight, change of prf from its preprogrammed position was made on the basis of the radar data received at the tracking station.

The total power consumed by the radar system in the operate mode is 2500 watts. The total weight of the five payload components is 348 pounds.

5. OPERATIONAL SUMMARY

The payload was launched by a thrust-augmented Thor booster and had a useful orbital life of approximately four days.

Radar radiation was confined (1) to the limits of the continental United States, and (2) to the limits of control of the Vandenburg and New Boston tracking stations. Doppler radar data were recorded simultaneously by the recorder unit contained in the vehicle and also by a ground-based recorder located at the tracking station. The data were transmitted to the controlling tracking station via a wide-band data link. There were a total of 14 mapping passes within the four-day period. The time interval for each pass varied from 1.4 to 3.7 minutes. The total mapping time was 32.91 minutes. The unprocessed vehicle data film was returned to earth in the recovery capsule. The resulting high-resolution imagery from the data films confirms the feasibility of doppler high-resolution radar techniques for space application.

## 6. CHRONOLOGY OF PROGRAM HISTORY

To give chronological perspective to the design and development phases of the program, a summary of events on a monthly basis is included as Appendix I to this volume.

## SECTION II - BASIC DOPPLER THEORY

### 1. GENERAL CONCEPT

The beam-sharpening process used in a doppler, high-resolution, side-looking radar may be described by means of a physical antenna analog. As the vehicle travels its orbital path a series of pulses is transmitted. Successive pulse transmissions are identified with the elements of an array of dipoles. The spacing between elements is the distance traveled by the vehicle between pulses. Each transmission is made with a controlled phase. The amplitude and phase of the reflected energy from the terrain at all ranges and angles within the physical beam width of the antenna is recorded on the data film.

The length of the antenna synthetically generated is basically limited to the distance instantaneously illuminated on the ground by the physical antenna. By the technique of optical processing, the amplitude and phase of the returns from the successive pulses are vectorially added to create the narrow synthetic beam. The results of these data are then recorded on a final film. Thus, the resolution equivalent to that of an antenna hundreds of feet in length is achieved with a small physical antenna.

### 2. BASIC EQUATIONS

The basic equations of a high-resolution radar are most easily developed if the analysis is restricted to the slant-range plane of a single-point target. Figure 1 shows the geometry involved. R is the distance to the target from the antenna at time t. At time $t = 0$, $R_1$ is the distance to the target. The angle $\theta_o$ is measured in the slant-range plane to the center of the antenna beam at slant range $R_1$. Several combinations of pitch and yaw will yield the same angle $\theta_o$.

From the geometry of Figure 1 the instantaneous range R to the target is

$$R = \left[R_1^{\,2} + (vt)^2 - 2R_1 vt \sin \theta_o\right]^{1/2} \quad . \qquad (1)$$

As the beam width of the physical antenna is small, the range during the period when the target is illuminated may be closely approximated by taking the first few terms of the binomial expansion of Equation (1):

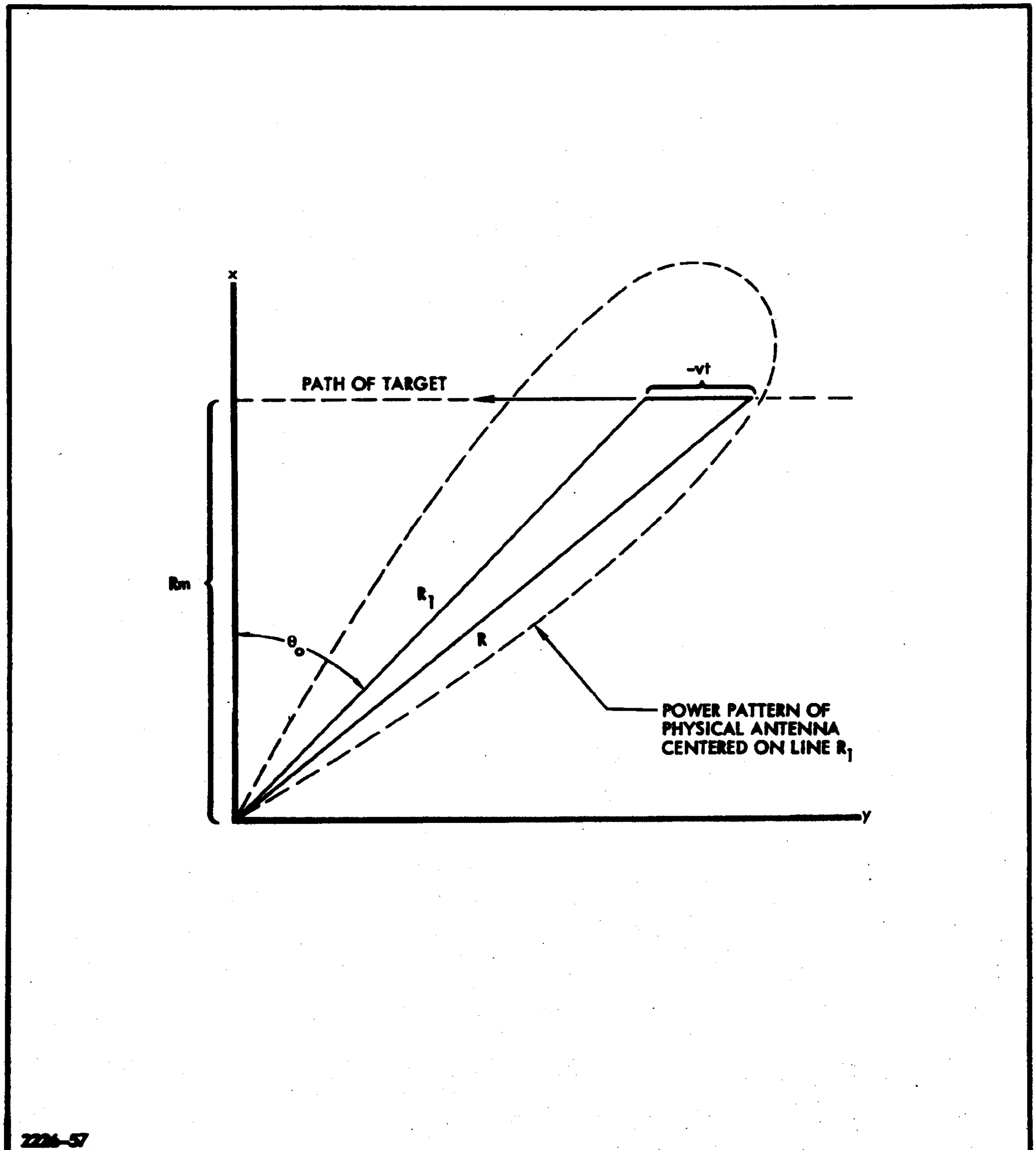


Figure 1 - Geometry of a Point Target in the Slant Range Plane

$$R \approx R_1\left(1 - \frac{vt \sin \theta_o}{R_1} + 1/2 \frac{(vt)^2}{R_1^2} \cos^2 \theta_o\right) . \tag{2}$$

The range dependence on time is reflected in a phase dependence on time of the return signal. The dependence of phase $\phi$ of the return signal on time is

$$\phi = 2\pi f_o t - \frac{4\pi R}{\lambda} + \phi_o \tag{3}$$

where

$f_o$ = the transmitted frequency

$\lambda$ = the wave length of the carrier

$\phi_o$ = the phase change caused by reflection.

Equations (2) and (3) may be developed into

$$\phi = 2\pi f_o t + \frac{4\pi}{\lambda} vt \sin \phi_o - \frac{2\pi(vt)^2}{R_1 \lambda} \cos^2 \phi_o + \phi_1 \tag{4}$$

where

$$\phi_1 = \phi_o - \frac{4\pi R_1}{\lambda} .$$

The return signal is synchronously demodulated with respect to some reference frequency to remove the carrier. It is desirable for the reference frequency to be the frequency of the return signal when the target is at the center of the beam. The phase of the return signal when the target is at the center of the beam and at range $R_1$ is given by

$$\gamma = 2\pi f_o t - \frac{4\pi R_1}{\lambda} + \phi_o . \tag{5}$$

The frequency will be

$$f_r = \frac{1}{2\pi}\frac{d\gamma}{dt} = \frac{1}{2\pi}\left(2\pi f_o - \frac{4\pi}{\lambda}\frac{dR_1}{dt}\right) . \tag{6}$$

From Figure 1, however,

$$\frac{dR_1}{dt} \equiv \left.\frac{dR}{dt}\right|_{t} = 0 \quad . \tag{7}$$

Therefore, from Equation (2)

$$\frac{dR_1}{dt} = -v \sin \theta_o \quad . \tag{8}$$

Then, substituting into Equation (6),

$$f_r = f_o + \frac{2v}{\lambda} \sin \theta_o \quad . \tag{9}$$

Therefore, $f_r$ is the frequency that will be used for synchronous demodulation. The synchronous demodulated signal will have the form

$$S(t) = A(t) \mathrm{Re} \left[ e^{-j2\pi f_r t} (e^{j\phi}) \right] \tag{10}$$

$$= A(t) \cos \left( \frac{2\pi (vt)^2 \cos^2 \phi_o}{R_1 \lambda} - \phi_1 \right) \tag{11}$$

where A(t) denotes the amplitude of the return which is a function of the reflectivity of the target and its position in the antenna beam. When

$$\phi_1 = n(2\pi)$$

$$\theta_o = 0$$

and

$$A(t) = K$$

Equation (12) reduces to the familiar expression

$$S(t) = K \cos\left(\frac{2\pi(vt)^2}{\lambda R_m}\right) . \tag{12}$$

The signal recorded on film at range $R_m$ will be of the form

$$S(x, R_m) = T_b + K' \cos\left(\frac{2\pi x^2}{\lambda R_m}\right) \tag{13}$$

where

$T_b$ = the transmissivity of the film

$K'$ = some constant times K.

From Equation (9) it is seen that all scatterers at an angle $\theta_o$ and with velocity v will have the same frequency. It follows that the locus of all possible scatterers whose returns have the same frequency is one nappe of a right circular cone with semi-apex co-angle $\theta_o$ whose axis contains the velocity vector.

The locus of points on the earth can be visualized if the intersection of the above doppler cone with a plane tangent to the earth at midmapping range is considered Since the range interval mapped is small, the mathematical model so described is a good approximation near the point of tangency.

## 3. AMBIGUITIES

Two types of ambiguities – range and azimuth – are inherent in a coherent high-resolution radar and provisions must be made to avoid them. The range-ambiguity problem is common to all pulsed radar and is usually avoided by lowering the prf so that the so-called "second-time-around" targets are not seen by the radar. However, the consideration of azimuth ambiguities yields another set of constraints on the choice of prf.

For a processor operating about zero doppler the information spaced at $\pm\gamma_n$ from zero doppler is ambiguous. This angular spacing is given by

$$\gamma_n = \frac{n\lambda F}{2v} \tag{14}$$

where

$n$ = a positive integer, 1, 2, 3, . . .

$\lambda$ = carrier wave length

$F$ = prf

$v$ = radar velocity.

The focused processor used with this system operates about an offset of prf/4 and is unable to distinguish between positive- and negative-going frequencies so that the ambiguity spacing is given by

$$\gamma_n = \frac{n\lambda F}{4v} . \tag{15}$$

For most high performance radars it is desirable to choose a prf such that the first azimuth ambiguity is placed in the vicinity of the first null of the physical antenna azimuth pattern. This choice of prf places an upper bound on the size of the mapped interval. This constraint in turn dictates the antenna height, since from the range-ambiguity standpoint the vertical antenna pattern is employed to avoid range ambiguities. It is readily deduced that ambiguity constraints are a determining factor in choosing antenna dimensions for a satellite radar. These considerations will be discussed further in Section III.

## 4. DATA PROCESSORS

The most successful type of high-resolution processor thus far is the optical correlator.* Considerable insight into the optical processor is possible if

*These devices are commonly known as correlators because the original conception, developed at the University of Michigan, was an optical cross-correlator.

the properties of a sine wave diffraction grating are considered. Figure 2 shows the three principal emergent rays from a sine-wave diffraction grating resulting from an incident plane wave of coherent light. The angle $\theta$ is defined thus:

$$\sin\theta = \lambda' f \tag{16}$$

where

$\lambda'$ = the wave length of the coherent light

f = the spatial frequency of the sine-wave diffraction grating.

Now consider a diffraction grating of the form $\cos(2\pi x^2/\lambda' R_m)$. This is of the same form as the demodulated return signal from a point target (Equation (13). Assuming a one-to-one scale factor in recording the demodulated return, the spatial frequency is $2x/\lambda' R_m$. From Figure 3 the distance r to the crossing of the zero axis is given by

$$r = \frac{x}{\tan\theta} \quad . \tag{17}$$

For small angles

$$\tan\theta = \sin\theta = \theta \quad . \tag{18}$$

Then,

$$r = \frac{x}{\lambda' f} = \frac{x\lambda' R_m}{\lambda' 2x} = \frac{R_m}{2} \tag{19}$$

which is to say that the diffracted light focuses on the zero (doppler) axis at a distance $R_m/2$ from the grating (data film).

From Figure 2 it is recalled that there are three principal emergent waves. For the cosine $x^2$ grating the three waves are defined thus (see Figure 4):

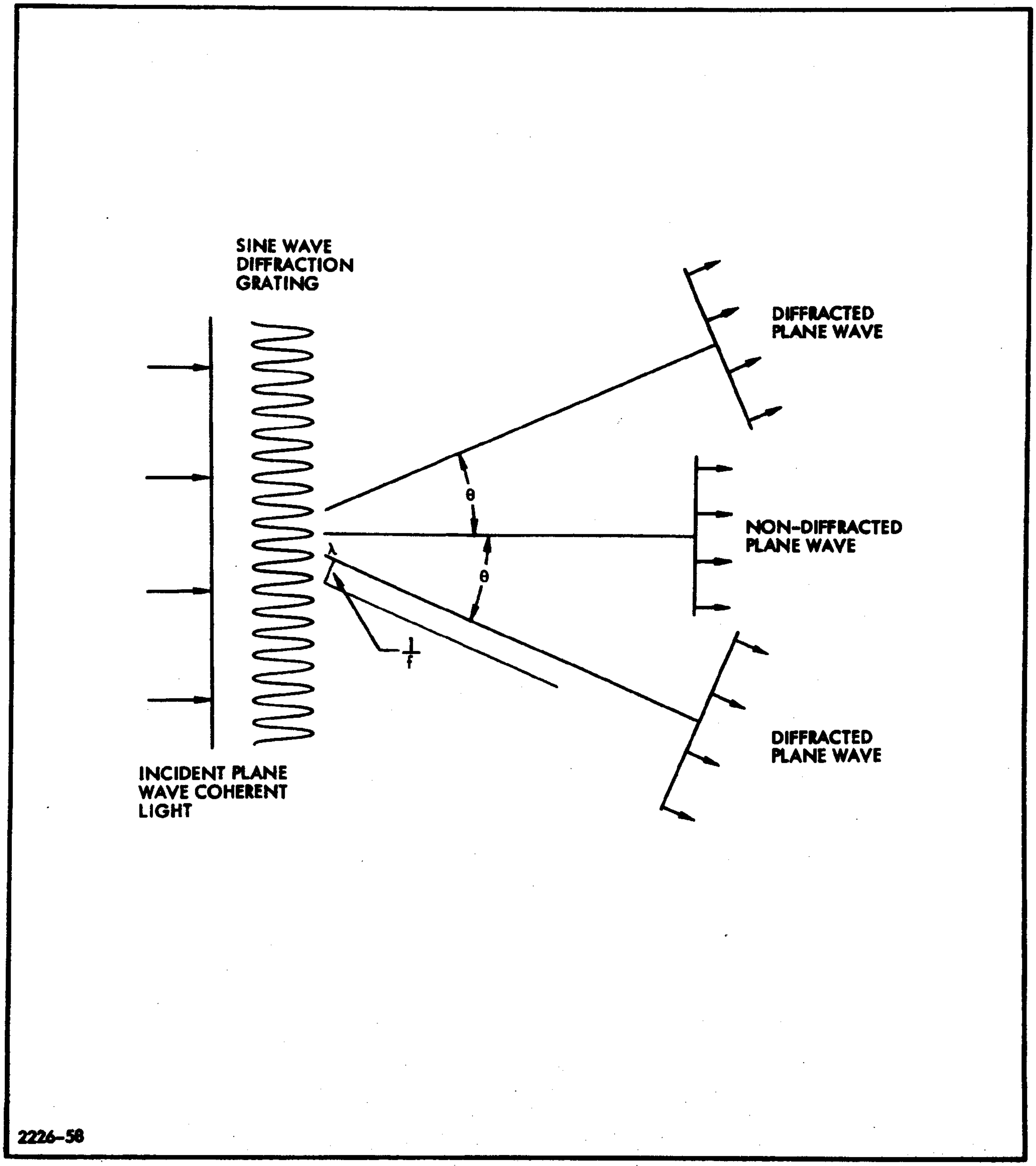


Figure 2 - Geometry Illustrating Fruenhofer Diffraction

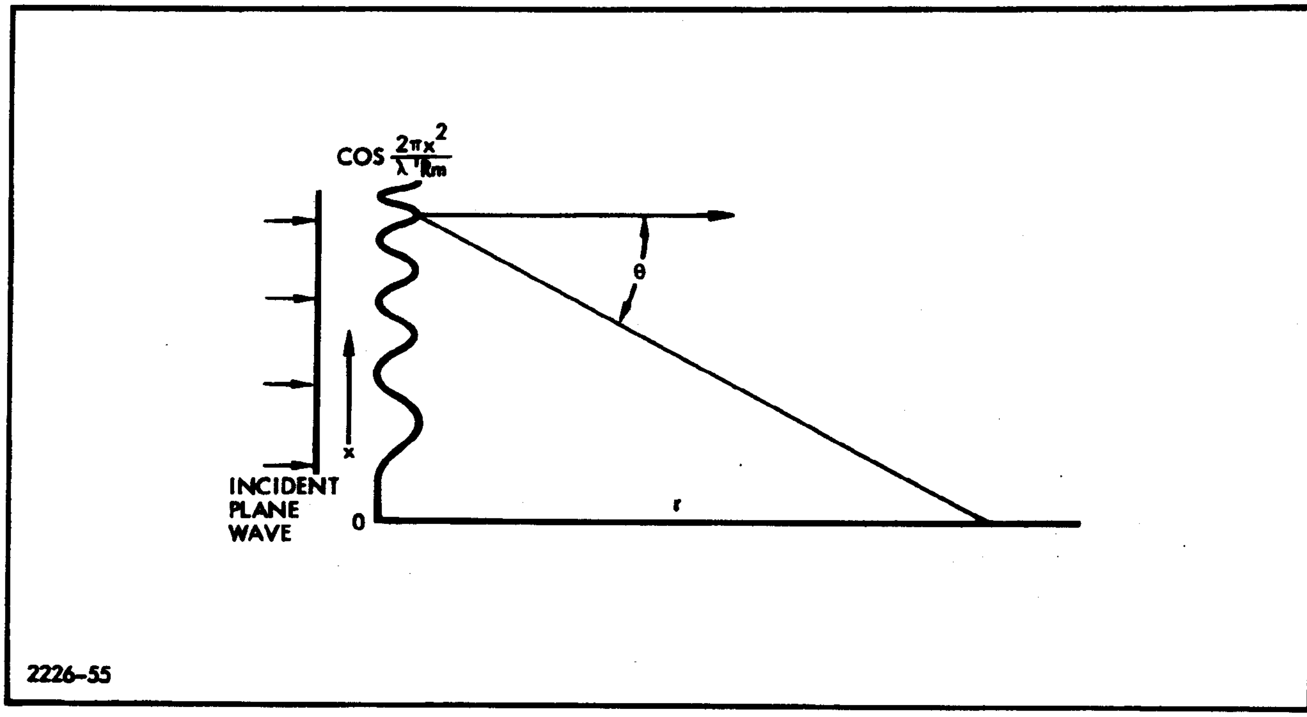


Figure 3 - Diffraction from $\frac{\cos 2\pi x^2}{\lambda' R_m}$ Grating

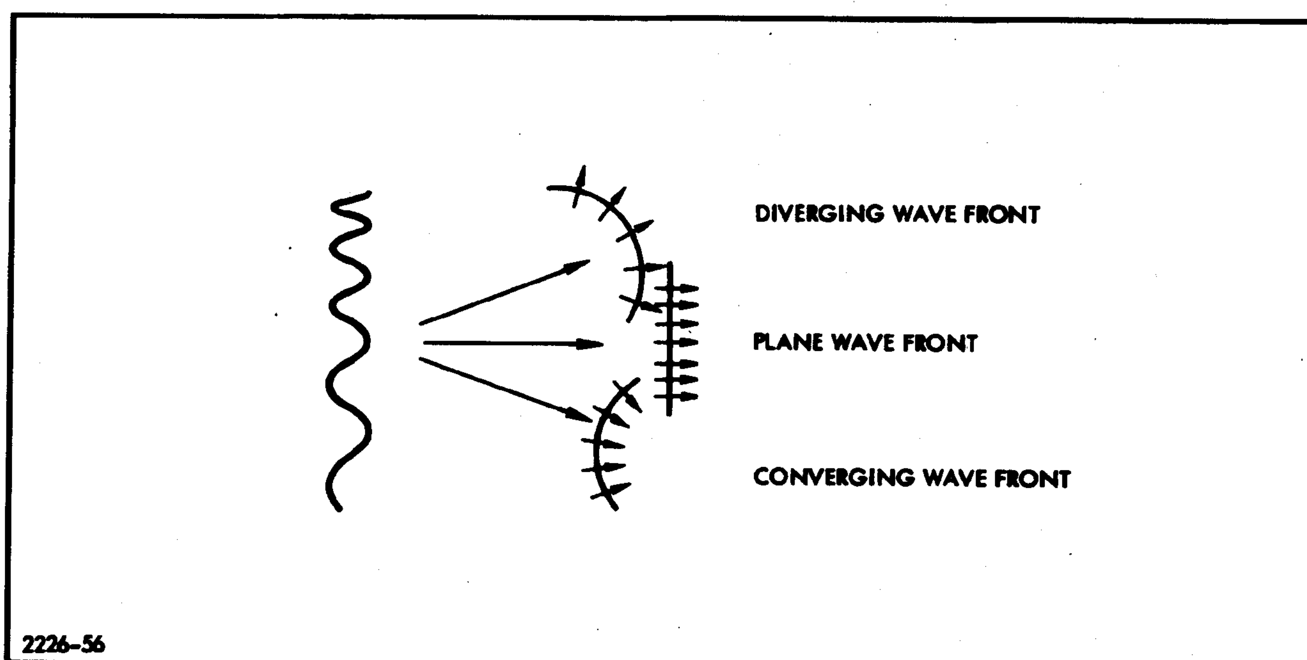


Figure 4 - Three Wave Fronts of a Parabolic Phase History

1. Converging wave front focused at a distance r on the axis
2. Diverging wave front with a virtual image at a distance -r on the axis
3. Plane wave front focused at infinity.

The converging wave front focuses at that angle and at that distance away from the recorded phase history which corresponds to the same angle and the scaled-down distance (proportional to the ratio of light-to-radar wave lengths and aircraft motion-to-film-scale factors) of the radar space where the data were recorded. Unfortunately, in a practical case the ratio is not nearly high enough and a converging lens must be used to bring the desired spot into focus at a convenient distance. Of course the other two wave fronts also come to a focus then but since they lie at different angles they can be blocked off from the final film with an appropriate optical stop. However, from Equation (19), the focal distance is a function of range; therefore, the lens must have a converging power which varies with range, giving rise to a conical shape. A cylindrical lens is also required to maintain target separation in range.

Thus, the basic elements of an optical processor are a coherent light source, optics to focus range and azimuth data onto a single plane, and film drives for transporting both the data and image films.

The optical processor for this system is being provided by the [redacted]

## SECTION III - SYSTEM ANALYSIS

### 1. ANTENNA LENGTH RELATIONSHIPS

Equation (9) demonstrated that the basic equation for the doppler frequency of a scatterer is

$$f_d = \frac{2V_r}{\lambda} \sin \theta \tag{20}$$

where

$V_r$ = relative velocity

$\lambda$ = radar wave length

$\theta$ = angle to scatterer measured from the perpendicular to the relative velocity vector.

Using Equation (20) with Equation (15) and the small angle approximation, the first ambiguous frequency is seen to be F/2. To avoid illumination of this frequency it should be placed at or beyond the first null of the physical antenna pattern. Using this criterion,

$$\frac{F}{2} = \frac{2V_r}{\lambda} \sin \frac{K_a \lambda}{D} \tag{21}$$

or

$$F \approx \frac{4V_r K_a}{D} \tag{22}$$

where

$K_a$ = constant greater than unity

D = length of physical antenna.

The value of $K_a$ varies depending on the type of antenna illumination used in the horizontal plane and the degree of suppression of azimuth ambiguity that is desired.

The basic equation for conditions of range ambiguity is

$$F = \frac{C}{2\Delta R_s \max} \tag{23}$$

where $\Delta R_s$ max = maximum unambiguous slant range interval. Equation (23) assumes a vertical antenna pattern which has a square-shaped beam illuminating only the desired slant range interval. To account for the actual vertical beam shape, Equation (23) may be rewritten as

$$F = \frac{C}{2K_r \Delta R_s} \tag{24}$$

where

$K_r$ = constant greater than unity

$\Delta R_s$ = slant range interval mapped.

The value of $K_r$ varies depending on the type of antenna illumination used in the vertical plane and the degree of suppression of range ambiguity which is desired. By using Equations (22) and (24) and solving for $\Delta R_s$, the following relationship is obtained:

$$\Delta R_s = \frac{CD}{8K_a K_r V_r} \quad . \tag{25}$$

This equation shows that the slant range interval which can be mapped is directly proportional to the length of the physical antenna. It is also seen that increasing $K_a$ or $K_r$ to reduce ambiguity levels will reduce the interval mapped.

Because of the physical limitations imposed by the vehicle, the length of the antenna was chosen to be 15 feet. To have as narrow a beam as possible, uniform illumination was chosen for the horizontal plane.

## 2. ANTENNA HEIGHT RELATIONSHIP

In this system the vertical pattern of the antenna is used to control the level of the range ambiguities. The geometry of the problem is shown in Figure 5. In this figure, the distance C/2F is the slant range interval between points of ambiguity such as A, A', and B, B'. The angle $\alpha$ is the angle between the ambiguous returns. The slant range to point A is $R_1$ and to A' is $R_2$. The slant range to point B' is $R_{mid}$ and is measured along the bore sight of the antenna. The problem is to illuminate as much of the slant range interval from A to A' as possible while maintaining the level of range ambiguity to a reasonable value. The final choice of antenna height must also be within the physical limitations imposed by the vehicle.

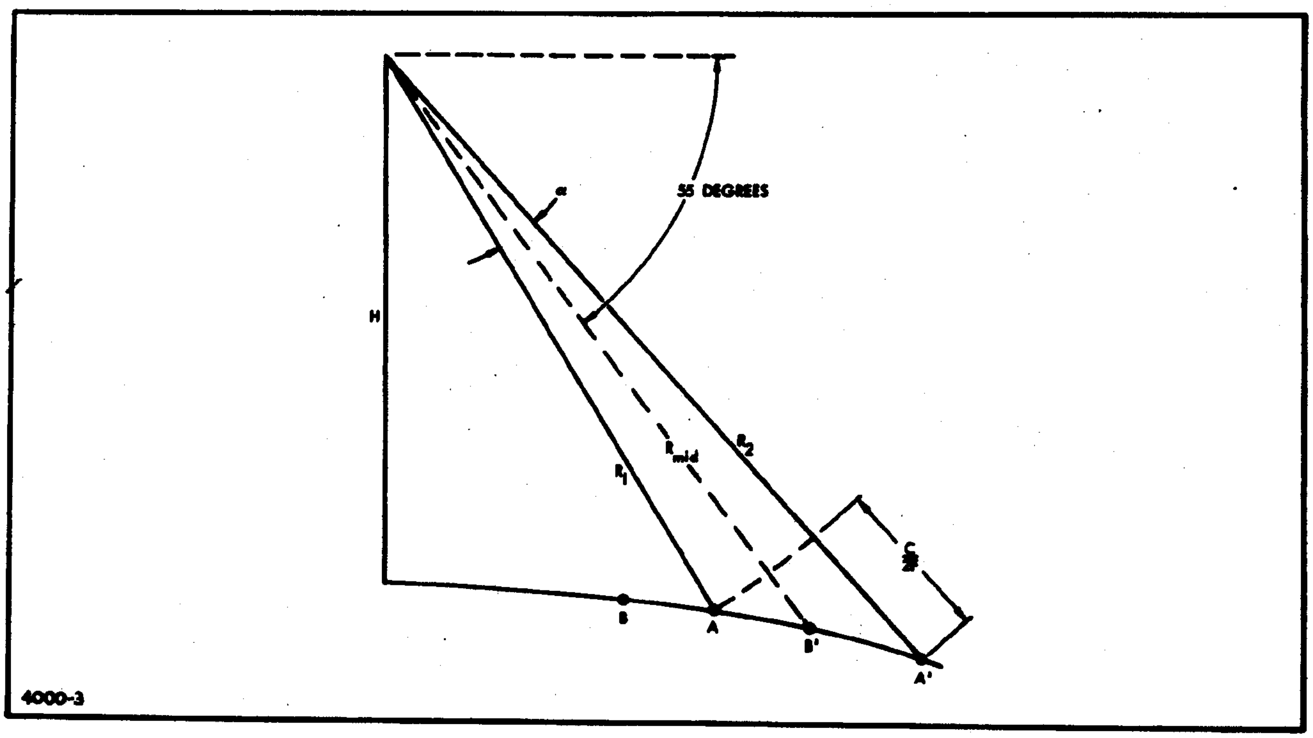


Figure 5 - Range Ambiguity Geometry

A typical two-way power pattern is shown in Figure 6. The dotted lines indicate the useful portion of the beam. This portion was selected to be the 6-db width since this choice leads to a realistic sensitivity time control requirement. There are two types of range ambiguities which can be encountered. The first occurs when targets illuminated by the sides of the main beam are ambiguous with respect to targets in the useful portion of the beam. This type can be referred to as main lobe ambiguity and is illustrated by points C, C' of Figure 6. The second type occurs when targets illuminated by side lobes are ambiguous with respect to targets in the useful portion of the beam. This type, referred to as side lobe ambiguity, is illustrated by points D, D' of Figure 6.

For a given prf or for a given ambiguity angle $\alpha$, a fixed set of points on the pattern becomes ambiguous with points in the useful portion of the beam. To illustrate graphically an ambiguity situation, the pattern of ambiguous points can be shifted by the angle $\alpha$ or multiples of $\alpha$ so that the ambiguity points are placed directly beneath the useful portion of the beam. This technique is shown in Figure 7. In this figure only the ambiguity caused by the first right-hand side lobe is shown for clarity of illustration. By varying the amount of shift, different amounts of ambiguities are introduced. In the case shown no ambiguity is being caused by the sides of the main lobe.

In the course of the original investigation, a number of types of antenna illuminations were considered and various spacings evaluated. The results of this study showed that by choosing the angle $\alpha$ so that main-lobe ambiguity was minimal, the largest portion of the slant range interval could be mapped consistent with low ambiguity levels. Increasing the ambiguity angle did not rapidly reduce the ambiguity level but did reduce the amount mapped. The results of this study are shown in Table I.

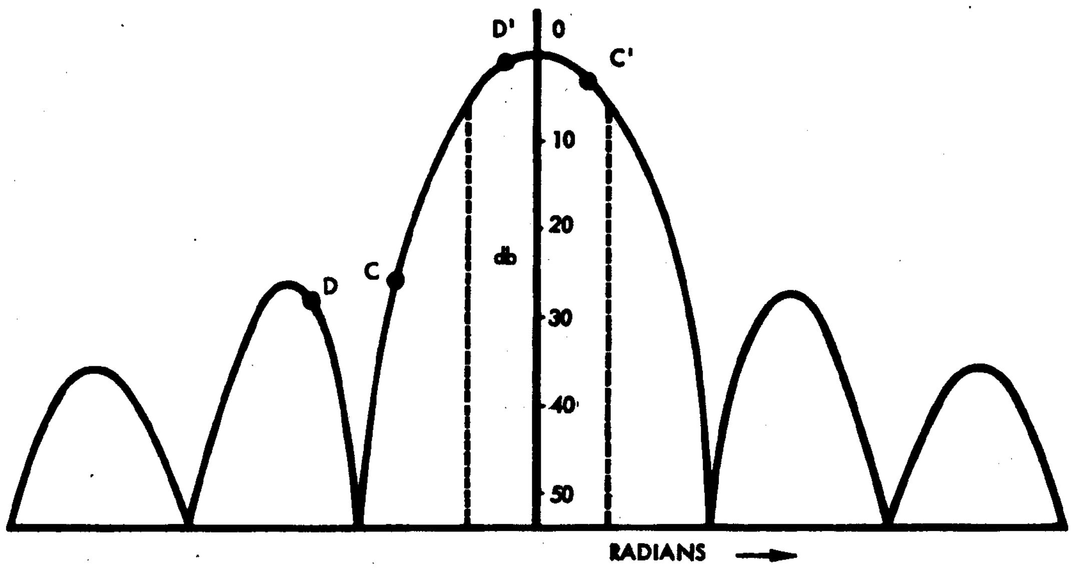


2226-53

Figure 6 - Typical Two-Way Power Pattern

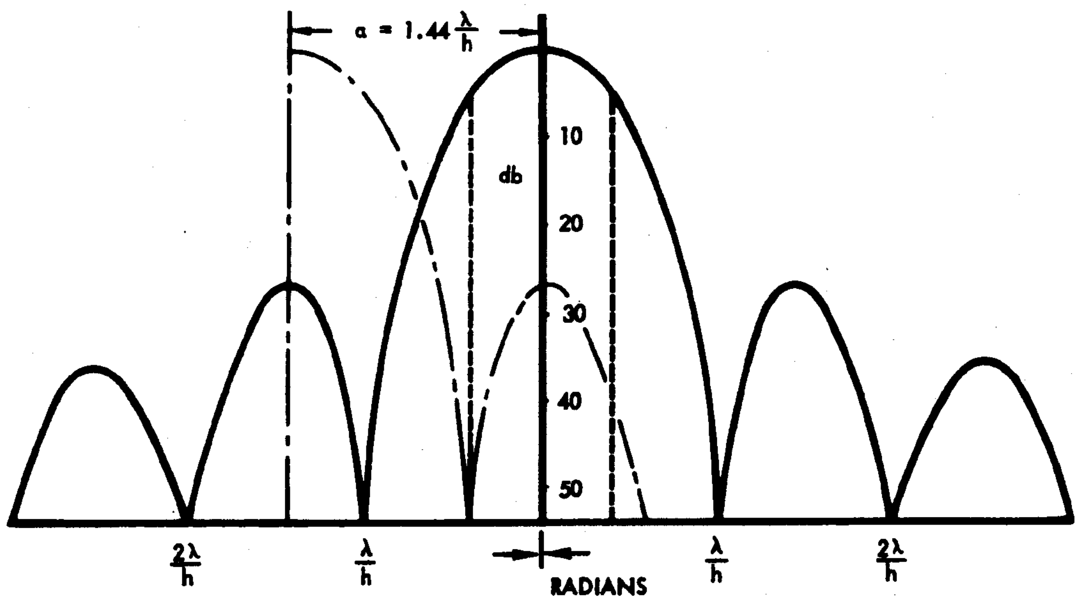


Figure 7 - Two-Way Power Pattern for Uniform Illumination and $\alpha = 1.44\lambda/h$

TABLE I - SUMMARY OF AMBIGUITY SPACING RELATIONSHIPS

| Type of illumination | Ambiguity spacing $\alpha$ | Level of first side lobe (two-way)(db) | Percentage of maximum interval mapped |
|---|---|---|---|
| Uniform | $\frac{1.44 \lambda}{h}$ | 26.4 | 0.61 |
| Cosine | $\frac{2.10 \lambda}{h}$ | 46.0 | 0.57 |
| Cosine$^2$ | $\frac{2.72 \lambda}{h}$ | 64.0 | 0.53 |

Referring to Figure 5, the value of $\alpha$ was calculated to be 0.0801 radian for the nominal altitude of 130 nautical miles, a prf of 8500 cps, and a depression angle of 55 degrees. This value of prf was based upon azimuth ambiguity studies. Using this value of $\alpha$ and the ambiguity spacing relationships shown above, the required antenna heights for the various types of illuminations were found to be:

| | |
|---|---|
| Uniform | 1.8 feet |
| Cosine | 2.7 feet |
| Cosine$^2$ | 3.5 feet . |

Because of physical limitations of the vehicle, the uniform illumination type was chosen with a height of 1.8 feet. This choice also allowed mapping of the largest portion of the slant range interval.

## 3. MAPPING INTERVAL

In paragraph III.2 the choice of uniform illumination and the height of 1.8 feet for the antenna in the vertical plane were discussed. Since the useful portion of the beam was chosen to be the 6-db width measured on a two-way pattern, the mapping angle for this type of illumination is

$$\alpha_m = \frac{0.88\lambda}{h}$$

$$= \frac{0.88 \times 0.102}{1.8}$$

$$= 0.05 \text{ radian} \quad . \tag{26}$$

At the nominal altitude of 130 nautical miles, this illuminates a slant-range interval of 5.95 miles. To minimize recorder electronics and to keep a fixed-range scale factor, this interval is kept constant independent of altitude variations.

## 4. AMBIGUITY LEVELS

### a. Azimuth Ambiguity

A measure of the azimuth ambiguity level for this system was obtained by the following considerations. Because of the pulsed nature of this system, targets which are separated by an angle given by Equation (15) have identical doppler frequencies. Since these targets have the same doppler frequencies they pass through the optical processor and each contributes energy to the final image.

The returns coming from the center region of the antenna pattern are the desired signals and all other ambiguous returns are the undesired signals. Therefore, the ratio of the energy of the undesired signals to the energy of the desired signal is a measure of the relative azimuth ambiguity level. This can be expressed as

$$\text{Az Amb} = \sum_{i=1}^{\infty} \frac{A_i}{A_o} \tag{27}$$

where

$Ao$ = the energy of the desired target

$\sum_{i=1}^{\infty} Ai$ = the energy from the ambiguous targets separated from the center target by $n\gamma$ (n being an integer).

These energies are graphically illustrated by the cross-hatched areas in Figure 8. A one-way amplitude pattern is shown rather than a two-way power pattern to illustrate better the ambiguous energies. The relative aperture width shown corresponds to an azimuth resolution of 25 feet in this system. It can be seen that the relative position of the ambiguity terms with respect to the signal can be varied by changing the pulse repetition frequency.

To determine this ratio a computer was programmed to evaluate the terms of Equation (27). The theoretical two-way power pattern of a 15-foot antenna with uniform illumination was used. It was assumed all targets had the same back-scattering coefficient. The ratio was calculated over a range of pulse repetition frequencies and for a number of azimuth resolutions. The results of these calculations are shown in Figure 9. These results were first used to establish that the prf should be in the range from 8,000 to 9,000 cps. This choice was made on the basis that it was desirable to obtain azimuth resolutions in the order of 10 feet with low ambiguity levels. The values for prf were then further defined to be 8215 to 8735. Based upon these values the azimuth ambiguity level for this system will be approximately -24 db.

**b. Range Ambiguity**

A measure of the range ambiguity level was obtained by calculating the ratio of the amounts of power returned from points of ambiguity as compared to the amount of power returned from the desired point. Analysis has shown that the greatest contribution to this level is made by the first

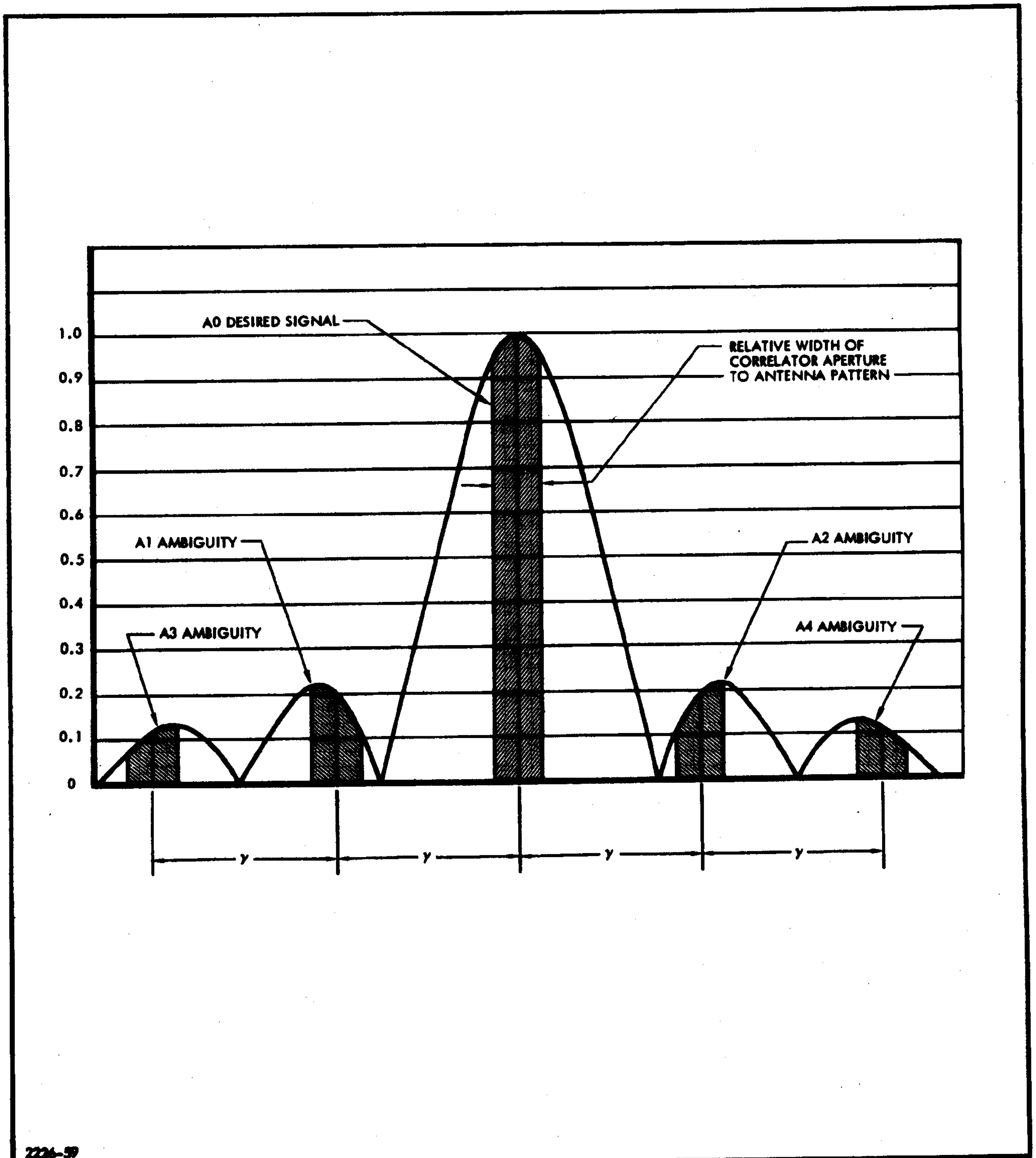


Figure 8 - Desired and Ambiguous Signals

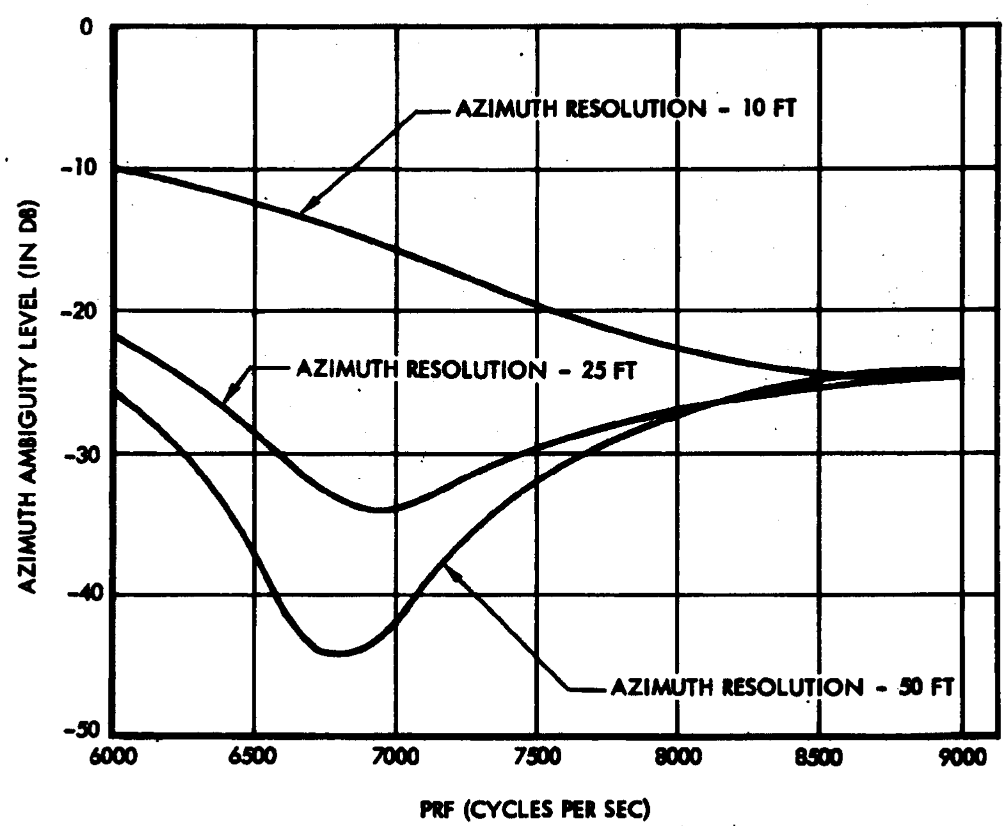


2226-60

Figure 9 - Measure of Relative Ambiguity Level

side lobes of the antenna. Side lobes near vertical incidence do not contribute a large factor. In this analysis, distributed terrain was considered as the model rather than a field of point targets. A theoretical antenna pattern was also used. Results show that for the nominal altitude the maximum level for combined range ambiguity is -22 db. This figure will vary slightly as a function of altitude and prf used.

## 5. RADAR POWER REQUIREMENTS AND SIGNAL LEVELS

### a. Radar Equation and Peak Power

There are a number of equations for the calculation of peak transmitter power required for coherent radars. Usually these equations contain a term which reduces the power required because of coherent integration. Since there is no general agreement as to the magnitude of this term, the traditional radar equation will be used here. This equation may be written as

$$P_t = \frac{(4\pi)^3 P_r R^4}{G^2 \lambda^2 \sigma} \tag{28}$$

where

$P_t$ = peak transmitter power

$G$ = antenna gain

$\lambda$ = wave length at $f_o$

$\sigma$ = apparent target cross-section

$R$ = slant range

$P_r$ = signal power at receiver.

The signal power $P_r$ is further defined as

$$P_r = KTB(NF)S/N \tag{29}$$

where

$K$ = Boltzmann's constant

$T$ = absolute temperature

$B$ = receiver band width

$NF$ = noise figure of receiver

$S/N$ = signal-to-noise ratio.

The quantity $\sigma$ is defined as

$$\sigma = A\sigma_o \tag{30}$$

where A is the area illuminated by a single pulse packet and $\sigma_o$ is the back scattering coefficient per unit area for a particular type of terrain. From the radar geometry the area A is seen to be

$$A = \frac{C\Delta tR\phi \sec\theta}{2} \tag{31}$$

where

$C$ = velocity of propagation

$\Delta t$ = radar pulse width

$R$ = slant range

$\phi$ = azimuth beam width

$\theta$ = aspect angle to the terrain.

Figure 10 shows experimental curves obtained by Goodyear Aerospace relating $\sigma_o$ to types of terrain and aspect angle. The selected value for $\sigma_o$ for the subject system is indicated by the dotted coordinates on the graph.

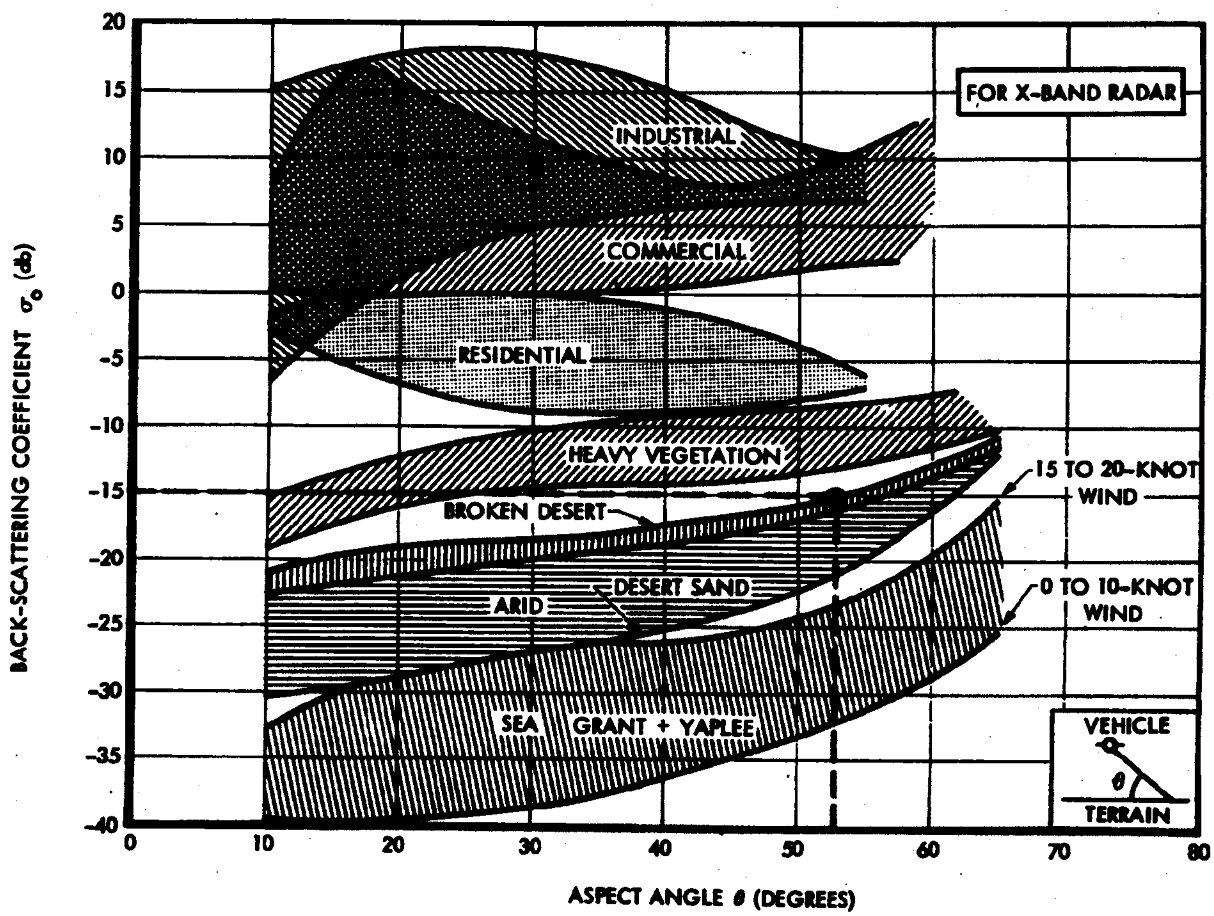


Figure 10 - Back-Scattering Coefficients versus Aspect Angle

Combining Equations (29), (30), and (31) with Equation (28) yields

$$P_t = \frac{(4\pi)^3 KTB(NF)S/N\, R^3}{G^2\lambda^2 0.5C\Delta t\phi\sigma_o \sec\theta} . \tag{32}$$

The values used for these parameters were selected as follows:

| | | |
|---|---|---|
| G, | antenna gain | = 43 db |
| $\lambda$, | operating wave length | = 0.102 foot |
| $\Delta t$, | transmitted pulse length | = $1.0 \times 10^{-6}$ sec |
| B, | band width | = 16 mc |
| $\phi$, | half-power azimuth beam width | = 0.0064 radian |
| (NF), | noise figure | = 10 db |
| S/N, | signal-to-noise ratio | = 10 db |
| $\sigma_o$, | back-scattering coefficient | = -15 db. |

From the operational geometry,

R = slant range at maximum altitude = $1.09 \times 10^6$ feet

$\theta$ = aspect angle = 53 degrees.

The physical constants are:

K = $1.38(10^{-23})$ watts/deg K

C = $9.85(10^8)$ ft/sec

T = 290 deg K.

Substituting the above values and allowing an additional 1.0 db for atmospheric attenuation,

$$P_t = 30.0 \text{ kw} \tag{33}$$

is obtained. This calculation shows a peak power of 30 kw will provide a 10-db signal-to-noise ratio at the receiver for terrain with a back-scattering coefficient slightly greater than broken desert. At the edges of the map the signal-to-noise ratio will be 4 db because of the drop-off of antenna gain. As previously mentioned, this calculation does not include a factor for improvement of the signal-to-noise ratio caused by coherent optical processing.

**b. Transmitter Average Power**

The average power of the transmitter is given by

$$P_{ave} = P_t F \Delta t \quad . \tag{34}$$

Since the pulse repetition frequency F is variable in 16 steps from 8215 to 8735, the average power varies from 246 to 262 watts.

**c. Effect of Pulse Compression**

In the above calculation for peak transmitter power, the actual expanded transmitter pulse length of 1.0 microsecond was used. This is the peak power actually required from the transmitter. Had the effective or compressed pulse length of 0.06 microsecond been used, the result of the calculation would be 497 kw or 16.6 times greater. Thus, the effect of pulse compression is to reduce the transmitter peak power required by the compression ratio. Of course the effect of pulse compression can also be considered to improve range resolution from the standpoint that a long pulse is transmitted and, after compression, a short pulse is received. The use of pulse compression, however, in no way alters the requirements for receiver band width or transmitter average power.

**d. Receiver Gain and Automatic Gain Control Requirement**

Having selected the noise figure for the receiver it is now possible to calculate the noise level at the receiver input as

$$n = KTB(NF) = 1.38(10^{-23})\ (290)\ (1.6)\ 10^{7}\ (10)$$

$$= 6.5\ (10^{-13})\ \text{watts} \quad . \tag{35}$$

The nominal signal return from -15 db terrain is, of course, 10 db above the noise, or 6.5 $(10^{-12})$ watts.

The automatic gain control circuitry in the Reference Computer was designed to have a threshold level of 80 mv rms at 50 ohms. Since this signal also represents the output of the RF-IF unit, the required over-all r-f/i-f gain can be immediately calculated. Optimum system operation dictates that in the absence of signal, agc will be at the threshold of operation. Therefore, the 80 mv at 50 ohms must represent the input noise times the r-f/i-f gain. The gain H is

$$H = \frac{(80)^2 \times 10^{-6}}{(50)\ (6.5 \times 10^{-13})}$$

$$= 2.0 \times 10^{8} = 83\ \text{db} \quad . \tag{36}$$

With the selection of the agc threshold at the noise level, the range of agc action required can now be determined.

The action of the agc circuit is to vary the gain of the i-f amplifiers as a function of the average level of received signals. The necessity for this type of circuitry can be seen from the following considerations. Figure 10 illustrated that for this system the back-scattering coefficient from terrain can vary from the chosen minimum value of -15 db to perhaps +10 db for cultural targets.

Since the noise at the receiver will be 10 db below the signal from -15 db terrain, the total variation from noise level up to maximum signal level may exceed 35 db. Unfortunately, the dynamic range capability of the recorder-film combination is limited to 20 db or less. The purpose of the agc circuit is thus to keep the average signal return centered within the dynamic range capability of the recorder.

For this system the range of operation for the agc circuit has been chosen to be a minimum of 27 db.

e. The Sensitivity Time Control Requirement

In addition to the agc circuitry, it is also necessary to employ sensitivity time control (stc) in the receiver chain. This circuitry is used to vary the gain of the receiver, as a function of time, to compensate for the difference of antenna illumination across the mapping interval. At the nominal altitude of 130 nautical miles the mapping interval is defined between the 3-db points of the vertical pattern. On a round-trip basis these points are 6-db down with respect to the maximum. To compensate, a receiver gain function producing an opposite effect to that of the antenna pattern is used. The chosen function has 6-db attenuation corresponding to the arrival time of energy from targets at the center of the illuminated area and has maximum gain corresponding to the arrival times of energy from targets at the edge of the map.

Variations caused by the difference in range of the near edge and the far edge of the map are about 12 percent or less than 0.6 db, and may be neglected. Optimum compensation is obtained for the nominal 130-mile altitude. Operation at other altitudes between 117 and 143 nautical miles will produce only slight compensation errors.

6. RANGE RESOLUTION

There are a number of system factors which tend to reduce the range resolution. These factors are:

1. Transmitted pulse length
2. Time jitter
3. Lateral film displacement
4. Spot size limitation in Recorder.

The transmitted pulse at half amplitude in terms of slant range is

$$\Delta s = 1/2\ CT = 1/2(9.85 \times 10^8)\ (0.06 \times 10^{-6}) = 30 \text{ feet} \quad . \tag{37}$$

Actually the receiver degrades the pulse to approximately 33 feet.

Time jitter in the transmitted pulse and sweep will appear as a resulting jitter at the film position. Since these are derived from counters in the Reference Computer they are not entirely independent but have been treated as such. Jitter from each has been limited to ±10 nanoseconds. In terms of radar distance this represents, for each jitter component,

$$S = 1/2(9.85 \times 10^8)\ (10 \times 10^{-9})$$

$$= 4.9 \text{ feet} \quad . \tag{38}$$

Lateral film displacement during the build-up period also produces an equivalent jitter in the range direction. The lateral displacement is about $\pm 0.7 \times 10^{-4}$ inches. Since the sweep is 1.08 inches for 5.95 miles, the displacement in terms of radar distance is

$$S = \frac{0.7 \times 10^{-4} \times 5.95 \times 6080}{1.08}$$

$$= 2.4 \text{ feet} \quad . \tag{39}$$

From previous analyses, it was found that the spread function for the cathode ray tube (crt) lens and film combination is $0.65 \times 10^{-3}$ inches at the half-amplitude level. This corresponds to:

$$S = \frac{0.65 \times 10^{-3} \times 5.95 \times 6080}{1.08}$$

$$= 22 \text{ feet} \quad . \tag{40}$$

Combining the above factors, using the root sum square method, yields:

$$Sr = 40 \text{ feet} \quad . \tag{41}$$

Test results on the system show that slant range resolution considerably better than 50 feet is being achieved.

7. AZIMUTH RESOLUTION

A major factor in determining the final azimuth resolution of the system is the effect of phase errors across the synthetic aperture. Consideration of the correlation process in the azimuth direction shows that it is necessary to maintain a prescribed phase history over some period of time, T. The expression for T as a function of azimuth resolution is given by

$$T = \frac{0.6\,\lambda R}{V_r A_z} \tag{42}$$

where

$\lambda$ = radar wave length

$R$ = slant range

$V_r$ = relative vehicle velocity

$A_z$ = azimuth resolution .

Since emphasis, in this system, has been placed upon obtaining the best possible resolution, a design goal of 10 feet was chosen. Using this value for azimuth resolution in Equation (42), the value for T is determined to be 0.25 second and the corresponding azimuth aperture is 1.25 inches on the data film.

Phase errors introduced by the system may be considered as being composed of linear, quadratic, and higher order terms. A linear phase error term corresponds to a fixed frequency error in the system and has an effect identical to an angular offset of the synthetic array with respect to the zero doppler plane. On the map film this error causes an angular displacement of the image. Since such errors affect all returns equally, the net result to a good approximation is equivalent to a displacement of the entire radar image and is usually small. For these reasons linear, or so called "squint", errors will not be further considered.

More serious are the effects of quadratic and higher order phase errors. These errors produce resolution degradation. For the purpose of determining an upper limit on the magnitude of phase errors, it was assumed that most errors generated by the system could be regarded as pure quadratic terms. Phase errors introduced by different portions of the system were considered to be independent and the over-all phase error limit was chosen to be 1.0 radian. A list of the sources of phase errors considered is given below:

1. Clutterlock drift
2. Local oscillator and 70-mc frequency drift
3. Film speed variations
4. Pulse-to-pulse transmitter phase jitter.

The phase error for any frequency drift may be written as

$$\phi = \int (W_o - W_1)\, dt \tag{43}$$

where $W_o/2\pi$ is the frequency at the start of the period of interest and $W_1$ is a function of time. For quadratic errors, $W_1$ varies linearly with time and can be written as

$$W_1 = W_o + \alpha t \quad . \tag{44}$$

Since $W_o$ may be taken at the center of a build-up period, the time of interest is $T/2$.

Hence,

$$\phi = \int_0^{\frac{T}{2}} \alpha t \, dt$$

or

$$\phi = \frac{\alpha t^2}{2}\Bigg]_0^{\frac{T}{2}} = \frac{\alpha T^2}{8} \quad . \tag{45}$$

By assigning a maximum phase error of 0.5 radian to this source, the following expression can be obtained:

$$\alpha_{max} = \frac{4}{T^2} \text{ radians/sec}^2$$

or

$$\alpha_{max} = \frac{2}{\pi T^2} \text{ cycles/sec}^2 \quad . \tag{46}$$

Using the previously calculated value of T as 0.25 second, the basic stability requirement applied to the clutterlock is found to be

$$\alpha_{max} \approx 10 \text{ cycles/sec}^2 \quad . \tag{47}$$

In the case of the local oscillator and the 70-mc oscillator, the result is modified by the fact that both are subtracted out of the return at demodulation. Drift of these frequencies is important, however, because it causes an apparent change in the path length from the radar to the target. A linear rate of change of radar path length contributes a doppler offset or squint error to the map being generated but does not degrade resolution. Higher order derivatives of $f_o$ will affect resolution and the level of side lobes.

Omitting all terms higher than second order, an expression for $f_o$ can be written as

$$f_o = f + \alpha t + \beta t^2 \quad . \tag{48}$$

The phase of the detected signal, referenced to the transmitted phase, is

$$\phi = \frac{4\pi R f_o}{C} = \frac{4\pi R}{C}\left[f + \alpha t + \beta t^2\right] \; . \tag{49}$$

This expression differs from an ideal phase history (with squint) only in the term involving $t^2$; hence, the error in phase is

$$\Delta\phi = \frac{4\pi R}{C}\beta t^2 \quad . \tag{50}$$

By assigning a maximum error of 0.5 radian and using the half build-up time for t, the value of $\beta$ is found to be 2420 cycles/sec$^3$.

Allowable errors in film motion may be calculated from a knowledge of the film speed and the azimuth frequencies of interest. Using a prf of 8500 cps, a 0.25 second build-up has 2125 range lines recorded in 1.25 inches of film.

At the frequency of prf/4 there are 531 cycles per build-up. By allowing an error of 0.5 radian, the maximum film displacement is found to be

$$S = \frac{1.25}{531 \times 4\pi} = 0.187 \times 10^{-3} \text{ inches} \quad . \tag{51}$$

Using this value of displacement and the time of 0.125 second, the allowable errors in acceleration and velocity are found to be

$$\Delta\alpha = 0.024 \text{ in/sec}^2$$

$$\Delta V = 0.003 \text{ in/sec} \quad . \tag{52}$$

Using this criterion for $\Delta V$, the limit on film speed variation is 0.06 percent.

Finally, the usual criterion can be applied to limit the transmitter pulse to pulse errors to 0.5 radian or 28.6 degrees.

In summary, the phase error sources and the established limit values are given in Table II.

TABLE II - PHASE ERROR SOURCES

| Error | Limit |
|---|---|
| Clutterlock drift | 10 cps/sec$^2$ |
| Local oscillator and 70-mc frequency drift | 2420 cycles/sec$^3$ |
| Film speed variation | 0.003 in/sec |
| Transmitter phase jitter | 28.6 degrees |

## 8. CLUTTERLOCK LOOP ANALYSIS

### a. General Requirements of Clutterlock Loop

The clutterlock loop is designed to orient the narrow synthetic array, generated by the coherent radar, along the axis of the physical antenna. It is generally assumed that the exact bore sight of the physical antenna with respect to the velocity vector is unknown and furthermore is changing at some limited maximum rate. The clutterlock must ascertain the antenna bore sight and cause the system to align its own synthetic pattern. Secondly, the clutterlock must follow the physical antenna with a small enough hang-off error to avoid ambiguities in the data and yet move slowly enough to avoid the destruction of coherent buildup in process at the recorder. A moment's reflection will show that complete compliance with these requirements is an impossibility, particularly if the rate of angular rotation of the physical bore sight is large.

Conceptually, the clutterlock operates by measuring the positive- or negative-going phase shift of the targets within the beam on successive returns. This process, of necessity, depends on the statistical nature of the return signals. Error may occur because of a predominance of targets in one side of the physical beam or because of very large targets not symmetrically located. These sources of error are largely eliminated if the time constant of the loop is long compared to the transit time of a single target across the beam. Further help is available in reducing the effect of very large targets by allowing the video used in the clutterlock to be limiting a substantial portion of the time, say 50 percent.

b. Clutterlock Servo Loop

Figure 11 is a simple diagram of the clutterlock servo.

(1) Storage and Approximate Multiplier

The storage and approximate multiplier is designed to compare the phase from corresponding range increments on successive prf returns. The design is such that the comparison of quadrature returns results in a zero output, while those having other phase angles give non-zero values of $E_c$.

Ideally, the function to be generated by the multiplier is $\overline{A} \cdot \overline{B}$ where A and B are vector notations for the two returns being compared. In fact the approximate multiplier generates the quantity

$$E_c = K(\left|\overline{A}+\overline{B}\right| - \left|\overline{A}-\overline{B}\right|) \tag{53}$$

where K is a proportionality constant. If $\overline{A}$ and $\overline{B}$ are of equal amplitude (i.e., the return amplitude does not change significantly between two successive prf pulses), the two functions can be analyzed as to whether their values are zero, positive or negative for various relative phases. Table III shows the result.

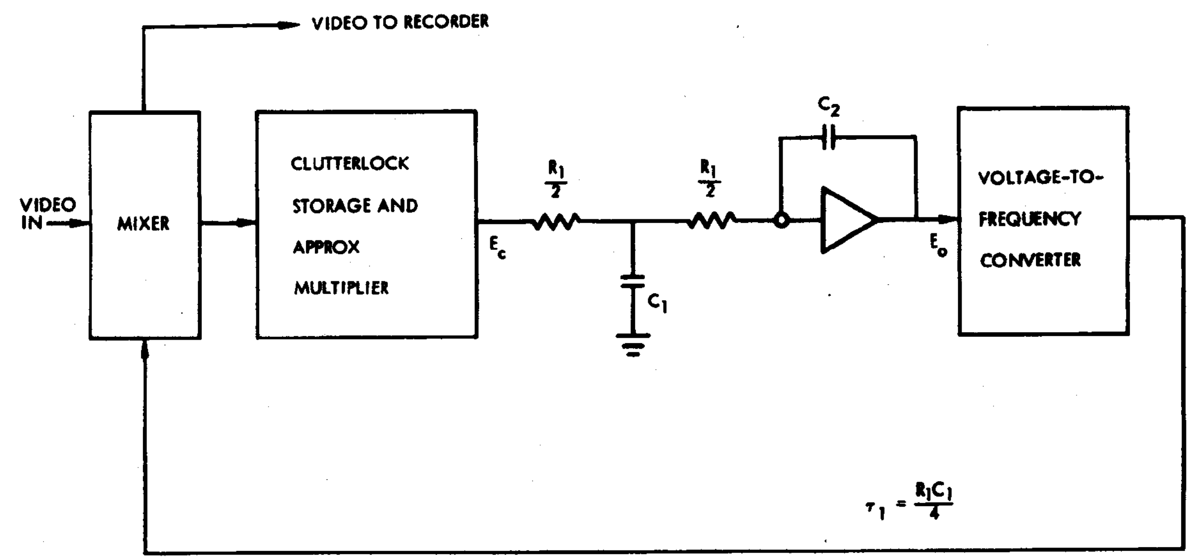


Figure 11 - Simplified Block Diagram of Clutterlock Loop

TABLE III - QUALITATIVE COMPARISON OF $\bar{A} \cdot \bar{B}$ and $|\bar{A}+\bar{B}| - |\bar{A}-\bar{B}|$

| Phase Angle, $\beta$ | $0^\circ$-$90^\circ$ | $90^\circ$ | $90^\circ$-$180^\circ$ | $180^\circ$-$270^\circ$ | $270^\circ$ | $270^\circ$-$360^\circ$ |
|---|---|---|---|---|---|---|
| $\bar{A} \cdot \bar{B}$ | + | 0 | - | - | 0 | + |
| $\lvert\bar{A}+\bar{B}\rvert - \lvert\bar{A}-\bar{B}\rvert$ | + | 0 | - | - | 0 | + |

As is evident from Table III, the sense of $|\bar{A}+\bar{B}| - |\bar{A}-\bar{B}|$ is always in agreement with $\bar{A} \cdot \bar{B}$. Further examination of the table shows that the output will be zero for either 90-degree or 270-degree phase angles. If the clutterlock servo is designed so that plus values lead to an increase in $\beta$, the point at 270 degrees will be one of unstable equilibrium and may be disregarded.

(2) Loop Transfer Function

Having made these choices, the clutterlock may be designed to make N range samples in each return, each sample having a width, W. For purposes of mathematical analysis, assume that the output of the multiplier is identical with the output of a true $\bar{A} \cdot \bar{B}$ multiplier. The output can then be written as

$$E_c = \left(\frac{WNF}{2}\right) E_s \left(\frac{4\pi V}{F\lambda}\right) \Delta\theta + \frac{WF\sqrt{N}}{2} E_n \tag{54}$$

where

$F$ = the prf

$E_s$ = a constant of the multiplier in volts

$V$ = the vehicle velocity

$\lambda$ = the operating wave length

$E_n$ = a noise voltage generated by the multiplier.

The quantity $\Delta\theta$ is the instantaneous alignment error between the physical antenna and the synthetic array being generated. It is seen that the quantity WNF/2 is the duty cycle of the clutterlock. The expression $4\pi V\Delta\theta/F\lambda$ represents the angular rotation of the second return B with respect to A, the first return, over one prf period. The last term is a noise input assumed to obey a random walk integration process.

The transfer function of the resistance-capacitance (r-c) filter and integrator may be written as

$$\left[ I_o + \frac{E_c}{R_1(T_1P + 1)} \right] \frac{1000}{C_2P} = \frac{2V}{\lambda} \theta_m \tag{55}$$

where

$$T_1 = \frac{R_1C_1}{4} \; .$$

$I_o$ is the quiescent current required at the input to the integrator, and $\theta_m$ is the angle off zero doppler to which the synthetic array is steered. Designating the angle off zero doppler of the center of the physical beam as $\theta_i$, and replacing $\Delta\theta$ by $\theta_i - \theta_m$,

$$\theta_m = \frac{\lambda(1000)}{2VCP} \; \frac{I_o + \frac{WFN}{2} E_s \frac{4\pi V}{F\lambda}(\theta_i - \theta_m) + \frac{WF\sqrt{N}}{2} E_n}{R_1 \; (T_1P + 1)} \; . \tag{56}$$

After some rearrangement, and defining a new constant $T_2$:

$$T_2 = \frac{R_1C_2}{1000WNE_s\pi} \; , \tag{57}$$

$$\theta_m = \frac{\lambda T_2 \; 500(T_1P + 1) \frac{I_o}{CV} + \theta_i + \left(\frac{\lambda F}{4\sqrt{N}\pi V}\right) \frac{E_n}{E_s}}{T_2P(T_1P + 1) + 1} \tag{58}$$

$$\theta_m = \frac{\theta_h(T_1P + 1) + \theta_i + \theta_{noise}}{T_2P(T_1P + 1) + 1} \quad . \tag{59}$$

is obtained. The first term $\theta_h$ is a steady-state hang-off error resulting from the practical requirement of a non-zero $I_o$. The term is minimized by providing large gain in the integrator (reducing $I_o$), and by making $C_2$ as large as possible consistent with other requirements. The last term, $\theta_{noise}$, is a noise term discussed previously. The denominator determines the rate at which the loop will track, as well as its stability.

(3) Time Constant Selection

The exact choice of $T_1$ and $T_2$ and their constituent parameters now depends on an engineering compromise and on the basic vehicle stability.

In the long run a continuous high-resolution map cannot be obtained if the vehicle continually moves the physical antenna at excessively high rates. If an attempt is made to hold the synthetic array steady to obtain high resolution, the level of relative azimuth ambiguities will rapidly increase.

If, however, the fact is considered that the vehicle has maximum rates of rotation, and further is provided with limits on its excursions in pitch and yaw, the values of $T_1$ and $T_2$ can be selected which just hold the ambiguities to an acceptable value, and thereby reduce the effects of vehicle instability a maximum amount.

From the geometry of the radar situation for a 55-degree depression angle, and an altitude of 130 nautical miles, the expression

$$\theta_i = 0.57\,\theta_a + 0.81\,\theta_p \tag{60}$$

can be written where

$\theta_i$ = the instantaneous angular offset of the real antenna beam from the zero doppler plane

$\theta_a$ = the instantaneous yaw angle with respect to the velocity vector

$\theta_p$ = the instantaneous pitch angle with respect to the velocity vector.

The problem will be analyzed assuming sinusoidal variations in $\theta_a$ and $\theta_p$ with amplitudes equal to the expected dead band and a frequency which is consistent with the fundamental of a triangular excursion from limit to limit. Given limits of ±0.25 degree and maximum rates of 0.003 degree per second, a worst case can be written as:

$$\theta_a = \theta_p = 0.25 \sin 0.02t$$

and substituting into Equation (60) yields

$$\theta_i = 0.35 \sin 0.02t \quad . \tag{61}$$

To minimize the effects of the noise term in Equation (59), it is desirable to select $T_1 = T_2$. This choice gives a minimum noise band width in the loop. If only the center term of Equation (59) is considered and

$$\theta'_m = \frac{\theta_i}{T_2 P(T_{1P} + 1) + 1} \tag{62}$$

is written, the quantity

$$\theta'_h = \theta_i - \theta'_m \tag{63}$$

can be evaluated for its maximum value with the expected input of Equation (61). The results are listed in Table IV. A maximum hang-off angle, $\theta_h$, may be chosen, as given by Equation (59). Setting this at 0.03 degree, the table may be completed.

If total errors of the order of one-tenth of the 3-db beam width are desired, $T_1 = T_2 = 2.5$ seconds must be chosen. The actual equipment design allows for choices of effective time constants of 2.5 and 5 seconds at command.

Values of the electrical components $R_1$ and $C_1$ may be calculated from the definition of $T_1$ in Equation (55), and of $C_2$ from Equation (57). The allowable $I_o$ is determined by setting Equation (59) equal to 0.03 degree.

TABLE IV - LAG ANGLES $\theta'_h$ AND $\theta_h$ FOR VARIOUS VALUES OF $T_1 = T_2$

| Time constant $T_1 = T_2$ (seconds) | Lag angle $\theta'_h$ (degrees) | Hang-off $\theta_h$ (degrees) | Total maximum error (degrees) |
|---|---|---|---|
| 1.0 | 0.007 | 0.03 | 0.037 |
| 2.5 | 0.019 | 0.03 | 0.049 |
| 5.0 | 0.034 | 0.03 | 0.064 |
| 10.0 | 0.085 | 0.03 | 0.12 |

This page intentionally left blank

## SECTION IV - ENVIRONMENTAL SYSTEM ANALYSIS

### 1. THERMAL EVALUATION

#### a. General

Thermal studies were conducted to determine the requirements for adequate environmental protection to the electronic equipment associated with the KP-II radar system. Analyses were also made to evaluate the adequacy of the equipment to meet these requirements.

The studies and analyses included a review of the basic thermal design philosophy, investigation of ascent heating conditions, orbital temperature studies, and a study of the thermal characteristics of the equipment during orbital operation. In addition, cooling requirements for ground operation of the equipment were investigated.

Unit design was based upon the requirements of satisfactory operation for three successive orbit duty cycles and a five-minute on-period per orbit with the environmental conditions specified below. These temperatures are average temperatures which are applicable to the vehicle skin with which the units exchange thermal energy during orbit.

| | Temperature range (F) | Pressure range (mm Hg) |
|---|---|---|
| Units (other than Recorder) | 0-100 | $10^{-1}$ to $10^{-8}$ |
| Recorder | 32-130 | $10^{-1}$ to $10^{-8}$ |

#### b. Thermal Design Philosophy

The KP-II radar system is adapted from the AN/UPQ-102 (RF-4C) Doppler Radar which uses internal forced air cooling. Use of forced air or similar active cooling systems in the KP-II system was not considered feasible. Thermal control of electronic equipment in space is most efficiently accomplished by passive means. The thermal design of the KP-II system was therefore based upon radiation thermal interchange which is the primary available mode of passive heat transfer. Thermal control of the various units occurs by radiation to the vehicle skin. Components within the various units experience thermal interchange with the unit walls and structure by radiation and conduction.

Space stable thermal coatings having desirable emittance characteristics are used on the equipment to obtain maximum thermal interchange. To assure high emissivities, black paint or black anodizing is used on the units which comprise the system. Black paints are used where anodizing is not possible or practical. Care has been taken in selecting paints which, by decomposition while in space, will not create a pressure environment in the equipment or vehicle. It should be noted that proper thermal treatment of the vehicle skin is also required for maximum thermal interchange between the system units and the vehicle. Thermal analyses presented herein presuppose such vehicle thermal coating.

The electronic equipment experiences transient heating and cooling conditions, with the maximum and minimum temperatures depending upon the particular orbit geometry, inasmuch as thermal control of the electronic gear is dependent upon thermal radiation interchange with the vehicle skin. The addition of thermal masses or heat sinks to temperature-critical components generally tends to stabilize these transient temperatures. Heat sinks are used in the equipment where local heating conditions, or particularly temperature-sensitive components indicate the necessity. Foils and highly conductive silicon grease are used extensively to reduce thermal contact resistance in these applications.

c. Method of Analysis

(1) Radiation

Thermal analysis in many cases was based solely upon radiation thermal interchange (either to a unit case or to the vehicle skin).

The following expression for radiation thermal balance was used:

$$Q = \sigma E_c F_c A_c (T_c^{\,4} - T_s^{\,4}) + (WC_p)_c \frac{dT_c}{d\theta} \tag{64}$$

where

$Q$ = heat dissipation (Btu/hr)

$\sigma$ = Stefan-Boltzmann constant
(0.1714 × $10^{-8}$ Btu/hr ft$^2$ degrees R$^4$)

$E_c$* = emittance

$F_c$ = radiation view factor

$A_c$ = radiating area (ft$^2$)

$W$ = weight (lb)

$C_p$ = specific heat (Btu/lb degrees R)

$\theta$ = time (hr)

$T_c$ temperature of component - emitting (degrees R)

$T_s$ = temperature of component - absorbing (degrees R).

For the steady state, Q can be expressed as:

$$Q = \sigma E_c F_c A_c (T_\infty^{\,4} - T_s^{\,4}) \quad . \tag{65}$$

Where $T_\infty$ is the steady-state component temperature, Equations (64) and (65) combine to form:

$$\sigma E_c F_c A_c (T_\infty^{\,4} - T_s^{\,4}) = \sigma E_c F_c A_c (T_c^{\,4} - T_s^{\,4}) + (WC_p)_c \frac{dT_c}{d\theta} \quad . \tag{66}$$

*Subscript "c" denotes properties of the component under study.

The variables $T_c$ and $\theta$ can be readily separated and for a differential time interval, $d\theta$, Equation (66) becomes:

$$\frac{dT_c}{(T_\infty^4 - T_c^4)} = \frac{\sigma E_c F_c A_c}{(WC_p)_c} d\theta \quad . \tag{67}$$

With an initial component temperature $T_o$ and a temperature at time $\theta$ of $T_c$ as limits, integration of Equation (67) yields:

$$f\left(\frac{T_c}{T_\infty}\right) = f\left(\frac{T_o}{T_\infty}\right) + \frac{4 E_c F_c A_c \sigma T_\infty^3 \theta}{(WC_p)_c} \tag{68}$$

where

$$f\left(\frac{T_c}{T_\infty}\right) = 2 \tan^{-1} \left(\frac{T_c}{T_\infty}\right) - \ln \pm \left[\frac{(T_c/T_\infty) - 1}{(T_c/T_\infty) + 1}\right] \quad . \tag{69}$$

It is noted that, for analytical purposes, heating is assumed to occur for a five-minute period and cooling to occur for 85 minutes during each orbital cycle. For repetitive cycles the component temperatures, therefore, vary between $T_{c1}$ and $T_{c2}$ at the beginning and end of the operate period, respectively.

Equation (69) can then be written as:

For Heating - ($\theta$ = 1/12 hr)

$$f\left(\frac{T_{c2}}{T_\infty}\right) = f\left(\frac{T_{c1}}{T_\infty}\right) + \frac{4 E_c F_c A_c \sigma T_\infty^3 \theta}{(WC_p)_c} \quad . \tag{70}$$

For Cooling - ($\theta$ = 85/60 hr)

$$f\left(\frac{T_{c1}}{T_\infty}\right) = f\left(\frac{T_{c2}}{T_\infty}\right) + \frac{4 E_c F_c A_c \sigma T_\infty^3 \theta}{(WC_p)_c} \quad . \tag{71}$$

It should be noted the $T_\infty$ is not the same for heating and cooling. For heating, $T_\infty$ is equal to the steady-state component temperature found in Equation (65). For cooling, $T_\infty$ is essentially the skin temperature $T_s$. The radiation parameter $f(\frac{T_c}{T_\infty})$ for both cooling and heating is plotted in Figure 12. Temperatures $T_{c1}$ and $T_{c2}$ are found by solving Equations (70) and (71) simultaneously.

(2) Conduction

Maximum temperatures of components mounted on large radiating heat sinks were found by assuming that all heat dissipation was conducted directly into the sink and from there radiated to an absorbing skin (vehicle or case). The sink temperature was then calculated by the method outlined above. The temperature difference between the component and the radiator was found from:

$$Q = U_{c-r} (T_c - T_r) \tag{72}$$

where $U_{c-r}$ is the surface conductance (in Btu/hr degrees R) between the components and the radiator.

In other cases the maximum component temperature was obtained by assuming that all heat dissipated during the five-minute operating cycle was fully absorbed by the component thermal mass. This approach was used where the component had a fairly large mounting area and where the thermal contact resistance between the component and the radiating heat sink or mounting plate was small. Under these conditions, the component temperature at the start of the operating cycle is essentially the sink temperature. Since the heat sink or base temperature can be found by considering the radiation thermal balance, a conservative value for maximum component temperature ($T_{c2}$) can then be found from:

$$Q_c\theta = (WC_p)_c \; (T_{c2} - T_{c1}) \; . \tag{73}$$

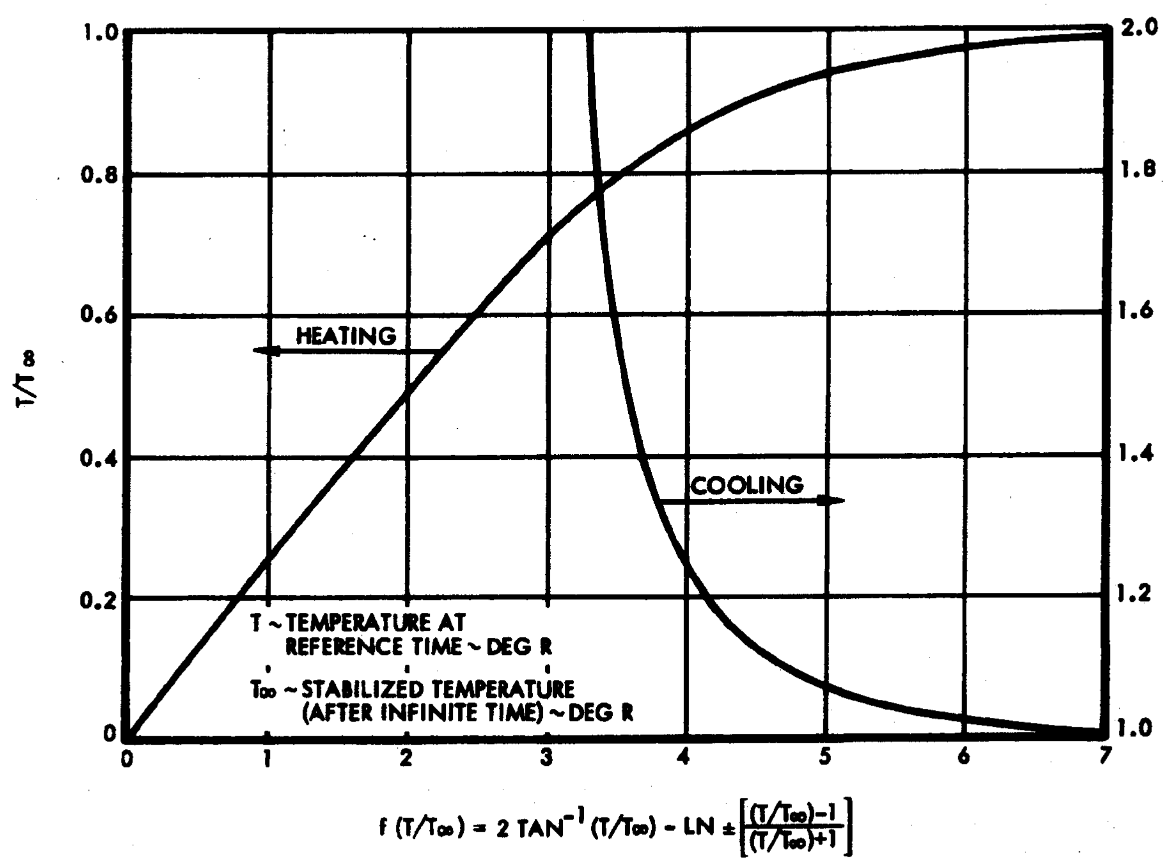


Figure 12 - Radiation Parameter

where $T_{c1}$ is the component (and heat sink) temperature at the start of the operating cycle.

(3) Special Considerations - Board Temperatures

Thermal characteristics of printed circuit boards used in the KP-II radar equipment were analyzed by considering radiation thermal interchange. The temperature difference between the board and the surrounding ambient (unit average temperature) was found for a particular board heat density by considering the following thermal relationship:

$$Q' = 2E_b F_{b-a} \sigma\left[(T_b + 460)^4 - (T_a + 460)^4\right] + (WC_p)' \frac{dT_b}{d\theta} \qquad (74)$$

where

$Q'$ = board heat density (Btu/hr ft$^2$)

$E_b$ = board emittance

$F_{b-a}$ = view factor

$T_b$ = board temperature (degrees F)

$T_a$ = ambient temperature (degrees F)

$(WC_p)'$ = board thermal capacity (Btu/ft$^2$ degrees F).

The above expression can be simplified by defining a radiant-heat transfer coefficient $\bar{h}_r$ (Btu/hr ft$^2$ degrees F) as:

$$\bar{h}_r = \sigma\left[(T_b + 460)^2 + (T_a + 460)^2\right]\left[(T_b + 460) + (T_a + 460)\right] . \qquad (75)$$

Equation (74) then becomes:

$$Q' = 2E_b F_{b-a} \bar{h}_r (T_b - T_a) + (WC_p)' \frac{dT_b}{d\theta} . \qquad (76)$$

Should fluctuations of $T_b$ be reasonably small, in the order of 50 degrees F or less, $\bar{h}_r$ may be treated as a constant 1.50 Btu/hr ft$^2$-degrees F. $T_a$ can also be presumed constant for simplicity.

The steady-state form of Equation (76) yields an expression for Q':

$$Q' = 2E_b F_{b-a} \bar{h}_r (T_{b\infty} - T_a) \tag{77}$$

where $T_{b\infty}$ is the steady state board temperature. Substitution for Q' in Equation (76) results in:

$$2E_b F_{b-a} \bar{h}_r (T_{b\infty} - T_b) = (WC_p)' \frac{dT_b}{d\theta} . \tag{78}$$

Integration of Equation (78) yields:

$$\frac{T_{b\infty} - T_b}{T_{b\infty} - T_{bo}} = \exp \left( - \frac{2E_b F_{b-a} \bar{h}_r}{(WC_p)'} \right) \theta \tag{79}$$

where $T_{bo}$ = board temperature at $\theta = 0$.

For repetitive orbital cycles the board temperature fluctuates between $T_{b1}$ and $T_{b2}$. During temperature decay, $T_{b\infty} = T_a$ so that Equation (79) reduces to:

$$\frac{T_a - T_{b1}}{T_a - T_{b2}} = \frac{T_{b1} - T_a}{T_{b2} - T_a} = \exp \left( - \frac{2E_b F_{b-a} \bar{h}_r}{(WC_p)'} \right) \theta \tag{80}$$

For temperature rise ($\theta$ = 1/12 hr) the corresponding expression is:

$$\frac{T_{b\infty} - T_{b2}}{T_{b\infty} - T_{b1}} = \exp\left(-\frac{2E_b F_{b-a} \bar{h}_r}{(WC_p)'}\right)\theta \qquad (81)$$

Temperatures $T_{b1}$ and $T_{b2}$ and found by simultaneous solution of Equations (80) and (81).

## d. Ascent Heating Conditions

Aerodynamic heating data on the Agena vehicle payload and forward rack skin areas were furnished by LMSC. The maximum average temperatures on the windward side during a yaw maneuver, occurring approximately 120 seconds after lift-off, were estimated to be 540 degrees F and 480 degrees F, respectively. Maximum average temperature given for the leeward side were 375 degrees F and 320 degrees F, respectively. An average of the windward and leeward temperatures was used for the analysis.

Ascent heating of system components occurs primarily by radiation from the vehicle skin. A heat balance indicating the radiation thermal interchange between the vehicle skin and a system component can then be written as:

$$\sigma E_e F_{c-s} A_c T_s^4 = \sigma E_e F_{c-s} A_c T_c^4 + (WC_p)_c \frac{dT_c}{d\theta} . \qquad (82)$$

Solution of the above expression by the method previously outlined (refer to paragraph c. preceding) results in maximum average payload ascent temperatures.

The average temperature of the Recorder unit (housed within the vehicle conical section) was found by conservatively assuming an ascent heating period of five minutes and a vehicle skin emittance of 0.9 at 460 degrees F. Assuming an initial temperature of 60 degrees F (520 degrees R) based on precooling during countdown, the integral form of Equation (82) becomes:

$$f\left(\frac{T_c}{T_s}\right) = f\left(\frac{T_{co}}{T_s}\right) + \frac{4\, E_e F_{c-s} A_c (T_s)^3 \theta}{(WC_p)_c} \tag{83}$$

where

$T_{co}$ = 520 degrees R

$T_s$ = 920 degrees R

$E_e$ = 0.9

$F_{c-s}$ = 0.9

$A_c$ = 13.5 ft$^2$

$(WC_p)_c$ = 19.4 Btu/degrees R .

Solution of Equation (83) using the radiation parameter method results in a maximum Recorder average temperature ($T_c$) of 110 degrees during ascent.

A similar solution to determine the maximum average temperatures of those units housed within the forward rack section with a 400 degrees F skin temperature indicates the unit average temperatures will reach 100 degrees F from an initial temperature of 60 degrees F.

The analysis indicates precooling the system components will provide an adequate margin for component temperature rise during ascent.

e. Equipment Thermal Analysis - Orbital Operation

Detailed thermal analyses were conducted on each unit comprising the radar system to determine the unit thermal characteristics while operating in a space environment. Studies were also made on component parts and individual electronic modules to determine heating and cooling response in a vacuum. Experimental investigations of techniques to enhance thermal interchange were also made.

Results of the analyses conducted on the various units are presented in Tables V through IX. Maximum predicted orbital temperatures are given for high heat dissipating or temperature sensitive components. Unit average temperatures are also given.

Results of the analyses and investigations indicate that in every instance the thermal design of the equipment is more than adequate to assure proper temperature control of all system components while operating in an orbiting vehicle. In each case maximum expected component temperatures have been shown to be below acceptable specification limits. Furthermore, it should be noted that temperatures given in the individual analyses are generally conservative and are based, for the most part, on an average vehicle skin temperature of 100 degrees F (Recorder analyses were based on an average vehicle skin temperature of 130 degrees F). Results of the computer analyses conducted on the Agena vehicle skin by the LMSC indicate that the average vehicle skin temperature will be considerably cooler than 100 degrees F. Maximum skin temperatures in the conical and barrel sections of the vehicle were found to be 80 degrees F and 73 degrees F, respectively. Minimum temperatures were 67 degrees F and 39 degrees F. Expected component temperatures can thus be reduced accordingly.

The analyses were based upon operation during each consecutive orbit. Actual duty conditions will not be this severe. Operation will not be required for more than three consecutive orbits. In view of this fact an additional margin of safety is indicated.

Results of the LMSC computer analysis further indicate no thermal problems should be anticipated at the low temperatures encountered during the orbital cycles. Minimum vehicle skin temperatures and unit temperatures are sufficiently warm for reliable operation of all components used within the KP-II radar system.

TABLE V - SUMMARY OF ANALYSES: TRANSMITTER-MODULATOR

| Telemetry signal number | Component | Calculated maximum orbital temperature (F) | Maximum allowable temperature limit (F) |
|---|---|---|---|
| F34 | Klystron collector | 452* | 572 |
| F35 | Klystron body | 240 | 250 |
| – | Klystron magnet | 150 | – |
| F36 | Unit case | 158 | – |
| – | Pulse-forming network | 164 | 185 |
| – | Charging choke | 165 | 185 |
| – | Heat sink for power resistor | 313 | – |
| – | Power resistors | 365 | 527 |
| F37 | Pulse transformer | 159 | 185 |
| – | Thyratron | 386 | 752 |

*See Figure 13

TABLE VI - SUMMARY OF ANALYSES: R-F/I-F UNIT

| Telemetry signal number | Component | Calculated maximum orbital temperature (F) | Maximum allowable temperature limit (F) |
|---|---|---|---|
| | Unit average temperature | 102 | – |
| F33 | Transmit-receive tube | 180 | 185 |
| F31 | Traveling wave tube | 135 | 185 |
| F32 | Frequency multiplier | 116 | 149 |

TABLE VI - SUMMARY OF ANALYSES: R-F/I-F UNIT (Continued)

| Telemetry signal number | Component | Calculated maximum orbital temperature (F) | Maximum allowable temperature limit (F) |
|---|---|---|---|
| – | High-voltage power supply | 137 | 185 |
| – | RE75 power resistors | 278 | 350 |
| – | Preamplifier vacuum tubes | 250 | 325 |

TABLE VII - SUMMARY OF ANALYSES: REFERENCE COMPUTER

| Telemetry signal number | Component | Calculated maximum orbital temperature (F) | Maximum allowable temperature limit (F) |
|---|---|---|---|
| F27 | Unit case | 110 | – |
| – | Printed circuit board (heat density - 20 watts/ft$^2$) | 123 | – |
| F22 | Video amplifier | 173 | 212 |
| F23 | Gate sequencer | 165 | 212 |

TABLE VIII - SUMMARY OF ANALYSES: CONTROL UNIT

| Telemetry signal number | Component | Calculated maximum orbital temperature (F) | Maximum allowable temperature limit (F) |
|---|---|---|---|
| F20 | Power supply | 165 | – |
| – | Power transistors | 248 | 257 |
| – | Transformer (-23.5 vdc) | 141 | 185 |
| F21 | Unit case | 130 | – |

TABLE IX - SUMMARY OF ANALYSES: RECORDER UNIT

| Telemetry signal number | Component | Calculated maximum orbital temperature (F) | Maximum allowable temperature limit (F) |
|---|---|---|---|
| F30 | Unit case | 134 | – |
| F28 | Deflection amplifier | 175 | – |
| – | (Heat sink) | 175 | – |
| – | (Power transistors) | 243 | 257 |
| F29 | High-voltage power supply | 145 | 185 |
| – | Drive motors | 205 | 300 |

### f. Ground Operation

Thermal design of the units comprising the KP-II radar system is based upon operational cycling in a space environment with a comparatively short duty period per cycle. Thermal conditions encountered during ground operation or bench testing for periods which exceed the normal space duty cycle must therefore be considered.

Analytical studies have been conducted to determine the time period that each of the KP-II system units can be operated during testing or other ground operations without exceeding the component design temperature limits. The analyses were based upon operation at full design power levels in the "buttoned-up" condition. Heat transfer was assumed to be accomplished by radiation and by free or forced-air cooling. The analyses showed that the Recorder, Reference Computer, Control and R-F/I-F units could be operated continuously in a laboratory environment using only natural radiation and free-convection cooling, without exceeding temperature design limits.

Analysis of thermal conditions encountered during ground operation of the Transmitter-Modulator unit indicates, however, that radiation and

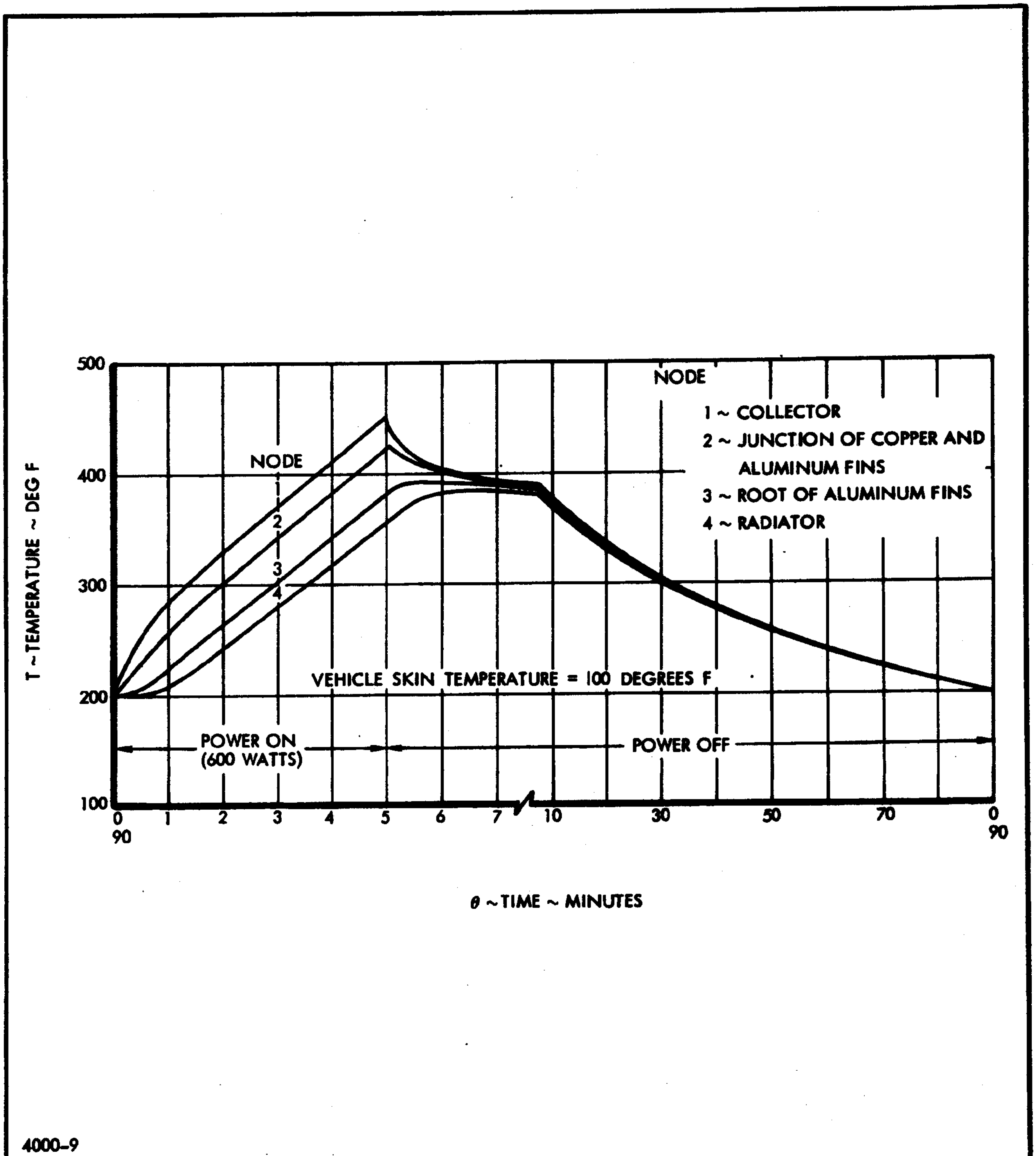


Figure 13 - Klystron Collector and Heat Sink Temperatures versus Time

free-convection heat transfer is not adequate to maintain critical component temperatures below design limits. Studies have shown that the klystron tube and several pulse components will exceed acceptable temperature limits if operated continuously without additional cooling protection.

As a result of the analytical studies, a duplex squirrel cage blower has been added as a part of the unit test apparatus. Forced-air cooling is therefore provided for the klystron and pulse components. A side cover on the unit is removed for cooling access to the pulse components.

Furthermore, analyses have shown that cooling air supplied to the vehicle on the launch pad (40 to 60 degree F air temperature) is adequate to maintain the equipment to an acceptable temperature level while operating.

## 2. STRESS ANALYSIS

### a. General

A comprehensive stress analysis of each unit comprising the KP-II radar system was conducted as a part of the mechanical design effort. Studies were performed to determine the adequacy of the equipment design to withstand the various service conditions.

Each unit was analyzed for structural integrity, static and dynamic load characteristics, load paths, adequacy of unit mounting methods, and weight-strength optimization. Dip-brazed structures and castings were given special consideration to assure compliance with stress design criteria. Methods of attachment of components with large concentrated masses were also investigated.

### b. Stress Design Criteria

Stress analysis of the individual units was based upon sustained loading of 20 and 30 g's, the latter being used in analyses of unit mountings. Both strength and stiffness of structural members were considered. Material properties were obtained from MIL-HDBK-5: Metallic Materials and Elements for Flight Vehicle Structures. Design fitting and safety factors were taken as 1.15 and 1.25, respectively.

Studies were made to determine the adequacy of the structure to resist loads without fracturing or incurring excessive deformation leading to permanent distortion of the members. Additionally, the natural frequency of load carrying members was examined. Structural stiffness was added where the natural frequency was too low. It was the design intent to keep the unit resonance frequency as high as possible within weight and size limitations. A third stress design criterion was required in certain instances where only minimal deformations could be tolerated. In these cases, it was necessary to analyze and design structural members for minimum elastic deformation.

Special yield point considerations were made on analysis of welded structures. The shear strength of "as welded" aluminum sheet and extrusions was reduced (as per MIL-HDBK-5) where heat treatment after welding was not feasible. Yield strengths of dip-brazed structures were also reduced accordingly. Dip-brazed structures were examined carefully for load characteristics. Dip-brazed joints were noted to satisfactorily support loads in compression and shear but not in tension or peel.

c. Method of Analysis

The detailed stress study of each unit consisted of the following checks and analyses:

1. Determination of unit weight and center of gravity
2. Examination of basic unit structure
3. Determination of load resisting stresses in load carrying members for comparison with yield stress limits
4. Determination of primary load paths
5. Determination of deflections and resonant frequencies of structural members
6. Analysis of mounting pad stresses and attach methods.

Other possible problem areas peculiar to particular units were additionally analyzed.

Discussions of the analytical studies and summary results for the individual units comprising the KP-II radar equipment are presented in the following paragraphs.

d. Transmitter Unit

The Transmitter unit structure consists of a welded tubular frame with welded aluminum sheet panels. The unit has a 1/4-inch thick base plate. The unit weighs (without mounting cradle) approximately 120 pounds and is mounted in the plane of the center of gravity. Large removable side and top skins are used as shear panels to transmit load and to assist the corner posts in transferring loads to the mount points.

Stress studies were conducted on the following parts of this unit:

1. Basic Unit Structure. Stress analysis of basic load paths indicated more than adequate strength for the service conditions.

2. Unit Base Plate. Design of this member was based upon thermal requirements and represents an overdesign from stress considerations. Deflection analysis showed no excessive deformation of the base plate.

3. Klystron Mounting. No stress or load distribution problems were found to exist as a result of klystron mounting techniques. Calculated stresses were far below yield limits.

4. Upper Component Support Deck. Analysis indicates that the design of this sheet metal member is more than adequate; maximum bending stresses of 4000 psi result from component loading. A resonant frequency of approximately 150 cps was found.

Additional stress studies were conducted on the cradle assembly which is used to enable center of gravity mounting of the Transmitter. The cradle is a welded aluminum assembly weighing approximately 15 pounds. The cradle consists of 1-1/2-inch square aluminum tubing and 1/8-inch to 3/16-inch thick aluminum sheet and structural shapes. Design of the cradle was predicated on vibration stiffness requirements (i.e., a high natural frequency) and thus dynamic load induced stresses are well within acceptable limits.

e. R-F/I-F Unit

Stress analysis of the R-F/I-F unit was concentrated in the areas of the mounting pads and the primary unit structure. This structure was fabricated by dip brazing. Care was taken to provide shear and compression loading because of the inherent weakness of dip-brazed structures to carry load in tension. Removable skins were used as structural shear panels to transmit load to the mounting points. Calculation of shear buckling strength of these panels showed them to be capable of carrying all of the load. Calculations of the basic extruded structure strength indicated that all loads can be carried without shear panels. It is thus evident that the resulting stress design is more than adequate. Furthermore, the design offers sufficient stiffness for a suitable unit resonant frequency.

f. Reference Computer Unit

Stress analysis of the Reference Computer unit consisted primarily of shear flow studies on structural sections and examination of mounting techniques. The unit chassis was fabricated from 6061-T4 aluminum sheet by spot welding and riveting. It was felt that the riveted structure would offer some vibration control by interface shear damping (damping by Coulomb friction). Studies indicate more than adequate structural strength for service conditions.

g. Control Unit

Detailed stress analysis of the Control unit was not required because the design was predicated on thermal requirements. These requirements resulted in an over-design from strength considerations. Thermal requirements necessitated the use of 0.250-inch and 0.190-inch thick aluminum sheet (6061-T4) to obtain a large thermal mass. The box was fabricated by dip brazing. A survey of the design indicated more than adequate structural strength.

h. Recorder Unit

Weight and vibration requirements imposed upon the KP-II Recorder unit necessitated the use of a magnesium casting for the primary unit structure. A cast magnesium structure was selected because of its high internal damping characteristics. Magnesium alloy AZ91C-T6, with a yield strength of 16,000 psi and an ultimate strength of 34,000 psi, was specified. The L-shaped casting was designed as a box beam with 1/8-inch thick walls. The box section was developed to obtain large moments of inertia (I) in each transverse direction. Covers on the casting were made structural members and shear fasteners were used to help transmit loads. Vehicle support structure made it necessary to use four mounting points which were unsymmetrical with respect to the unit center of gravity. Three mounting points were on the knee end of the Recorder. The Recorder was supported on these points. A fourth point was utilized on the opposite end of the Recorder. This point was used to stabilize the Recorder and to eliminate the cantilever effect about the fixed knee-end supports.

The Recorder casting was analyzed considering distributed and concentrated loads totaling 110 pounds. The beam was considered fixed at the knee-end and simply supported at the single support end for the analysis. Maximum stresses found were well within allowable limits.

Extensive stress studies were also conducted as part of the design effort on the film magazine. The magazine housing is a casting made of AZ91C-T6 magnesium. The magazine is supported from the Recorder unit by two hinge joints and a shear pin. Analysis of load paths and stress concentrations within the casting and mounting lugs indicated that the stress design was adequate to meet all service conditions.

Several other critical areas were given special consideration to assure adequate stress design: (1) Recorder supports; (2) structural cover plates; (3) film spool; (4) Recorder electronic compartment; (5) power supply mounting technique; and (6) magazine support lugs.

## 3. VIBRATION ANALYSIS

### a. General

As part of the design effort, vibration studies were conducted on each unit comprising the KP-II radar equipment. These studies were performed to determine the adequacy of the equipment to meet the vibration and sustained acceleration levels encountered during ascent and orbital conditions. In general, the analysis was based upon the short duration, high-level vibration which is normally encountered during the ascent conditions. It should be noted that vibration levels encountered while in orbit are nearly negligible and are of little concern. Design of the units was based upon the acceleration and vibration requirements summarized in Table X and XI.

### b. Design Philosophy

The vibration design philosophy called for design of fairly rigid unit structures with minimum amplification of vibration input at resonance. Units were designed for a natural frequency above 100 cps. Primary structure was utilized for placement of components whenever possible. In cases where components could not be mounted on primary structure, the secondary support members were made as rigid as possible and were securely tied into the main unit structure. This was done in an attempt to maintain amplification of vibration through the support structure to a minimum. Because of the relatively high primary vibration input during the ascent condition, a large amplification factor from mount input to an individual component could not be tolerated.

TABLE X - VIBRATION AND ACCELERATION LEVELS

| Axis | Unit weight (lb) | Vibration Input | | Acceleration |
|---|---|---|---|---|
| | | Frequency range (cps) | Amplitude* | |
| Longitudinal (x-x) | Below 75 | 5-14<br>14-400<br>400-2000 | 0.5 inch DA<br>5 g<br>7.5 g | 15 g |
| Normal (z-z) Transverse (y-y) | Below 75 | 5-10<br>10-200<br>200-400<br>400-2000 | 0.5 inch DA<br>3 g<br>5 g<br>7.5 g | 2.5 g |
| Longitudinal (x-x) | Between 75-250 | $5-f_1$**<br>$f_1-400$<br>400-2000 | 0.5 inch DA<br>$g_1$<br>$g_2$ | 15 g |
| Normal (z-z) Transverse (y-x) | Between 75-250 | 5-10<br>10-200<br>200-400<br>400-2000 | 0.5 inch DA<br>3 g<br>$g_3$<br>$g_4$ | 2.5 g |

*g = zero-to-peak acceleration

DA = peak-to-peak amplitude

$g_1 = 32(W)^{-0.43}$

$g_2 = 48(W)^{-0.43}$

$g_3 = 143(W)^{-0.776}$

$g_4 = 214(W)^{-0.776}$

where

W = weight of units in pounds

$g_1, g_2, g_3, g_4$ = g units

** $f_1 = (39.2 g_1)^{0.5}$

TABLE XI - RANDOM VIBRATION REQUIREMENTS

| Frequency range (cps) | Random density (g2/cps) | Rms acceleration (g) |
|---|---|---|
| 30-400 | 0.05 | 4.4 |
| 400-2000 | 0.12 | 13.9 |

c. Method of Analysis

Each unit was analyzed to determine forced vibration characteristics under both sinusoidal and random inputs as well as sustained acceleration. Because of the complexity of the KP-II radar equipment, purely analytical procedures were inadequate for exact determination of resonant frequencies and modes of vibration. The complicated structures, various load distributions, degree of damping present, and the undetermined properties of materials under strain introduce relationships and variables which cannot be accurately expressed in mathematical terms. Accordingly, the complex multiple-degree-of-freedom systems involved in this equipment were broken up into simplified models for analysis. Furthermore, the analytical vibration studies were restricted to major structural members and important component-supporting secondary structures.

To supplement these analytical studies, extensive testing was conducted on prototype and structural mockups of the various KP-II units. Mockups were used which simulated the weight, configuration, and load distribution characteristics of the proposed units.

These tests made possible more accurate determination of response characteristics of the units. Input to specific components was measured over the entire frequency spectrum from 5 to 2000 cps, thus giving a more realistic basis for specification of component vibration requirements.

d. Development Testing: Recorder Unit

Tests conducted on the Recorder unit indicated satisfactory vibration response in nearly every instance. The Recorder structure - a magnesium casting - offered a high degree of internal damping and maintained amplification factors through the structure to an acceptable level. Therefore, input to most components was within limitations of the component specifications. A vibration problem was experienced, however, with the cathode ray tube. This critical component could not withstand the acceleration levels experienced at box resonance.

Testing and inspection of the tube showed severe electron gun damage under vibration. Analysis of the tube vibration characteristics indicated that excessive vibration amplification was occurring within the tube shield and deflection yoke assembly. Design improvements were incorporated to strengthen the electron gun structure and to reduce vibration amplification within the tube shield and yoke assembly.

Additional tests verified the effectiveness of these design modifications and the adequacy of the Recorder unit design to meet vibration requirements.

e. Development Testing: Other Units

Initial tests on the Transmitter, R-F/I-F, Reference Computer, and Control units indicated that vibration amplification factors (Q) encountered with these units at their respective resonances was excessive. Resulting acceleration levels and component inputs were beyond the capability of some components. In many other instances the possibility of a decrease in component reliability was suggested by the resonant acceleration levels. It was necessary, therefore, to reduce these resonant effects.

Re-examination of the unit designs indicated that, without extreme weight penalties, little could be done to decrease amplification of vibration through the structure. Many of the vibration critical components were state-of-the-art devices and could not be modified to withstand the extreme environment. In view of these circumstances, it was deemed necessary to reduce the primary vibration input during unit resonances. This was accomplished by use of vibration isolators.

### f. Isolator Design

(1) General

Selection of appropriate isolation devices was based upon the following considerations:

1. Large vibration displacement at low frequencies
2. Base mounted units
3. Unit natural frequency as low as 100 cps
4. Unit center of gravity above mounting plane
5. Minimum sway space
6. Minimum isolator size
7. Low isolator transmissibility.

It was necessary to select an isolator with a natural frequency $fn_i$ so that:

$$fn_i < \frac{1}{\sqrt{2}} fn_u \quad (84)$$

where $fn_u$ is the unit resonant frequency. This resulted in a transmissibility of less than one ($Q<1$) at unit resonance. Furthermore, it was necessary that $fn_i$ be in a range where the input vibration displacement was small. This requirement was necessary to assure against bottoming or destruction of the elastic element since the transmissibility was between 2.5 and 5.0 at mount resonance.

It is noted that displacement for a particular acceleration level decreases with the square of the frequency, as shown in the following relationship:

$$D = \frac{19.6\,g}{f^2} \quad (85)$$

where

$D$ = double amplitude displacement in inches

$f$ = frequency in cps

$g$ = linear acceleration (g units).

It is thus evident that $fu_1$ should be as high as possible to satisfy the minimum displacement requirement.

The displacement and transmissibility design criteria were satisfied by selection of mounts with $fn_1$ between 45 and 80 cps.

(2) Reference Computer and Control Units

The Reference Computer and Control units were isolated by the addition of compression-type center bonded mountings (Lord type J-9534-1) to the base mounting pads. These are broad temperature range (BTR) silicon rubber isolators with high stiffness characteristics. Isolator stiffness was selected so that the natural frequency of the isolation system was 60 cps and 75 cps for the Reference Computer and Control units, respectively.

The isolators were located symmetrically around the unit center of gravity but below the plane of the center of gravity. This approach resulted in a six-degree-of-freedom system with coupled modes in the longitudinal and lateral planes for each box.

Effects of the coupled modes, however, were reduced by the stiffness of the resilient supports and no particular problems were encountered as a result of the base mounting technique. Testing of structural mockups indicated adequate vibration control over the entire frequency spectrum.

(3) Transmitter and R-F/I-F Units

Application of the base mount isolation technique was not possible with the Transmitter and R-F/I-F units because of unit weight and configuration and isolator size restrictions. Accordingly, center of gravity mounting systems employing HT2 series Lord BTR elastromeric mounts were selected for these units.

The BTR HT2 series of elastomeric mounts have approximately equal spring rates in all directions, assuring all-attitude protection for equipment. Transmissibility at resonance is 4.0 or less and varies little with temperature or loading. Isolator stiffness was selected so that the natural frequency of the isolation system was 50 cps and 65 cps for the Transmitter and R-F/I-F units, respectively.

The Transmitter unit was mounted on four HT2914-100 Lord elastomeric mounts located symmetrically with respect to the center of gravity of the unit. This resulted in a six-degree-of-freedom system with no coupled modes.

Because of the vehicle structural configuration the center of gravity mounting technique required use of an an adaptive mounting cradle. The cradle was designed to have a natural frequency of 350 cps. It was felt that amplification of primary vehicle input at this frequency would be negated by low isolator transmissibility.

Isolation of the R-F/I-F unit was accomplished by use of six HT2-50 Lord BTR elastomeric mounts located in a bottom-side diagonal configuration. Mounts were located symmetrically with respect to the center of gravity of the R-F/I-F unit. This resulted in a six-degree-of-freedom system.

Development tests conducted on the Transmitter and R-F/I-F unit indicate that the isolation systems specified for these units offer satisfactory vibration control over the entire frequency spectrum.

g. Effect of Sustained Acceleration on Isolation Systems

The effect of sustained acceleration on isolator performance was analyzed by examining isolator deflection characteristics under static load condition

An equivalent static load was assumed for the sustained acceleration and deflection and stiffness characteristics were determined by using component load-deflection curves. Under combined vibration and acceleration conditions the flexing element of the isolator will move about an equilibrium point, which is displaced from the normal rest point by an amount $\delta_s$ proportional to the sustained acceleration level.

Under the combined environment, the maximum isolator deflection $\delta_T$ is therefore the algebraic sum of the static deflection $\delta_s$ and the vibration displacement $\delta_v$. To prevent isolator damage, this deflection must be less than the maximum allowable element movement. These relationships can be expressed as

$$\delta_T = \delta_s + \delta_v \quad , \tag{86}$$

where $\delta_s$ is determined from the component load-deflection curves and $\delta_v$ is found from

$$\delta_v = \frac{9.8\,(Q)\,g}{f^2} \quad , \tag{87}$$

where Q is the isolator transmissibility at resonant frequency - f (cps) and g is the vibratory acceleration input in gravity units.

Analyses conducted on the various isolated units indicate that little change in isolation characteristics occurs as a result of exposure to the combined dynamic environment. Shift in resonant frequency of the isolators was insignificant because the spring rate is fairly linear for sustained acceleration up to 15 g's. Total deflection in each case was also well within allowable component limits.

## 4. SHOCK ANALYSIS

### a. General

A study of the effects of the shock environment was conducted on each unit of the KP-II radar equipment. This study was based upon the shock requirements listed in Table XII. The study consisted primarily of:

1. Determining the effect of isolation systems (used on the Transmitter-Modulator, R-F/I-F, Reference Computer, and Control units) on shock loading.
2. Determining the adequacy of the unit mountings to withstand exposure to the shock environment.

### b. Isolator Effectiveness

Isolators used on the Transmitter-Modulator, R-F/I-F, Reference Computer, and Control units are primarily required for vibration control. These devices, however, are also beneficial in reducing the effects of shock loads. The BTR elastomeric mountings have high energy storage capacity which cushions the shock loads gradually. Snubbing characteristics of the BTR mountings increase at an exponential rate and eliminate severe bottoming effects. For vibration control the isolators were selected for each unit so that their natural frequency ($fn_i$) was less than 70 percent of the unit resonant frequency ($fn_u$). In reality, the isolator natural frequency was found to be less than 50 percent of the unit natural frequency ($fn_i < 0.5\ fn_u$). In addition, the isolator damping ratio ($\zeta$ - ratio of damping to critical damping) was found to be much less than one. These factors result in shock transmissibility of less than unity. The isolated unit shock spectrum (response) is a complex decaying pulse attenuated by the isolator (and structure) damping.

TABLE XII - SHOCK REQUIREMENTS

| Unit weight (lb) | Axis | Shock level (Peak acceleration g's) | Pulse duration (milliseconds) |
|---|---|---|---|
| Less than 75 | All axes | 30 g | 8 |
| Between 75 and 250 | Longitudinal (x-x) | $A_1$ | 8 |
| | Normal (z-z) and transverse (y-y) | $A_2$ | 8 |

NOTE:

$A_1 = 184\ (W)^{-0.42}$
$A_2 = 83.2\ (W)^{-0.77}$
$W$ = Unit weight in pounds
Pulse shape to be half sine-wave

c. Adequacy of Mounting and Attach Structure

The mounting and attach structure and mounting hardware of each unit, including the hardmounted Recorder unit, was analyzed to determine stress levels of the various specified impact loads for comparison with yield limits. Units normally isolated were considered to be hard mounted for this analysis. Stress conditions under shock loading are complex and depend upon the material properties and the duration and pulse shape of applied load. In impact loading, the loaded member is required to absorb the kinetic energy of the impact. The energy is then stored as strain energy or dissipated as heat. The complexity of the mechanical systems involved and unknown damping characteristics make determination of dynamic stresses from strain information nearly impossible.

In view of these facts, unit stress characteristics were determined by using an equivalent static acceleration equal to the maximum dynamic acceleration. This approach is conservative in that damping and mechanical impedance was not considered. The dampening of the initial stress wave by elastic hysteresis in the structure, and the diminution of the intensity of the stress wave by the cushioning effect of the actually non-rigid moving body, serves to make the actual stress less than that found by equivalent static acceleration.

Results of the shock analyses indicate that the various units are fully capable of withstanding exposure to the shock environment. Shock induced stresses in mounting and attach structures were found to be below yield limits for all units. In addition, units mounted on isolators have a greater margin of safety because of shock attenuation through the isolators.

This page intentionally left blank.

## SECTION V - SYSTEM DESIGN DATA

### 1. MECHANICAL

#### a. General

The radar system components with the exception of the Recorder unit are located in the vehicle barrel or cylindrical section. The Recorder unit proper is installed in the vehicle conical section with the data take-up spool located in the vehicle nose cone.

#### b. Barrel Section

The vehicle barrel section is 5 feet in diameter with a 0.06-inch skin over structure rings spaced 15 inches apart. Flat surfaces constructed between the structure rings inside the barrel section are used for mounting the radar equipments. Radar units located in the barrel section are the Transmitter, R-F/I-F, Reference Computer, and Control units. The arrangement of the units in the barrel section is shown in Figure 14. The boxes are mounted to the barrel at four mounting points per unit except for the R-F/I-F unit. The R-F/I-F unit is mounted to the barrel at six locations. All mounting attachments are accessible through door openings and removable panels built into the barrel. Vibration isolators, flexible wave guide, and service loops on interconnecting cables are used to isolate the units from the vehicle vibration during ascent.

#### c. Conical Section

The vehicle conical section is forward of the barrel and attaches directly to the barrel section. The conical section is 5 feet in diameter at the base and 33 inches high with a 15-degree taper. The small end of the conical section is capped by a forward bulkhead. The Recorder unit is rigidly mounted to the conical section by three bolts at the small end and by four tubular webs at the base of the conical section. The unit is accessible through removable panels built into the conical section.

d. Nose Cone

Recorded raw data from the radar Recorder is stored in the nose cone for recovery. The nose cone is attached to the small end of the conical section and exposed film passes from the Recorder to the take-up spool through a chute connecting the nose cone with the conical section.

e. Weight and Volume Limitation

Weight and volume design-center values for the radar units are listed in Table XIII.

TABLE XIII - RADAR UNITS WEIGHT AND VOLUME

| Unit | Weight (lb) | Volume (cu ft) |
|---|---|---|
| Transmitter | 130 | 2.3 |
| RF-IF | 47 | 1.5 |
| Reference Computer | 46 | 1.2 |
| Recorder | 110 | 2.0 |
| Control | 37 | 0.5 |
| Totals | 370 | 7.5 |

The actual weight of the equipment flown was 348 pounds.

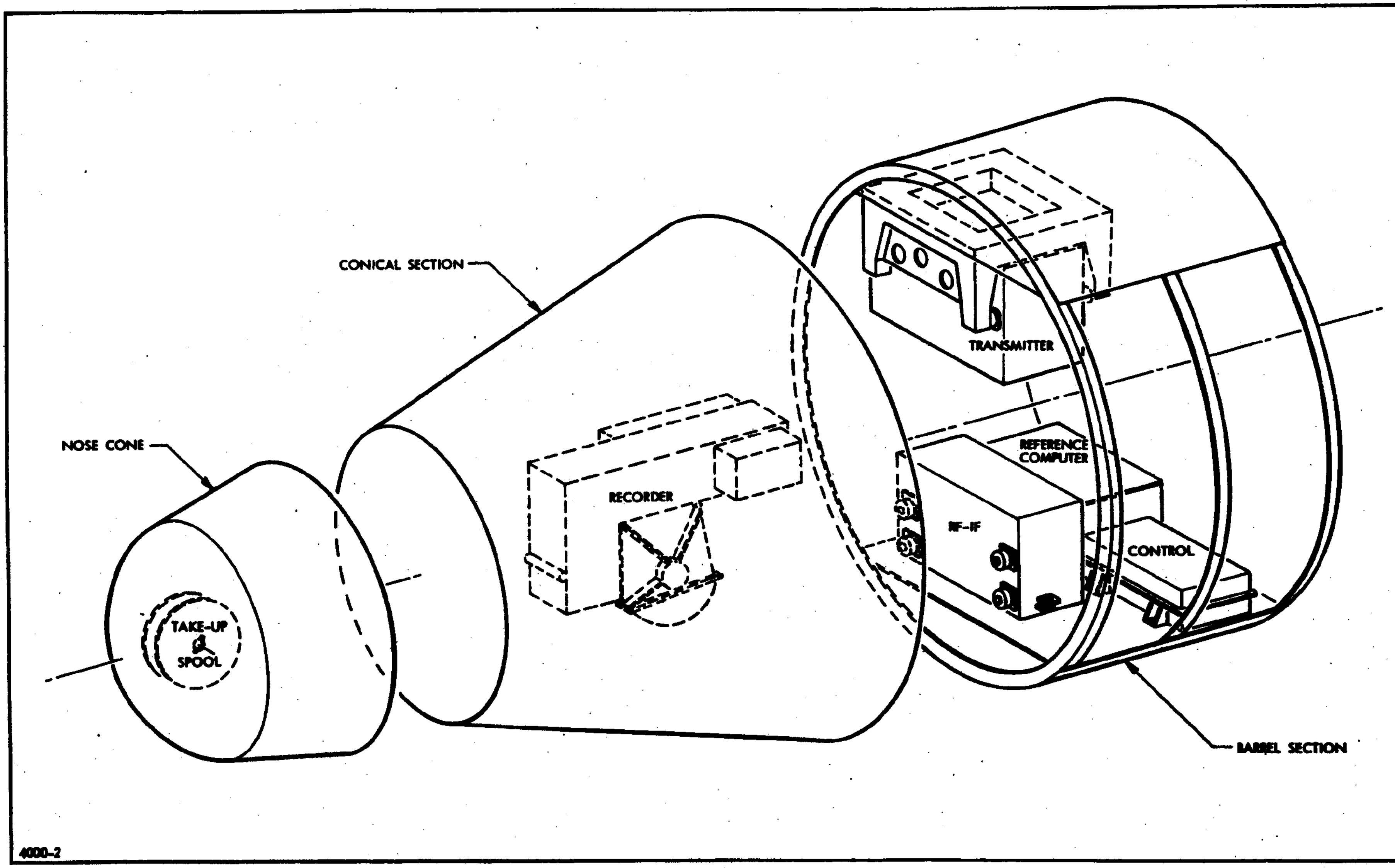


Figure 14 - KP-II Side-Looking Radar Installed in Forward Section of Agena Vehicle

This page intentionally left blank.

f. Modular Construction

Modular design and plug-in subassemblies are used wherever possible. Plug-in subassemblies and units are designed to be interchangeable. Modules and other subassemblies are designed for good thermal conduction to component structures.

2. ELECTRICAL

a. General

Radar units containing r-f and pulse circuits have their signal ground grounded to their respective unit cases. All primary power grounds are isolated from the unit cases. Power supplies are designed to provide electronic overload protection. A timer interlock is incorporated to ensure (1) proper warmup of the Transmitter unit before application of high voltage, and (2) all switching relays are used in a fail-safe mode. External unit connectors, other than coaxial connectors, are of the crimp bayonet coupling type and have a finish of gold iridite. These connectors conform to the requirements of Military Specification MIL-C-0026482A.

b. Electromagnetic Interference - Radio Frequency Interference

The radar equipment is designed to conform with Military Specification MIL-I-26600 requirements for electromagnetic and r-f types of interference. Good rfi design practices have been incorporated throughout the equipment to minimize EMI-RFI problems.

c. Power

Primary power required for the radar equipment is supplied by associated equipment in the vehicle. The required power is listed in Table XIV.

TABLE XIV - SYSTEM POWER REQUIREMENTS

| Voltage | Frequency | Power (watts) | | | |
|---|---|---|---|---|---|
| | | Off | Warm-up | Pre-operate | Operate |
| 115 ±2 percent ( 3-$\phi$) | 400 ±0.001 percent | 0 | 82 | 82 | 122 |
| 115 ±1 percent ( 1-$\phi$) | 2000 ±1 percent | 0 | 97 | 197 | 197 |
| 28.3 ±2 percent | DC | 5 | 5 | 215 | 215 |
| 4850 ±250 | DC | 0 | 0 | 0 | 2000 |
| Totals | | 5 | 184 | 494 | 2534 |

The power values in Table XIV are design-center values. The total load during operate was required to be within 2534 watts ±20 percent. Measurements on the equipment have shown the actual operate load to be about 2500 watts.

d. Duty Cycle

The radar system was designed for a total mission time of 80 minutes of intermittent operation extending over a 96-hour period. After a 5-minute warmup and a 30-second pre-operate period, the system is required to operate for a maximum of five minutes per orbit and for a maximum of three successive orbits.

# SECTION VI - SYSTEM FUNCTIONAL DESCRIPTION

## 1. BASIC RADAR SYSTEM

This section (1) discusses the basic KP-II radar system frequency and timing requirements, (2) examines the radar system block diagram in detail, and (3) reviews the radar system programming and control functions.

### a. Frequency Requirements

#### (1) Base Frequencies

Three basic frequencies are required to operate the system:

1. Transmitter carrier, $f_o$ = 9600 mc
2. Prf = 8215 to 8735 cps
3. I-f frequency = 70 mc.

Certain time functions or related frequencies must also be made available. These added requirements dictate the method of generating the three basic signals.

If the transmitter carrier $f_o$ is considered together with the fact that pulse-to-pulse phase coherence is required, it is apparent that the local oscillator which reduces the return signals to i-f must have known phase relationship to the transmitted signal. For this reason the local oscillator and transmitted signals are both derived from a single oscillator. A portion of the signal derived from this oscillator is offset in frequency for transmission.

#### (2) Frequency Requirements of Chirp

From practical considerations it is desirable that a single chirp network be used both for dispersing and recompressing the transmitted pulse. This choice eliminates the requirements for matched networks but creates the necessity of time sharing the chirp network and its associated amplifiers and compensating circuitry. It is further necessary that the spectrum of the signals to be recompressed be reversed with respect to the original dispersed spectrum.

Figure 15 shows the method of inverting the spectrum. In Figure 15(b) the carrier is first displaced by 140 mc to create $f_o + 140$. The spectrum to be transmitted is arranged about the i-f frequency as shown in Figure 15(a). This spectrum is then imposed on the $f_o + 140$ mc signal to give a carrier at $f_o + (140 - 70)$ which is the same as $f_o + 70$ mc. When the return signals are demodulated with respect to $f_o$, a 70-mc i-f carrier results whose side bands are reversed from Figure 15(a). This signal is then compressed by the identical network which dispersed the transmitted pulse.

(3) The Prf/4 Offset

In addition to the above strategem, it has been found desirable to generate maps with doppler frequencies around prf/4 instead of zero doppler. This choice yields an advantage in the correlation optics as well as in the required degree of transmitter-receiver leakage. It would be acceptable to further offset the carrier by prf/2 with a single side-band modulation causing the receiver i-f frequency to be 70 mc + prf/4. The same result may be accomplished by taking that portion of the 70-mc signal which is to generate the 140-mc offset and shifting its phase by 90 degrees each prf pulse. This signal multiplied by 2 then provides 140 mc + prf/2. When the transmitted signal is altered in this manner, returns from true zero doppler appear to have shifts of prf/4.

(4) Clutterlock Frequency

It is necessary to provide a means of bore-sighting the narrow synthetic antenna pattern generated by the final processing with the physical antenna pattern. The portion of the system which accomplishes this objective is referred to as the clutterlock loop (for a

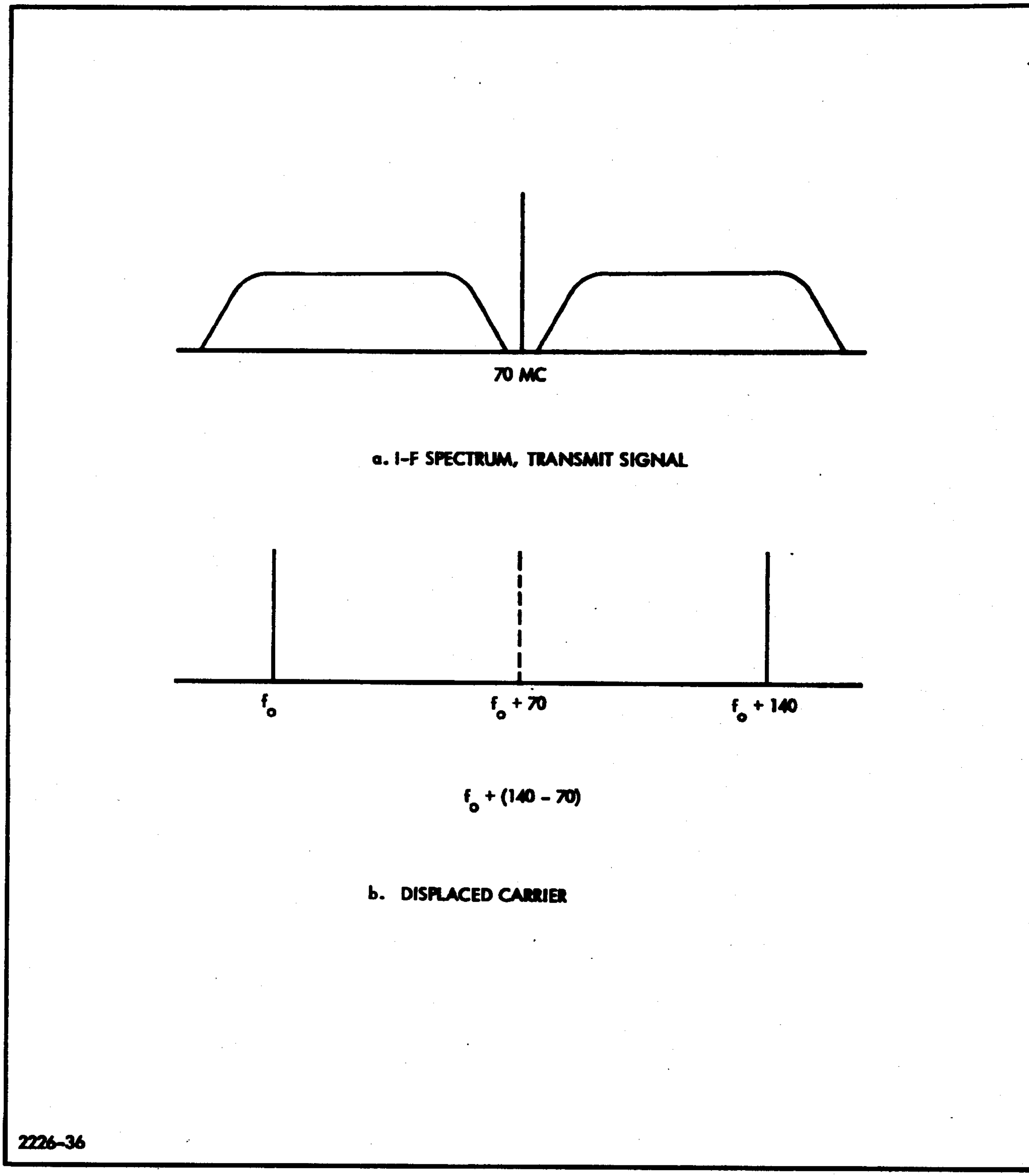


Figure 15 - Inversion of Transmitted Spectrum

detail analysis refer to Section VII, paragraph 3.b.(1)(c)). The clutterlock operates by comparing the phases of returns from successive prf pulses. For this reason a switching frequency at prf/2 is required which is generated in the same circuitry which operates the 90-degree phase-stepper in the 70-mc channel.

b. Time Pulses

Besides the noted continuous frequencies, it is necessary to generate a series of pulses at the prf rate which have various time delays with respect to the original prf. The system has a basic clock and counter chain which resets at the selected prf rate. For purposes of analysis the time of the clock pulse which generates reset is taken for the start of each prf cycle. The following pulses are then generated:

1. Reset pulse to return the counter to zero
2. A slightly delayed unblanking pulse which is available to disable any equipment during actual transmission
3. An On-Gate to prepare the chirp system and the traveling wave amplifier tube (twt) in the i-f unit for the transmit mode (as opposed to the receive mode) and to turn on the 140-mc offset frequency
4. A modulator trigger which initiates the spectrum to be transmitted and which causes the high-voltage pulse to be applied to the transmitter
5. A video-sync pulse which is telemetered along with the wide-band video and used for purposes of synchronizing remotely based equipment
6. A sweep trigger to initiate a recorder crt sweep at the time the return signal is expected. The sweep so initiated will in turn generate the correct stc, crt unblanking, and dynamic focus wave shapes.

(1) System Timing Diagrams

A clearer picture of the over-all timing requirements may be obtained by referring to Figures 16, 17, and 18.

(a) System Timing Diagram No. 1

Figure 16 shows the original clock train and the outputs of each section of the counter chain. The successive binary stages of the counter are designated A through H. The bar over the sixth binary (F) indicates that the complement or inverse wave is shown. The roman numerals located below some of the counter wave shapes indicate the time and the binary elements which contribute to the generation of certain timing pulses. No. I, for example, shows that at clock pulse 1, binaries A, B and C are so arranged as to generate the On-Gate shown further down the diagram. The arabic numbers shown at various points on the diagram refer to clock pulses. (A block diagram of the synchronizer timing logic is shown in Figure 26.) Near the right side of the diagram two vertical lines indicate a region of prf adjustment. The prf monostable indicated at clock 224 is adjustable in length and may end just before any clock pulse from 237 to 252 inclusive. Sixteen prf values are therefore available in equal increments of period.

Clock 32 initiates a fixed monostable whose output in turn is used to initiate the sweep trigger and trigger a series of eight blocking oscillators. These blocking oscillators are utilized to sample and store the return signal for comparison with the signal from the next transmitted pulse, the comparison providing clutterlock data.

The ramp, sweep and crt unblanking wave forms are all generated in the recorder as is the illustrated triangular stc curve.

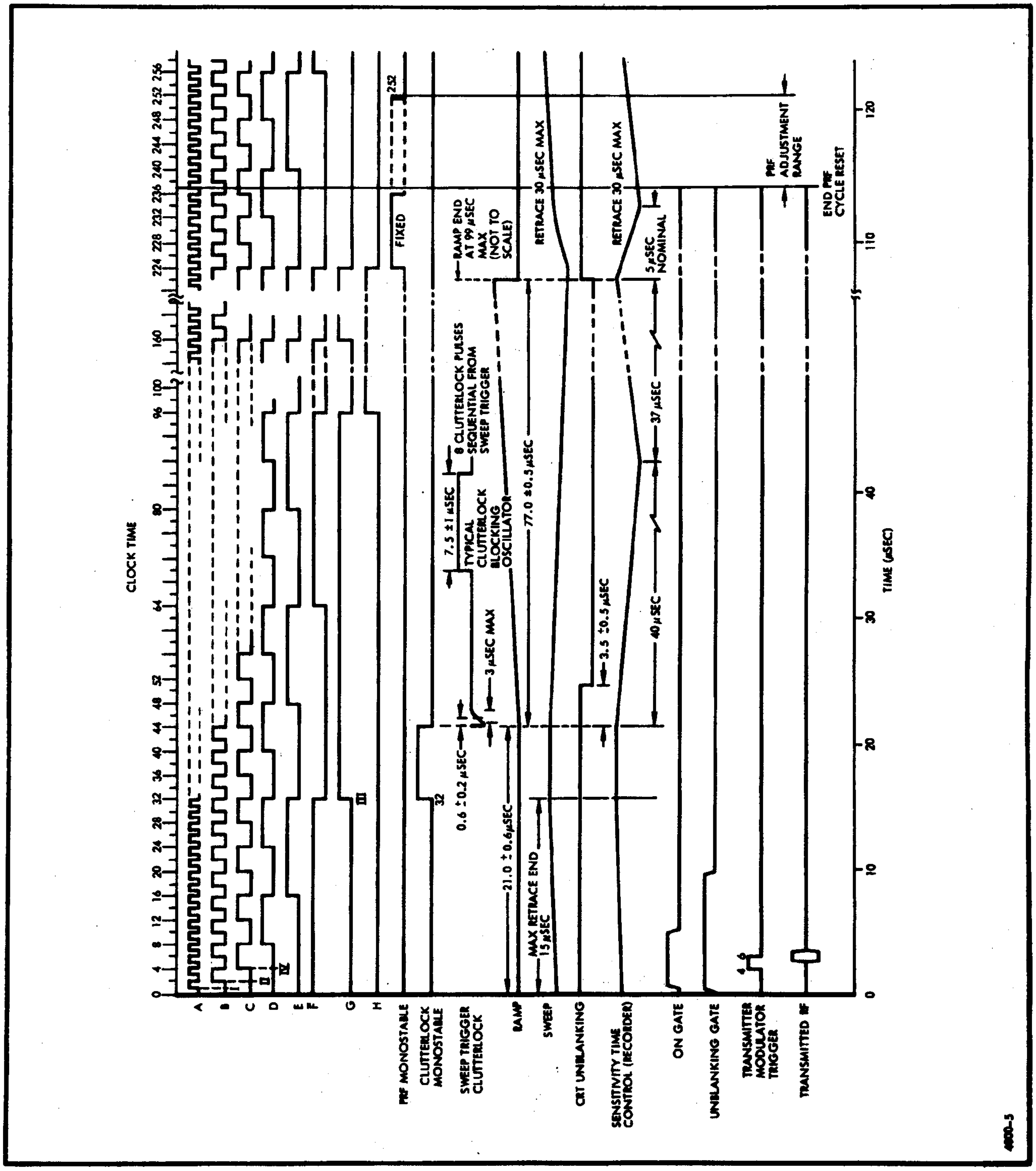


Figure 16 - Timing Diagram No. 1

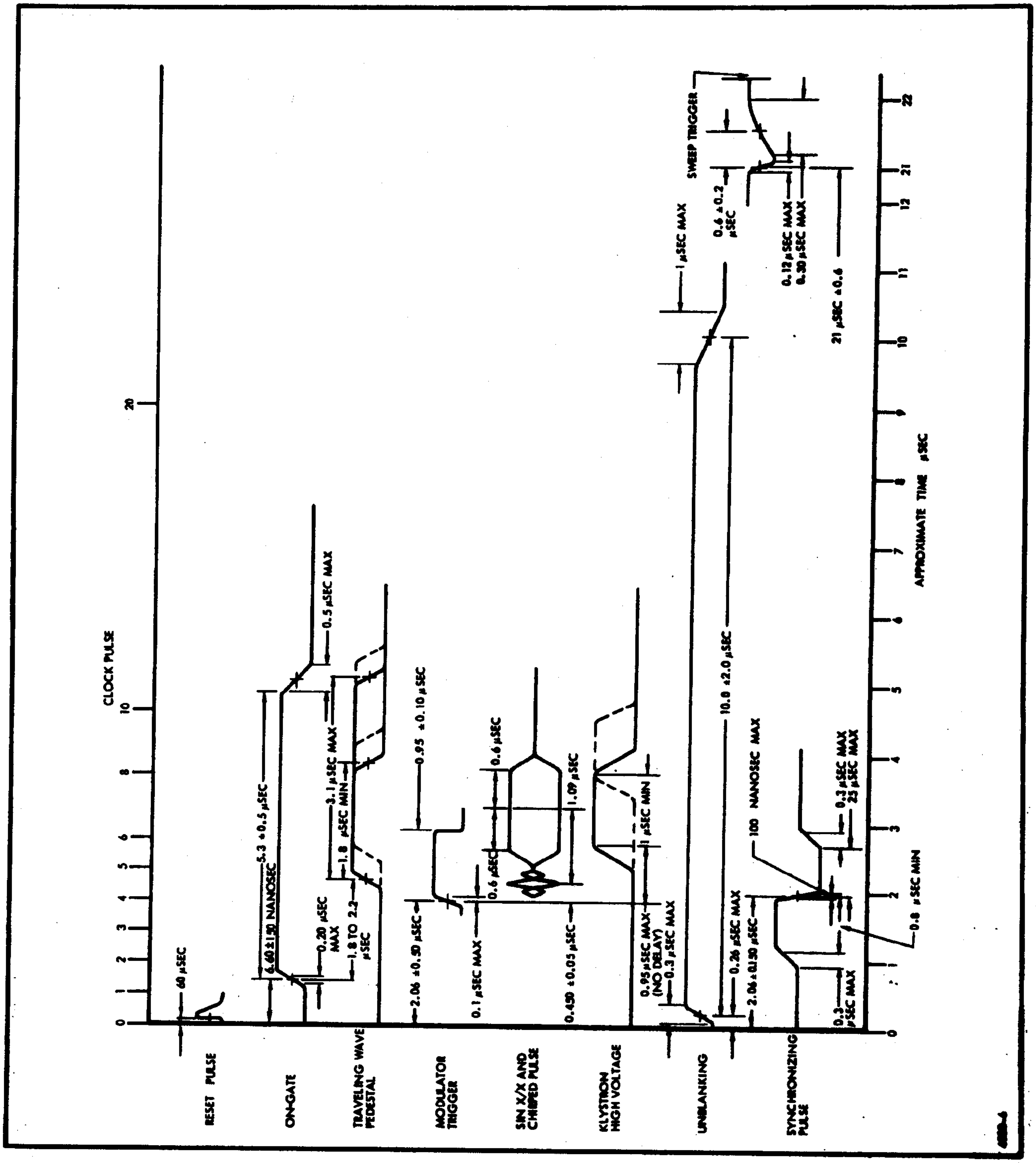


Figure 17 - Timing Diagram No. 2

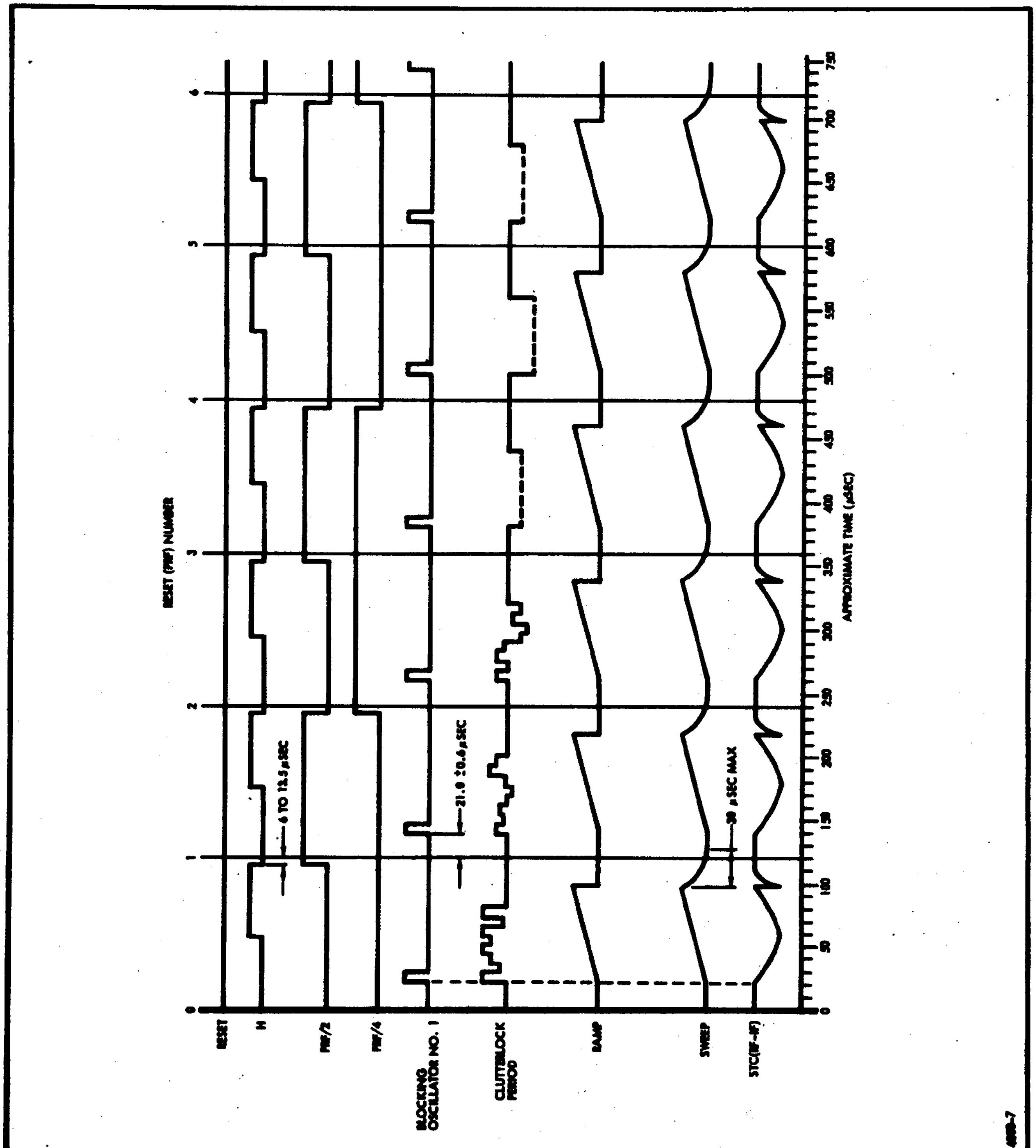


Figure 18 - Timing Diagram No. 3

(b) System Timing Diagram No. 2

Figure 17 shows the series of fast wave forms generated immediately following Clock 0 and reset. These have been previously listed excepting the twt grid pulse which is generated as a direct result of the On-Gate and the sine x/x pulse and chirped pulse which are initiated by the modulator trigger. The sine x/x and chirped pulse represent the transmitted spectrum before and after, respectively, the chirp networks.

The most important aspect of Figure 17 is the relationship of the twt grid pulse, the chirped pulse, and the klystron high-voltage pulse. These pulses must be simultaneous for transmission to occur. The klystron high-voltage pulse is adjustable in the system to coincide with or contain the chirped pulse. The twt grid pulse is adjustable to contain both. The dotted positions of the pulses represent the extreme end of the adjustment range as opposed to the earliest times (shown by solid lines in Figure 17).

(c) System Timing Diagram No. 3

Figure 18 shows a series of slower wave forms. Reset and H have been previously shown. The prf/2 is a signal-gating wave form employed in the clutterlock operation.

The prf/4 signal operates the phase stepper to give the 90-degree offsets to the 70-mc signal.

The clutterlock period shows the times during which clutterlock information is actually collected and indicates the sampled nature of the data. The indicated wave shape is only representative. The bottom wave shape is the actual stc curve in the R-F/I-F and is derived by a diode shaper from the triangular stc curve of Figure 16. The sharp negative spike following the desired curve is caused by the crt retrace and is neither functional nor objectionable.

## 2. . THE RADAR SYSTEM BLOCK DIAGRAM

### a. Simplified Block Diagram of KP-II Radar System

Figure 19 shows a much simplified diagram of the radar system. Block 1 provides the various timing pulses (refer to paragraph VI. 1. b. ) while block 12 generates the frequencies called for in paragraph VI. 1. a. (2). During the transmit mode the signal flow is via blocks 1 through 10 inclusive. The modulator trigger pulse triggers the 0. 06-microsecond pulser of block 2 and the modulator of block 11. The output of the 0. 06-microsecond pulser is filtered and imposed on a 70-mc carrier producing the 70-mc sine x/x pulse. The switches of blocks 4 and 6 are controlled by the On-Gate (present in the transmit mode) so that the sine x/x pulse is passed down the i-f chirp line to the mixer of block 7. Block 7 converts the signal to $f_o$, at which frequency further amplification is obtained in the twt, block 8. Next, the twt output goes to the transmitter (block 9) in coincidence with the high-voltage pulse from the modulator (block 11). The transmitter output passes finally through the TR/ATR box (block 10) and on to the antenna.

With the disappearance of the On-Gate the system reverts to the receive mode. The signal flow in the receive mode is via blocks 10, 13, 4, 5, 6, 14, 15, and 16.

The returning signal passes the TR/ATR box (block 10) and is immediately reduced to 70 mc by the mixer (block 13). The switches (blocks 4 and 6) allow the signal to pass the i-f and chirp line (now a dechirp line) and continue to the demodulator (block 14).

Because of the side band inversion process (refer to paragraph VI. 1. a. (2)) the output of the i-f line (block 5) is recompressed into a series of 0. 06-microsecond target returns. Block 14 reduces these returns to bipolar video which is amplified and recorded. The recorder (block 16) is also the recipient of a sweep trigger which controls all recorder timing and the stc function.

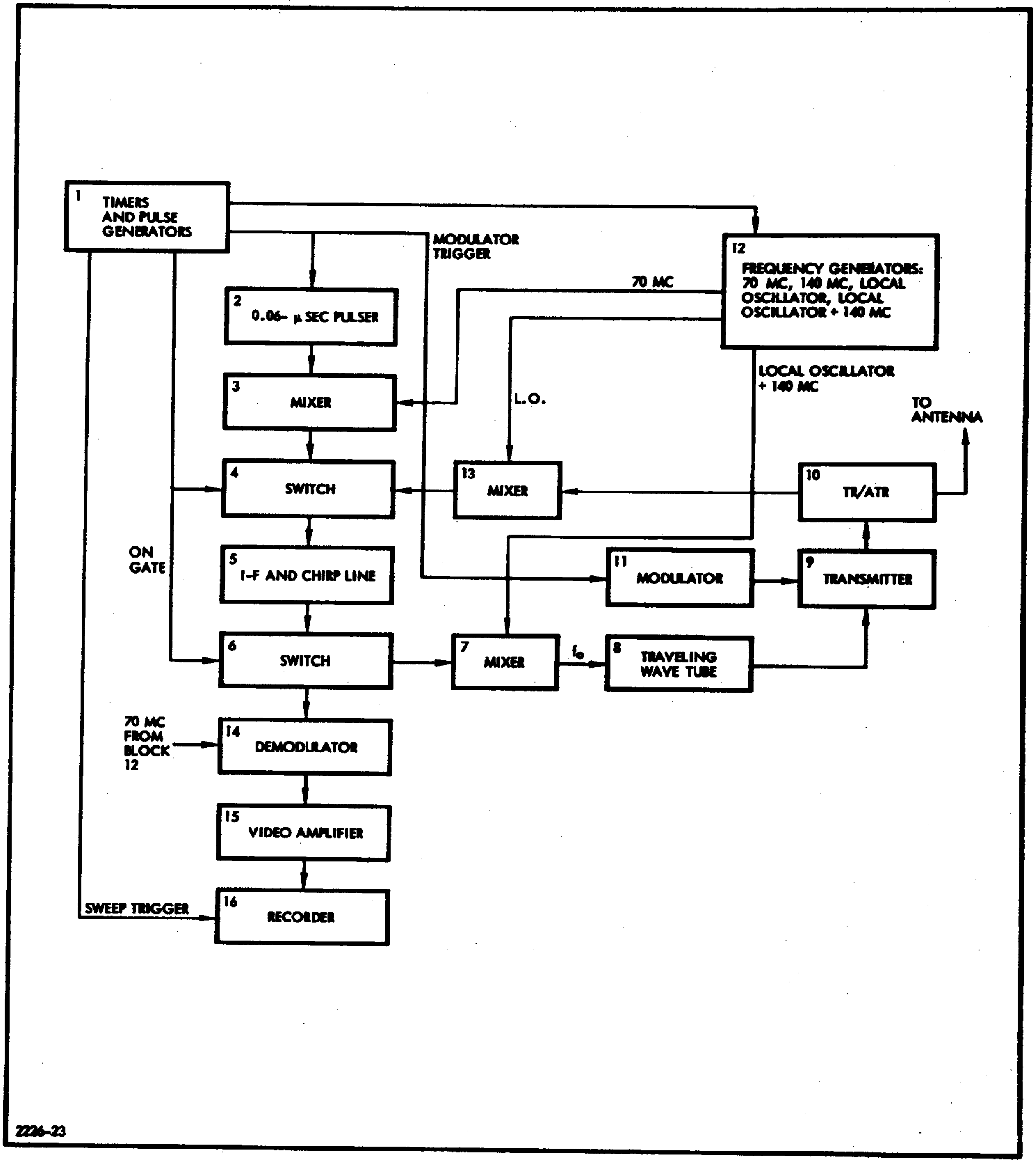


Figure 19 - Simplified Block Diagram of KP-II Radar System

b. Detailed Block Diagram of KP-II Radar System

Figure 20 shows some of the additional complexities required for a practical system. As shown in this diagram, the signal flow on transmit is via blocks 1 through 14 inclusive, while the received function is performed via blocks 14, 21, 4 through 10, and 22 through 27. The remaining blocks indicate auxiliary operations. (Refer to Figure 26 for a detailed block diagram of the counters and pulse generators as discussed in Section VI, paragraph 3: Reference Computer.)

Blocks 15, 16, and 17 generate 70 mc and a phase-stepped 140 mc as previously discussed. Blocks 18, 19, and 20 provide the local oscillator (LO) and LO + 140 mc signals.

Blocks 30, 31, and 32, together with blocks 23 and 24, are the clutterlock loop. The loop provides a low-frequency offset signal proportional to the antenna pointing error. This signal is in turn used to offset the 70-mc reference prior to demodulation in block 23.

Block 33 fulfills a standard agc function providing a d-c voltage proportional to signal level. The resulting voltage adjusts the receiver gain to maintain a constant output. Although not shown on the block diagram, both the clutterlock video and the agc video signals are gated to operate only during the time when data are being recorded on film. Their outputs are therefore not a function of signal levels occurring at other times.

Block 34 provides an auxiliary video output with an added synchronizing pulse which is transmitted to the ground through a wide band video link.

Block 20 is activated by the sweep trigger from the pulse generator block. The sweep generator block in turn generates a crt sweep and a crt unblanking pulse, turning on the recorder crt at the proper time. Light from the crt is focused on the film which is in continuous motion.

3. RADAR SYSTEM MODES

The radar set is programmed by means of an in-flight tape system, or commanded via the ground-based radar, into its various operating modes or

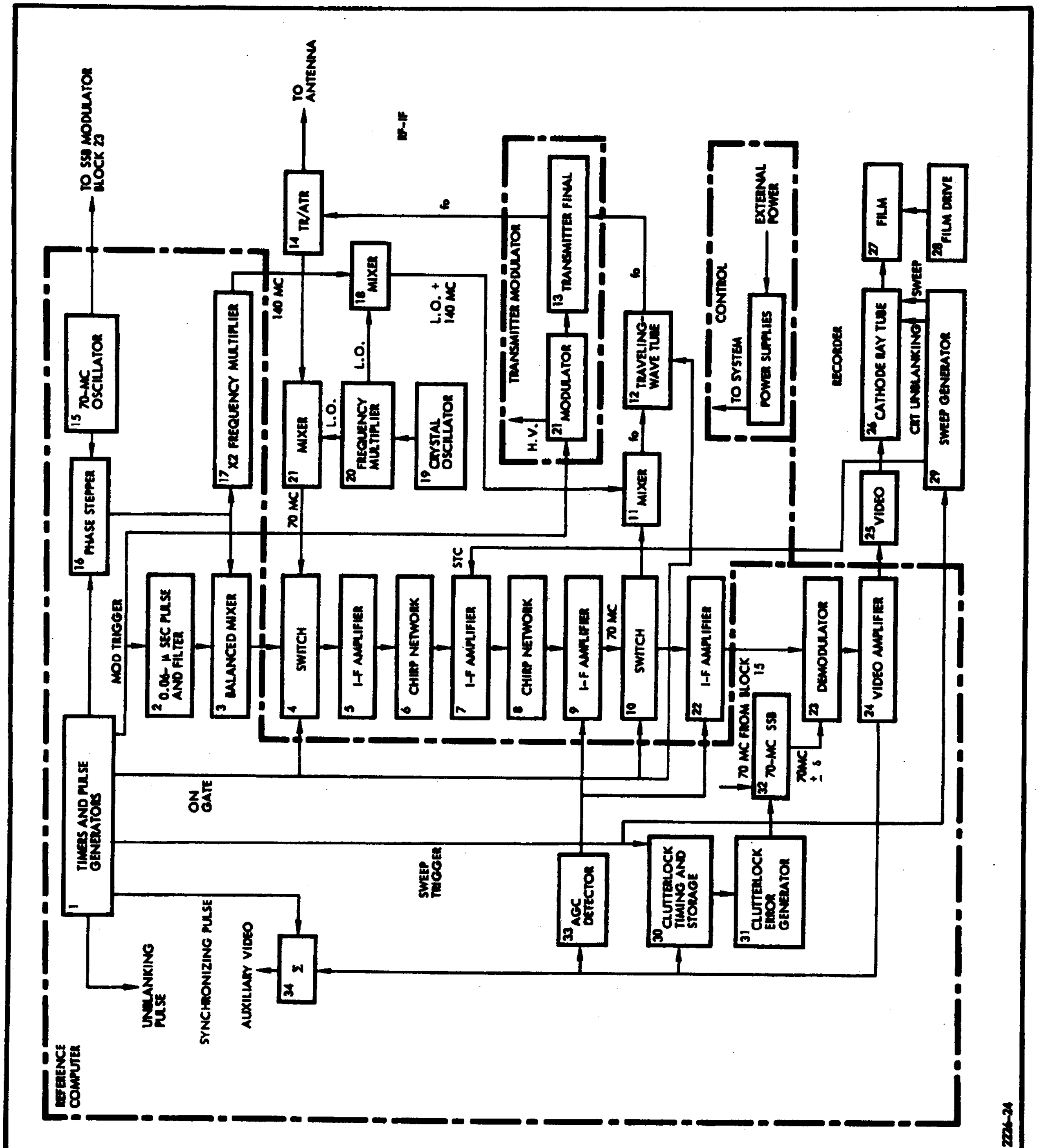


Figure 20 - Detail Block Diagram of KP-II Radar System

conditions of operation. These modes are indicated in Table XV. Further details are found in the operation sections for the various units.

TABLE XV - RADAR SYSTEM MODES

| Command | Type of command | Description |
|---|---|---|
| Warm-up | Momentary +28.3 vdc | 28.3 vdc; 115 v, 3 $\phi$, 400 cps, and 115 v, 1 $\phi$, 2000 cps to various units. Filaments and conditioned signals energized. Time delay circuit initiated in transmitter. |
| Pre-operate | Momentary +28 vdc | D-c power supplies energized (+23.5 vdc, -23.5 vdc, and 300 vdc). |
| Operate | Momentary +28.3 vdc | Transmitter high voltage and film drive on. Clutterlock loop closed |
| Off | Momentary +28.3 vdc | System to Warm-Up from Pre-Operate or Operate |
| Warm-up off | Momentary +28.3 vdc | Warm-up relay de-energized. Power off except +28.3 vdc |
| TDO No's 1, 2, 3 | Continuous +28.3 vdc via 3 input "and" gate | Time delay circuit in transmitter-modulator bypassed when all three signals are present |
| Attenuator select No's 1, 2, 3 | Momentary +28.3 vdc; 3-digit relay chain | Any one of eight receiver gain positions selected (including one position for agc) |
| Attenuator reset No's 1, 2, 3 | Momentary +28.3 vdc; 3-digit relay chain | Reset conditions for above relays |
| Clutterlock timer Constant No's 1, 2 | Momentary +28.3 vdc | Clutterlock time constant either 2.5 sec or 5.0 sec |
| Clutterlock short | Momentary +28.3 vdc | Clutterlock loop opened |
| Prf select No's 1 2, 3, 4 | Continuous +28.3 vdc; 4-digit relay chain | Any one of 16 prf's selected |
| BIT on | Continuous +28.3 vdc | Built-in test circuit operated to test clutterlock loop |
| Film drive on-off | Momentary +28.3 vdc | Film motor energized or de-energized |

This page intentionally left blank

## SECTION VII - COMPONENT DESCRIPTION

### 1. TRANSMITTER-MODULATOR

#### a. Mechanical Design

Three environmental factors - pressure altitude, vibration, and temperature - dictated to a great extent the mechanical design of the Transmitter-Modulator (see Figure 21). Each of these and their influence on the design will be discussed in the following paragraphs.

(1) Altitude

The problem of high-voltage breakdown in the low pressure environment was a very difficult one to solve. Each voltage component and wire connection had to be completely potted or oil-filled. Not only was it necessary to use potting, but because of the voltage gradient these parts had to be surrounded with a grounded shield to completely eliminate corona. Further details of this problem are discussed in Section VIII.

(2) Vibration

The vibration requirements were met by mounting the heavy components on a rugged, shock-mounted box structure. The most difficult part of the design was to provide center-of-gravity mounting while retaining ready access to the removable covers of the box. One of the most critical items in regard to vibration is the klystron tube. The large heat-dissipating mass mounted on its anode had to be anchored securely to prevent breakage of the collector from the body of the klystron under conditions of high g loading. At the same time it was necessary that the fixture allow for movements caused by thermal expansion.

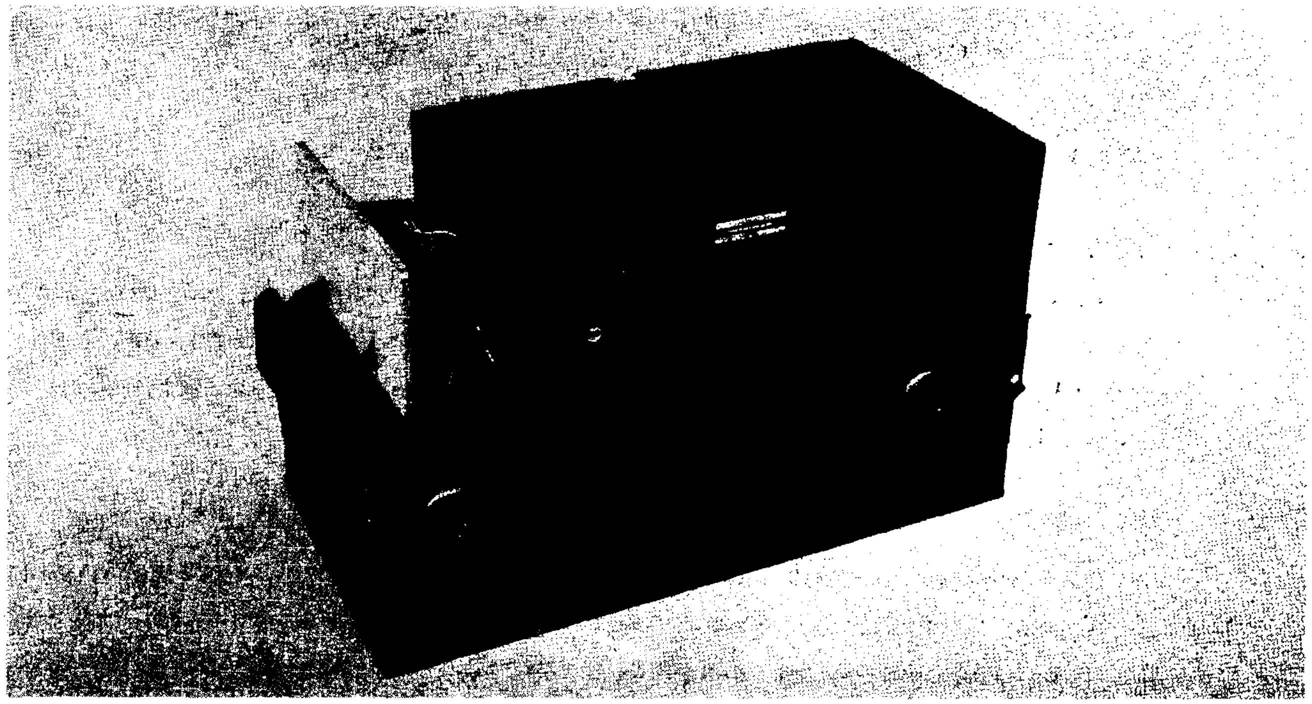

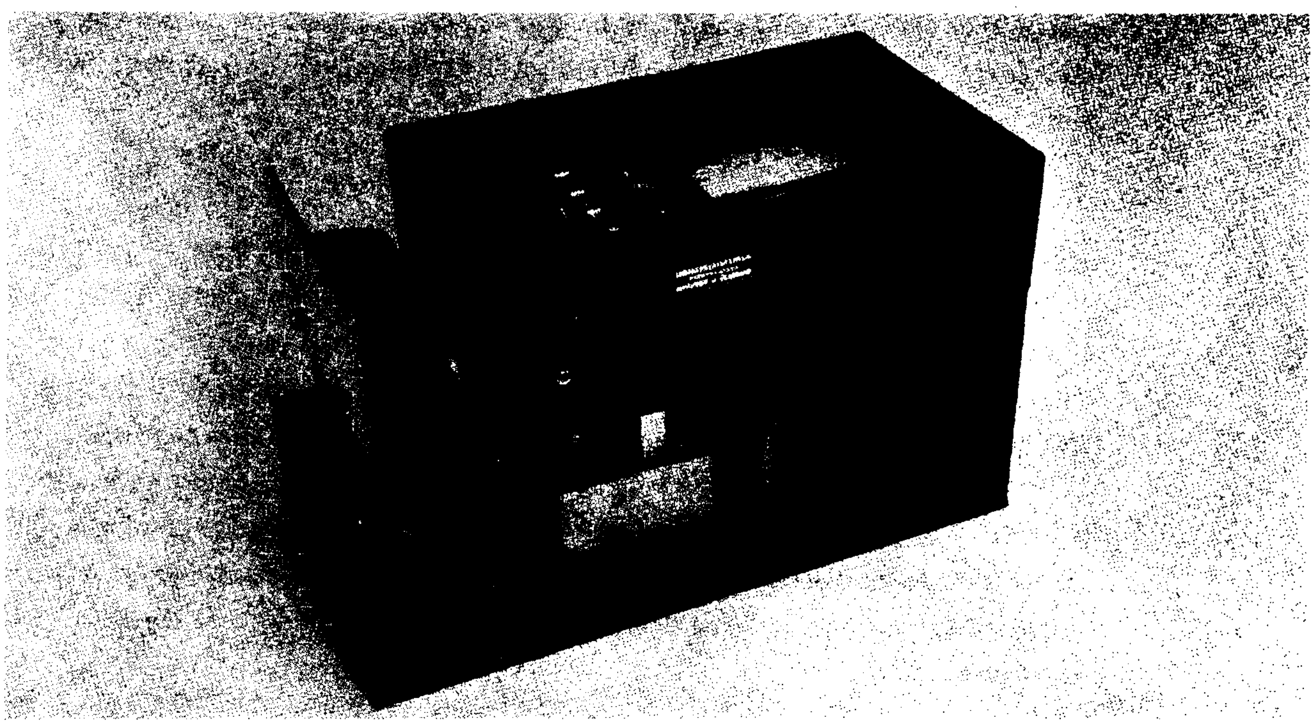

Figure 21 - Transmitter-Modulator

(3) Temperature

The temperature environment also influenced the box design in that all the heat had to be removed by radiation. This was accomplished by heat-sinking all components to the base of the Transmitter-Modulator box to absorb the energy during the on time, and cooling the components by radiation during the off time. The special problem of cooling the klystron collector was solved by providing an attached mass to serve as a heat sink during the on time, and a large surface with good radiation properties for removing the heat during the off time. The body of the klystron is cooled by direct radiation into the box structure.

b. Electrical Design

The function of the Transmitter-Modulator is to provide a high-power pulse of at least 30-kilowatts peak by amplifying the chirped signal from the R-F/I-F unit. This amplification is provided by the five-cavity klystron which is cathode-pulsed by a line-type modulator. This klystron provides linear amplification and preserves the amplitude and phase characteristics of the input drive pulse.

The Transmitter-Modulator will be described by breaking it down into three major divisions: modulator, timing and trigger circuit, and overload and protection circuit. Each of these functions will be discussed in the following paragraphs.

(1) Modulator

The function of the modulator is to provide the proper voltage for operation of the klystron r-f amplifier. This voltage is applied as repetitive negative pulses to the cathode of the tube. Each pulse is about 28 to 30 kv in amplitude and approximately 1.2 microseconds in width. The circuit produces these pulses at a rate of 8215 to 8735 pulses per second.

A simplified diagram of the modulator is shown in Figure 22 along with some of the voltage and current wave shapes. These pulses are produced in the following manner:

At the beginning of the charging cycle the capacitance of the pulse-forming network (pfn) is almost completely discharged and the thyratron is cut off. The inductance of the pulse transformer is small compared to that of the charging choke. The constants of the pfn are chosen for the pulse width desired and the inductance of the charging choke is chosen so that it forms a series resonant circuit with the capacitance of the pfn. The resonant frequency is approximately one-half the lowest prf:

$$f \leq \frac{PRF}{2} = \frac{1}{2\pi\sqrt{LC}} \quad . \tag{88}$$

In the absence of the charging diode CR1, the inrush of current to the pfn would normally cause a damped oscillation to be set up with the voltage E across C rising to approximately twice the power supply voltage (assuming negligible drop across the pulse transformer) and finally approaching the power-supply voltage as a steady-state value. This discharge action is prevented and the charge is maintained on the pfn because of the forward diode in the charging circuit which will not allow the current to reverse.

The timing is such that the peak voltage on the pfn occurs just before the trigger pulse to the thyratron. When the thyratron is triggered it shorts the input of the pfn to ground. The pfn is now directly across the pulse transformer and the energy of the pfn is completely discharged through the pulse transformer to the klystron. Since the characteristic impedance of the pfn is matched to that of the pulse transformer and its load, a voltage pulse approximately E/2 in amplitude and 1.2 microseconds long, is impressed across the pulse transformer. This pulse is stepped up by the pulse transformer to a

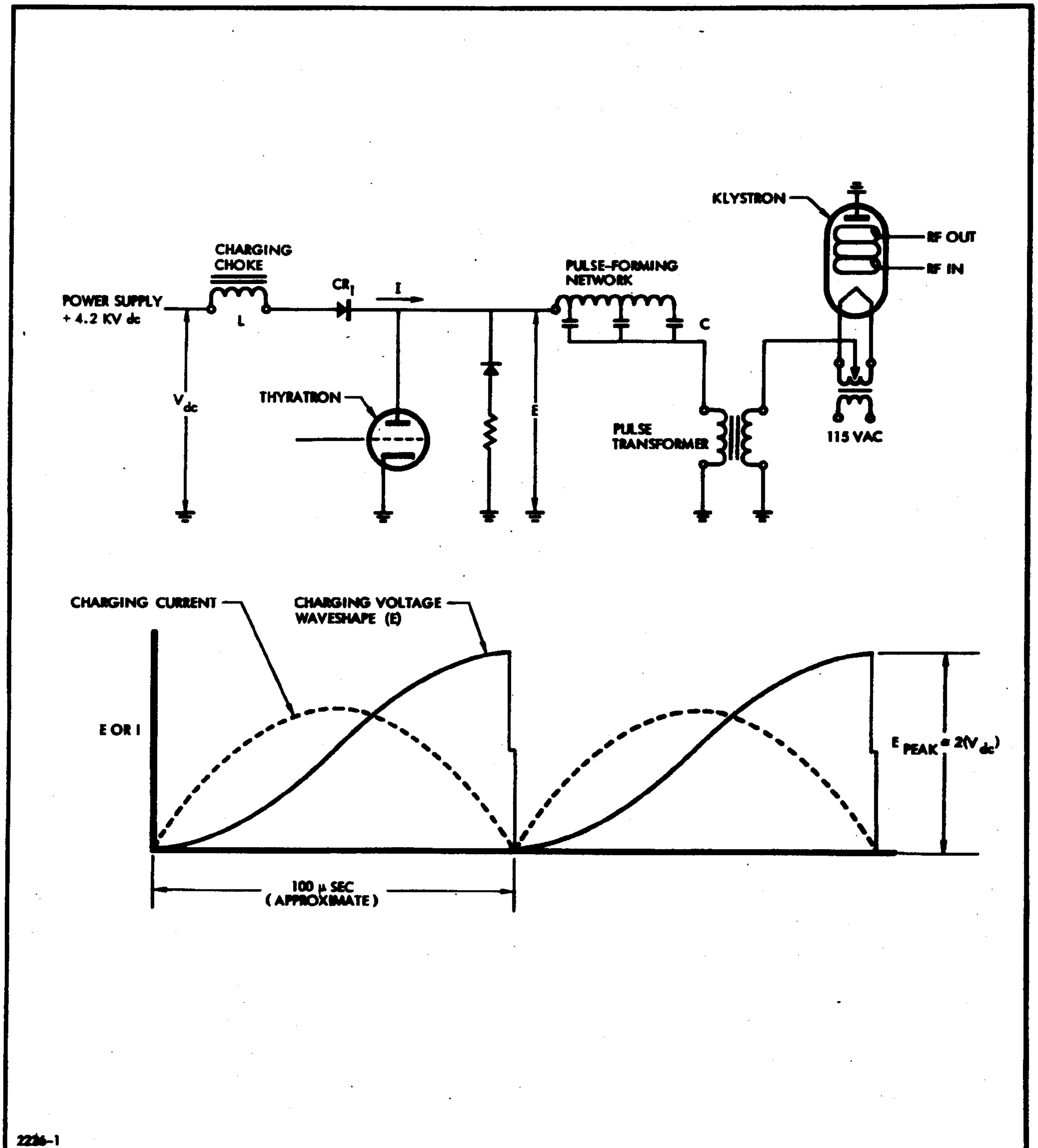


Figure 22 - Simplified Schematic of the Modulator

30-kv pulse across the klystron amplifier. This causes the tube, during the high-voltage pulse, to amplify the r-f signal being applied to its input cavity.

In practice, the impedance of the pfn is designed to be slightly higher than that of the pulse transformer and its load. This causes the voltage E to go slightly negative at the end of the discharge and effectively cuts off the thyratron.

This charge and discharge process is repeated at the prf rate causing the klystron amplifier to amplify the r-f input pulse to 30-kw peak each prf period. This pulse is then radiated by the antenna.

(2) Timing and Trigger Circuit

This circuit makes use of a delay line, an avalanche-trigger amplifier, and a blocking oscillator. The function of the circuitry is to properly delay and develop the voltage trigger required by the grid of the thyratron.

The incoming 5-volt modulator trigger is coupled to the delay line which is adjustable from 0 to 0.65 microsecond in 0.05-microsecond increments to a value as required to properly align the system pulses with the inherent delays found in the existing cables and circuits.

The output of the delay line is used to trigger a transistor delay line controlled avalanche stage. The avalanche stage develops sufficient voltage to drive the grid of the cathode follower which in turn triggers the blocking oscillator circuit. The cathode-follower method of triggering the blocking oscillator was chosen since it is adaptable to high prf rates.

The blocking oscillator, which is of conventional design, develops a high-voltage, medium-power pulse to drive the grid of the hydrogen thyratron. The grid pulse amplitude, pulse width, rise time, and driving impedance are specified by the thyratron manufacturer. To assure stable and reliable operation all these conditions must be met, particularly when operating at high prf rates. This blocking oscillator has an amplitude of 250 volts and is capacitively coupled to the thyratron grid. A despiking network in this circuit prevents large voltage spikes produced by the hydrogen thyratron during ionization from being reflected into the blocking oscillator circuit.

(3) Overload and Protection Circuit

This circuit monitors the inverse current, power-supply overload, the time delay, and the temperature of the klystron collector. All of these signals either operate or feed through relays to provide a voltage to turn off the high-voltage power supply in case of malfunction.

2. R-F/I-F UNIT

a. Mechanical Design

(1) Main Structure

The main structure of the R-F/I-F unit provides (1) a framework on which all the wave guide and associated parts are mounted, and (2) an electronic box which houses the plug-in modules. The complete R-F/I-F unit is pictured in Figure 23. The unit is mounted to the structure through six vibration isolators. These isolators are so located that the box will vibrate about its center of gravity and thereby provide the maximum isolation of the box from its vibration environment. Since it is not necessary to operate during vibration the isolation is required only for survival of the components.

(2) Component

Certain mechanical considerations were given to the component parts within the unit because of the environmental conditions, e. g:

1. Temperature. Adequate temperature control was provided by the box design, which proved adequate for the extremes expected to be encountered.

Figure 23 - R-F/I-F Unit

2. Vibration. To protect adequately the component parts, it was necessary to mount the entire R-F/I-F unit with vibration isolators so that the moment arms pass through the center of gravity. By this and proper selection of the resonant frequency of the isolator, it was possible to keep the g-loading on the box within safe limits for the component parts.

3. Altitude. The requirement for operation at high altitude slightly influenced the design. The steps required to eliminate problems of corona and voltage breakdown are described in detail in Section VIII.

**b. Electrical Design**

(1) General Description

The R-F/I-F unit has two basic functions: it generates the chirped pulse that is amplified by the Transmitter-Modulator, and it serves as the receiver section of the radar system. Since most of the unit concerns itself with chirping and dechirping pulses, it is necessary to explain what these processes are before discussing the detailed circuitry.

In the transmit section of the circuit this unit receives a 0.06-microsecond, sine x/x pulse from the Reference Computer from which it generates a linear sweep-frequency pulse for the r-f drive to the transmitter. This is achieved by feeding the sine x/x pulse through a chirp network where all the frequencies are delayed according to their frequencies. The chirped pulse emerges as a 1.0-microsecond pulse. The rf in the 1.0-microsecond pulse is a linearly frequency-modulated signal with the start of the pulse being $f_1$ and the end of the pulse being $f_2$. The frequency content of these pulses requires an information band width of 15 megacycles which is sufficient for the required 50-foot resolution with some additional allowance provided. All of the chirping circuitry is designed around a 70-megacycle frequency. The chirped pulse is later mixed with the appropriate signals to translate it to an X-band frequency. It is then amplified by the transmitter and becomes the transmitted signal. This burst of energy upon being reflected by a target is then detected by the receiver.

The receiver portion of this unit includes X-band wave guide sections, t-r tubes, a microwave mixer, circuits for dechirping the returned signal, and circuits for providing amplification at the i-f frequency. The wave guide and t-r tubes perform the duplexing function of the system and provide protection for the receiver from the high-powered pulse from the transmitter. The losses in this wave guide and the performance of the microwave mixer-amplifier determine the minimum sensitivity of the system. Once a returned signal is detected and amplified it is sent through the chirp network where the linear sweep-frequency pulse is recompressed into the original 0.06-microsecond sine x/x pulse. How well this pulse resembles the original pulse is a measure of proper system performance. In actual operation the returned signal has experienced a doppler shift that results in the sine x/x pulse having slightly different frequency content. In the reference computer this pulse is detected in a synchronous demodulator where it is compared with the reference frequency for determination of the doppler shift.

(2) Transmitter Circuit Function

The R-F/I-F unit functional block diagram is shown in Figure 24. The transmitter and receiver sections time-share the center i-f amplifier portion of the circuit. The signal flow through the transmitter section, beginning with the 99-megacycle oscillator, is as follows:

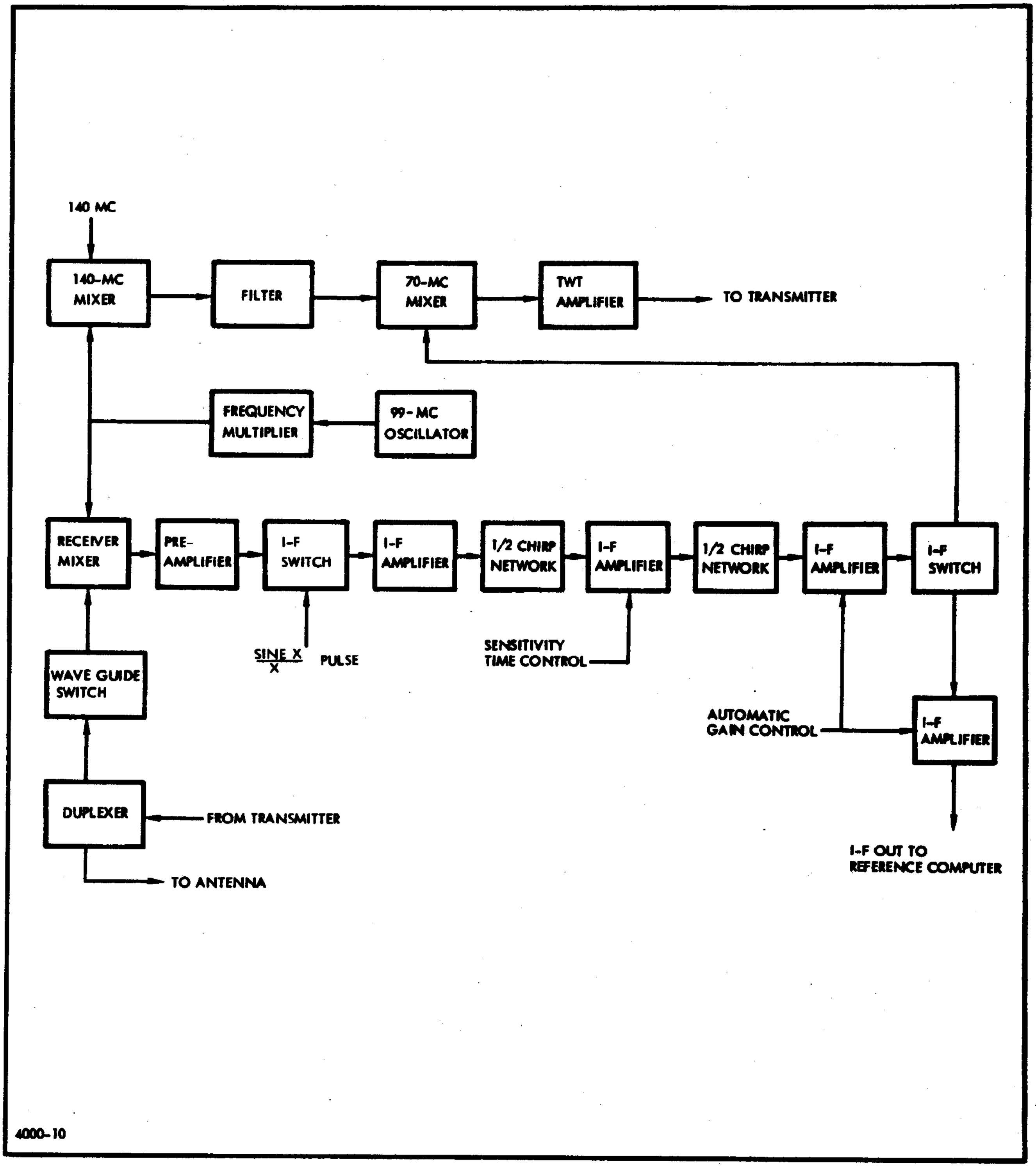


Figure 24 - Functional Block Diagram of R-f/I-f Unit

(a) 99-Megacycle Oscillator

This oscillator is the stable local oscillator (stalo) of the radar system. It is highly stable over short-term periods and is tuned to a frequency of 99.275 megacycles. This frequency is multiplied to the X-band region in the frequency multiplier.

(b) Frequency Multiplier

The frequency multiplier utilizes the harmonic generation property of varactor diodes to multiply the stalo frequency 96 times and provide enough power at this frequency to drive the receiver mixer and the 140-megacycle mixer.

(c) 140-Megacycle Mixer

The output of the frequency multiplier is mixed with a 140-megacycle signal from the Reference Computer and forms two side bands in the X-band region. One of these side bands is filtered out before reaching the 70-megacycle mixer. The 140-megacycle from the Reference Computer is derived from the basic 70-megacycle oscillator to maintain phase coherence. This mixing operation is required only in the transmitter chain since the transmitter signal must be frequency-inverted so that is can be sent back through the same chirp network. Otherwise the returned pulse would be further expanded instead of being recompressed.

(d) Filter

This unit is an X-band wave guide filter that selects the upper side band from the 140-megacycle mixer so that the transmitter signal is frequency-inverted.

(e) 70-Megacycle Mixer

The 70-megacycle mixer, during the transmit period, accepts the 9670-megacycle signal from the filtered 140-megacycle output, and the linearly swept 70-megacycle pulse from the i-f channel, and mixes them. The two resulting side bands are frequency swept, one sweeping from low frequency to high frequency, the other doing the opposite. The lower one, which is in the pass band of the transmitter, is amplified while the undesired side band is reflected from the transmitter and absorbed in a load isolator at the output of the twt amplifier.

(f) TWT Amplifier

This tube amplifies the relatively small 9600-megacycle power output to about 250 milliwatts which is sufficient to drive the klystron amplifier in the transmitter. Operation of this tube is such that it provides linear amplification of the signals without appreciable phase shift.

(3) Receiver Circuit Function

In the preceding transmitter discussion (paragraph VI. 2. b. (2)) the passage of the stalo signal to the receiver mixer and the local oscillator was discussed. The receiver description will therefore begin with a signal returning to the duplexer:

(a) Duplexer

The duplexer consists of wave guide sections, a 3-db hybrid, and a t-r tube. During the transmit period the duplexer protects the receiver from the high-power transmitter pulse and directs the transmitter pulse to the antenna. During the receive period the duplexer allows the low-energy level received pulses to pass on to the receiver.

(b) Wave Guide Switch

A wave guide switch is included in the wave guide run to the receiver mixer. This switch provides protection for the receiver crystals when the system is not in operation and might be damaged from high-level pulses from some outside source.

(c) Receiver-Mixer Amplifier

This unit has a balanced crystal detector input stage followed by a 70-megacycle preamplifier. The mixer converts the X-band return pulses to the 70-megacycle i-f frequency by mixing with the local oscillator frequency. The design of this unit is such that it will provide a receiver noise figure of 10 db when installed in the unit. There is a gain of about 24 db in the preamplifier which ensures that the noise figure of the amplifiers following the mixer-amplifier will not degrade the over-all noise figure of the system. The output of the unit is an i-f signal (70 megacycles) that is further processed elsewhere in the system.

(d) I-F Switch

The i-f switch allows the chirp network to be time-shared by the transmitter and the receiver. During the interval of time that the transmitter is on, the receiver's normal function is disconnected. At that time the sine x/x pulse from the Reference Computer is fed through the i-f amplifiers and chirp networks so that it is changed into a 1.0-microsecond pulse having a linear frequency change during the pulse. At the end of the transmitting period the switch returns the receiver/i-f amplifiers and chirp networks to their normal functions of amplifying and dechirping the return echoes.

(e) I-F Amplifiers

These amplifiers are provided to amplify the return signals and to overcome the losses of the chirp network. They operate at a center frequency of 70 megacycles and have a band width of about 15 megacycles, which is the information band width of the amplified pulses. Each amplifier has a gain of about 30 db and has provisions for adjusting the gain by 6 db with a three-position step attenuator on the front of the unit.

(f) Chirp Network

The chirp network is divided into halves and interspaced with i-f amplifiers to overcome the losses in the networks and to keep the signal above noise level. These networks are passive filter elements taking the form of a bridged "T". Their design is such that they exhibit a linear phase delay versus frequency characteristics for all frequencies within the pass band. Therefore, whenever a sine x/x band of frequencies, centered at 70-megacycles, is fed into the chirp network, it produces an expanded pulse of nearly constant amplitude with a linear frequency change from the start of the pulse to the finish of the pulse. When the expanded pulse is inverted in frequency and fed back into the network, the original sine x/x pulse is reconstructed by the network. This reconstructed pulse is then amplified and sent to the Reference Computer as a detached target return.

(g) Automatic Gain Control and Sensitivity Time Control

These functions are inputs to the R-F/I-F unit from the Reference Computer and Recorder, respectively, and are described in the sections covering these units.

3. REFERENCE COMPUTER

a. Mechanical Design

(1) Description

The Reference Computer (see Figure 25) is designed as a basic sheet metal box with printed circuit boards carrying the circuitry. The printed circuit boards are mounted in pairs on magnesium castings. The

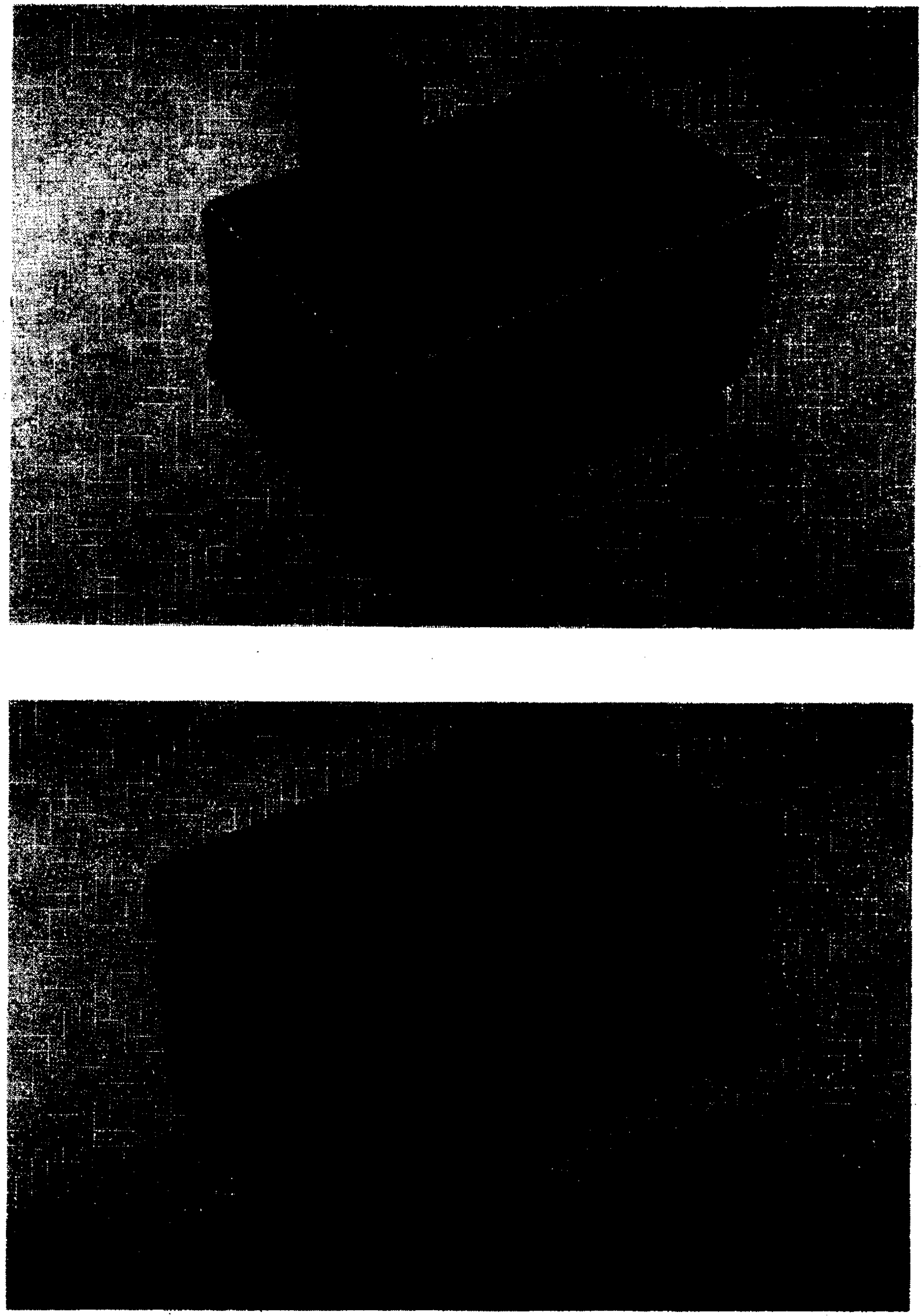

**Figure 25 - Reference Computer**

castings are fastened in the chassis by means of shear pins on the connector end and machine screws on the front end. An alignment pin on the chassis fits into a hole in the module castings. The modules utilize double read-out edge connectors. The connectors are paralleled to provide a more reliable connection.

The top and bottom access panels cover the entire face of the unit, thereby providing complete access to the modules and the wiring harness upon removal.

b. Electrical Design

(1) Operation

The operation of the Reference Computer is best described by breaking it down into four major divisions: synchronizer, r-f section, clutterlock, and self-verification and signal conditioning.

(a) Synchronizer

The synchronizer section generates the basic timing and control signals for the radar. These signals are sweep trigger, modulator trigger, on-gate, and unblanking gate. The synchronizer section also generates the following signals for control and timing of the computer: prf/4 and complement, prf/2 and complement, blocking oscillator trigger and doubler gate.

The synchronizer section consists of a crystal-controlled clock at 2.07065 mc ±1000 cps and a counter with controlled feedback. The feedback is controlled by four digital-control lines. The state of the four control lines is either +28 or 0 vdc and is determined by the prf selection. The four input-control lines are applied to four control relays. This enables a total of 16 prf selections which vary from 8.735 to 8.215 kc with a separation of approximately 35 cycles. This method of producing a variable prf has proven very successful in minimizing jitter. Jitter is less than 0.01 microsecond.

During each cycle of the counter, a modulator trigger, on-gate, sweep trigger, unblanking gate, doubler gate and B. O. trigger are generated, using the logic provided by the counters, to trigger the necessary circuitry. (See Figure 26. Refer to Section V, paragraph 1. b. (1)(a) for the waveform timing diagram and a further description.)

(b) R-f Section

The r-f section generates the following signals: 140-mc pulse; 0.06-microsecond, 70-mc (sine x/x) pulse; 70-mc reference signal offset by 90 degrees each prf; and an agc control signal. See Figure 27 for a block diagram of the r-f section.

The r-f section is composed of a crystal-controlled, 70-mc oscillator which has two isolated outputs. One output is fed to a phase-stepper which is also supplied with the logic of prf/4, prf/4 complement, prf/2, and prf/2 complement which causes the reference signal to be stepped 90 degrees in phase each prf. The output of the stepper is the offset 70-mc reference supplied to the doubler and to the balanced modulator. The logic lines supplied to the stepper are generated in the gate sequencer by counting down from the prf. This logic is also fed to the video gate board.

The 140-mc pulse is generated by a doubler circuit from the 70-mc reference and is gated by an inverted on-gate.

The 0.06-microsecond, 70-mc pulse is generated by first triggering a blocking oscillator circuit which utilizes an avalanche transistor to produce a 0.06-microsecond square wave. The 0.06-microsecond square wave is fed to a special Fourier transform filter designed for a flat pass band and linear phase shift between limits of 0 to 7.5 mc. The output from the pulser,

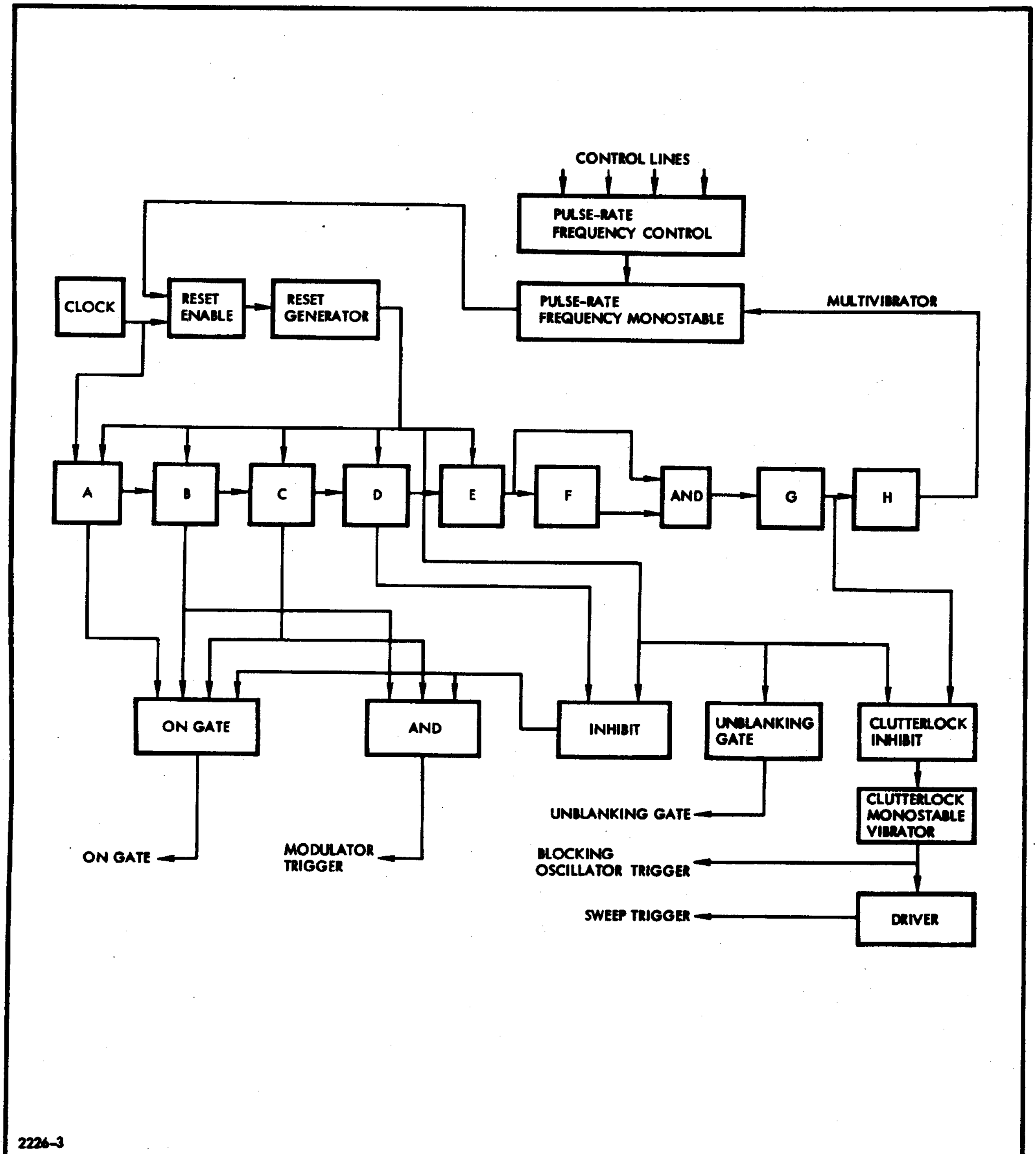


Figure 26 - Synchronizer Timing Logic

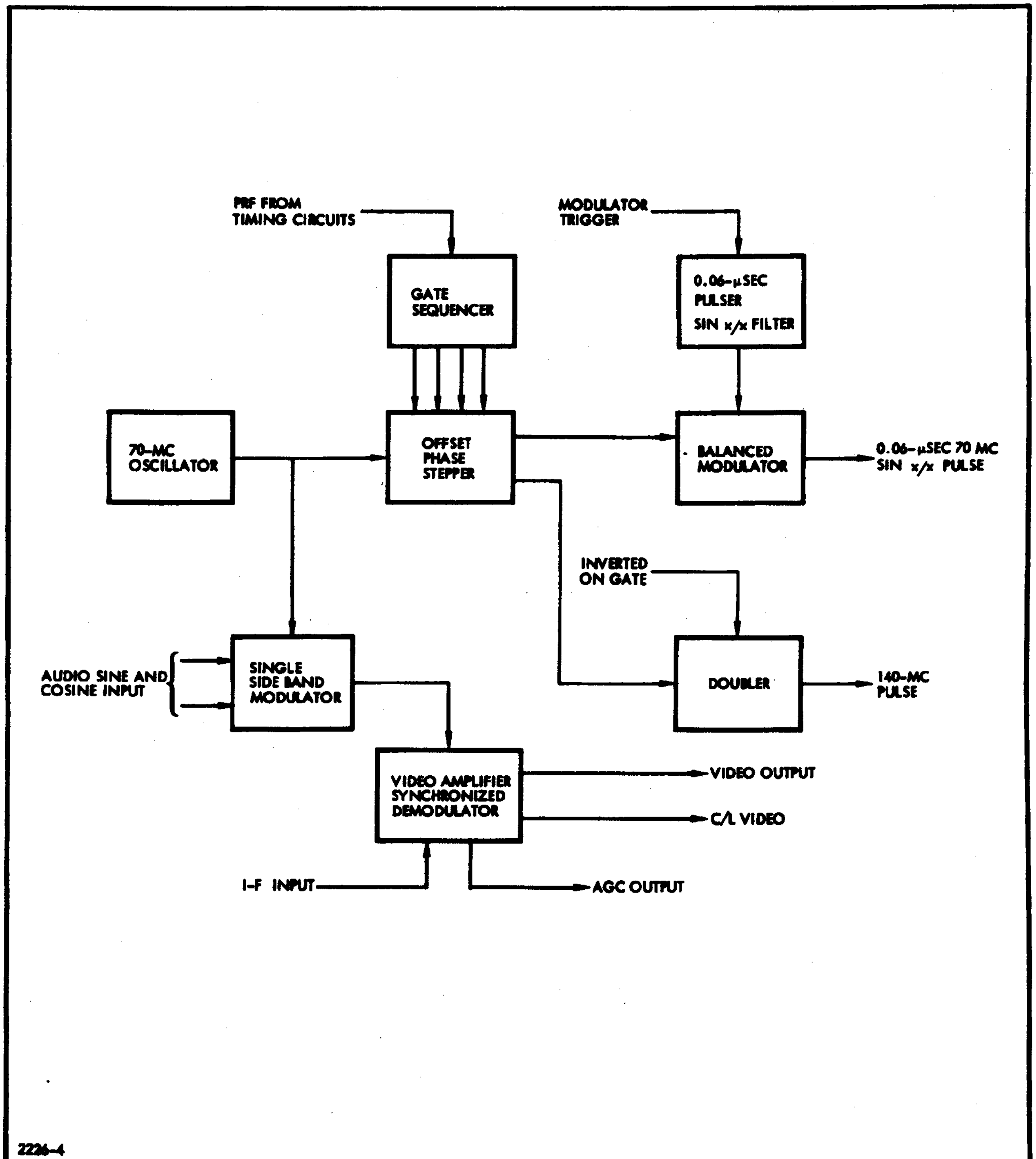


Figure 27 - Block Diagram of R-f Section

a classical sine x/x time domain spectrum distributed symmetrically about the Y-axis center frequency, is fed to a balanced modulator where the 70-mc offset reference is modulated by this signal producing a 0.06-microsecond, sine x/x, 70-mc suppressed carrier signal to the radar.

The r-f section also has a high-resolution synchronous demodulator which demodulates the i-f input using as a reference the output of the single side-band (ssb) modulator whose output is offset from the 70-megacycle reference by the audio frequency from the clutterlock section. An agc voltage of 0 to -6 volts is produced as a function of the i-f input signal.

(c) Clutterlock Section

The basic purpose of the clutterlock section is to generate sine and cosine error signals to the ssb modulator to compensate for angular displacement of the antenna beam with respect to the zero doppler direction.

The clutterlock section (see Figure 28) consists of a video amplifier, video gate, storage and switching module, approximate multiplier, audio synchronous demodulator, audio filter, 50-kc reference generator, voltage-controlled oscillator, and an integrator reset.

An output from the synchronous demodulator (Figure 27) is amplified and fed to the video gate. The video gate transfers the signal to the approximate multiplier and the storage and switching module. The signal transferred by the video gate is 60 microseconds of information following the blocking oscillator trigger. The information transferred to the storage and switching module is stored on eight sampling capacitors. Following the next blocking oscillator trigger these capacitors are sampled and the output is fed to the approximate multiplier through the video gate.

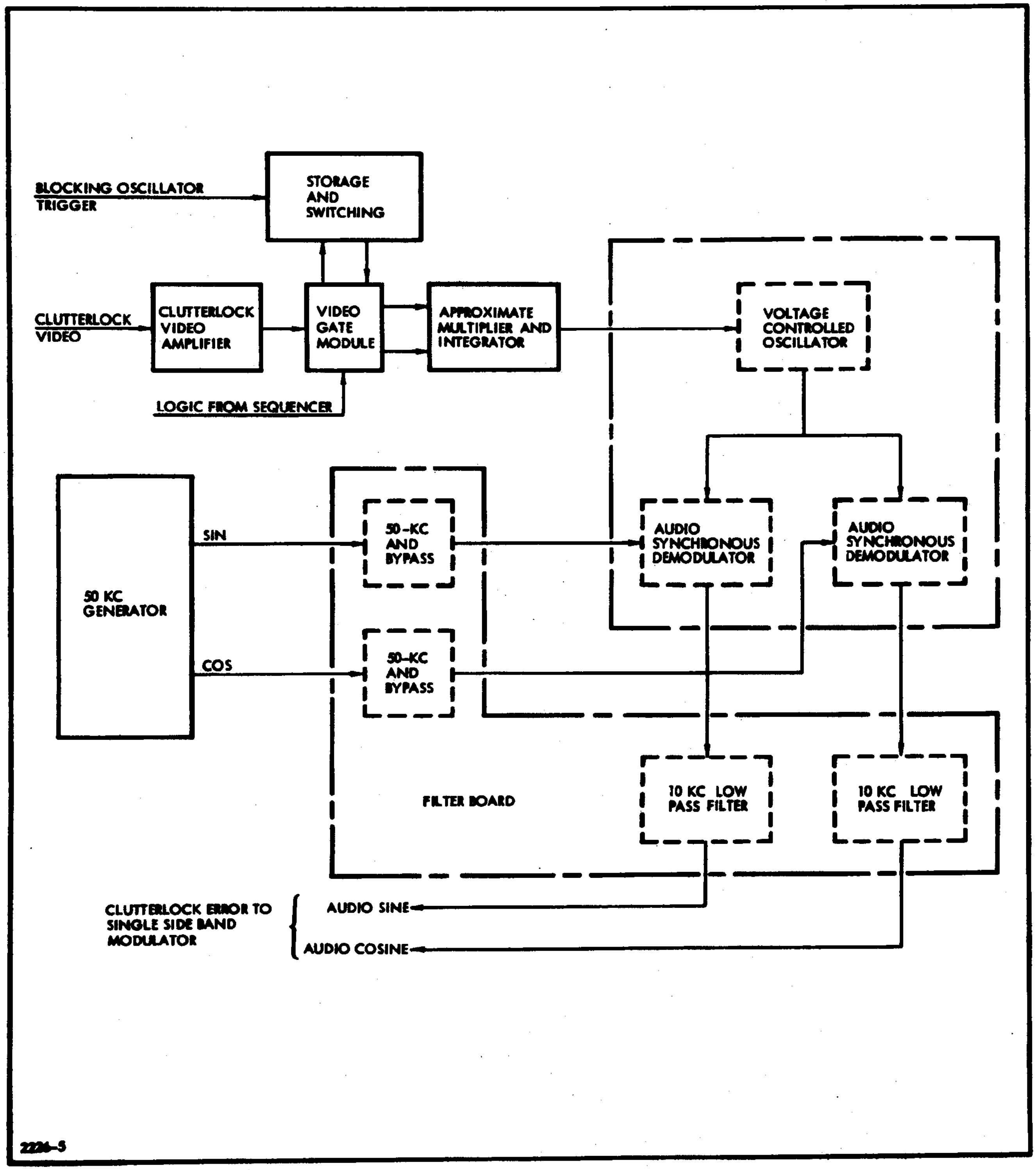


Figure 28 - Block Diagram of Clutterlock

In the approximate multiplier the phase difference between the transferred and the stored video is detected. This means that the phase of the return from consecutive pulses is compared. Because of the 90-degree offset between prf's (providing the synthetic beam is centered with respect to the zero-doppler plane) the video signals will be 90 degrees out of phase and will be zero. The detector output will be one polarity for a forward misalignment of the antenna beam and of opposite polarity for an aft misalignment.

The output of the integrator is fed to a voltage controlled oscillator (vco) whose output is from 40 to 60 kc, depending on the output of the integrator. The output from the audio synchronous demodulator module is then two quadrature sinusoidal signals chopped at the vco rate. These quadrature signals are then applied to a low-pass filter which eliminates all except the difference components. These two signals, sine and cosine, are fed to the ssb modulator.

The inputs to the ssb modulator are the sine and cosine signals and a 70-mc reference signal. The ssb module consists of two balanced modulators which are driven by the sine and cosine signals, respectively. The references applied to the balanced modulators are the 70-mc and the 70-mc phase shifted by 90 degrees. The output of the two balanced modulators is then fed to a summing network which suppresses the carrier and the lower side band. The upper side band is then amplified and fed to the synchronous demodulator for demodulation against the input i-f signal. The output of the ssb is a 70-mc signal which is offset by an audio frequency which is proportional to the original antenna beam misalignment from the zero doppler plane. The remaining circuitry in the clutterlock section is an integrator reset. The purpose for the reset is to sense the integrator output voltage and to discharge the integrator capacitors when this voltage exceeds +8.5 vdc or falls below -8.5 vdc. These values correspond to approximately ±1 degree of beam displacement and approximately ±prf.

(d) Self Verification

The built-in test (BIT) circuit generates a 70-mc signal chopped at a 30-kc rate which is fed to the high-resolution synchronous demodulator when so commanded by the operator. This is used to simulate an i-f input signal. When the BIT loop is closed the clutterlock circuit nulls out at prf/4 and holds in this condition until the BIT switch is opened.

## 4. CONTROL UNIT

### a. Mechanical Design

Two views of the Control unit are shown in Figure 29. The chassis is constructed of 5/16-inch and 1/4-inch aluminum plates interlocked and dip-brazed together. The heat-generating components are mounted on the upright walls to achieve adequate heat transfer to the outer surface. The chassis weight is nine pounds.

### b. Electrical Design

(1) Operation

The Control unit serves primarily as a control and junction box. Power from the vehicle system power supplies is distributed to the other side-looking radar (slr) units through the Control unit. It also provides three regulated voltages not otherwise available to the other slr units. The Control unit will be described by breaking it down into five major functions or divisions: control and junction box, -23.5 vdc power supply, +23.5 vdc power supply, +300 vdc power supply, and the timer override circuitry. The Control unit is shown in simplified schematic form in Figure 30.

[redacted]

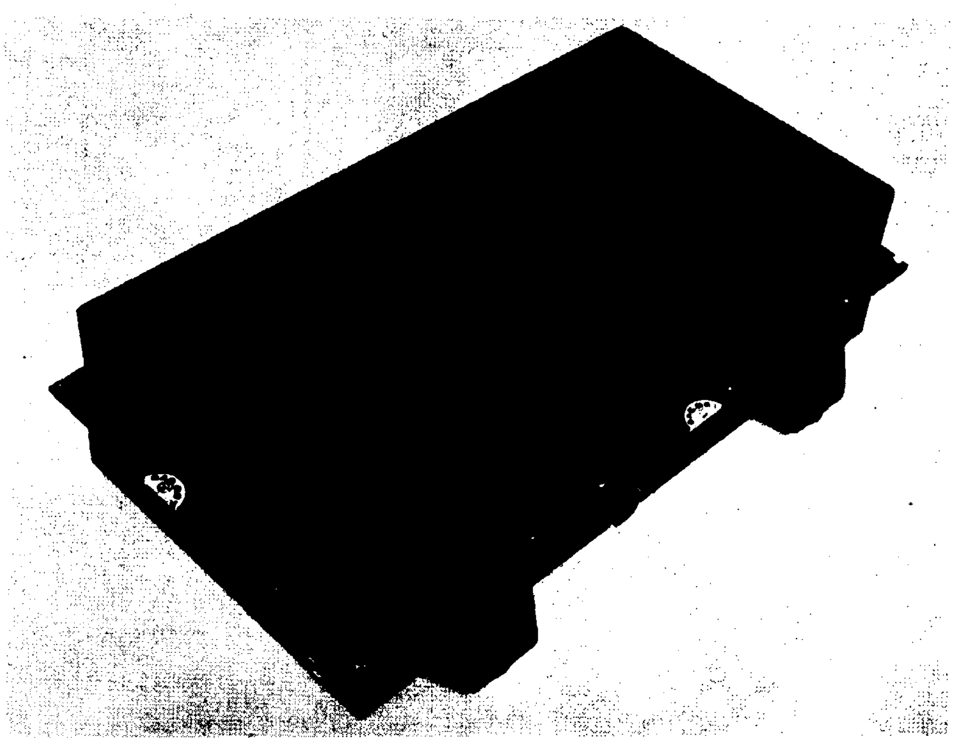

Figure 29 - Control Unit

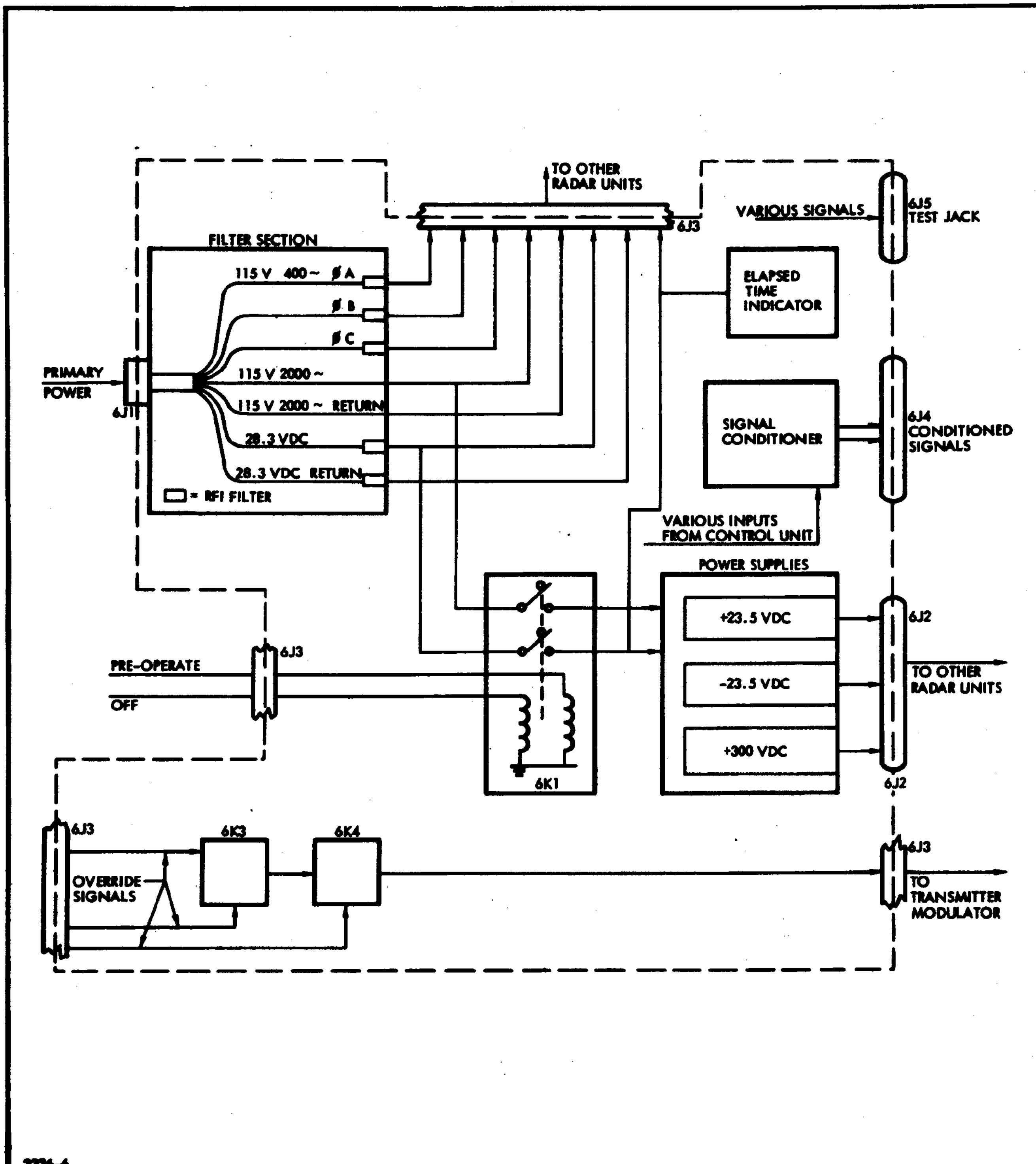


Figure 30 - Simplified Schematic of Control Unit

(a) Control and Junction Box

When the slr system is in the warm-up mode, (1) 28.3 vdc, (2) 115 v, 3 phase, 400 cps, and (3) 115 v, 1 phase, 2000 cps voltages are applied to the Control unit from the vehicle power supplies. These voltages are distributed to the other units in the slr system.

When the slr system is in the pre-operate or operate mode, 28.3 vdc and 115 v, 2000 cps power is applied to the circuits in the Control unit which generate +23.5 vdc, -23.5 vdc, and 300 vdc. This is accomplished with relay 6K1. The relay is of the latching type and is energized from the vehicle command subsystem by applying 28.3 vdc momentarily to the pre-operate input of the Control unit. The Control unit is commanded from the pre-operate mode with the momentary application of +28.3 vdc to the OFF input of the Control unit. The slr is commanded to the operate mode by momentary application of +28.3 vdc to the OPERATE input. In OPERATE, the film drive motor (Box 7), the transmitter high-voltage (Box 3), and the integrator time constant (Box 5) relays are energized. No Control unit functions are involved when the OPERATE command is given.

(b) +23.5 Vdc Regulated Power Supply

The +23.5 v power supply (shown in block-diagram form in Figure 31) is a series regulated supply. The regulator was designed to deliver an output voltage of 23.5 v ±1.0 percent for all load currents from 0 to 5 amperes. The maximum peak-to-peak output ripple at full load is less than 18 millivolts. A series-type regulator circuit was chosen because it is best capable of providing a constant output voltage to a variable load while maintaining a high efficiency. An overload-protection circuit was also incorporated to prevent destruction of the

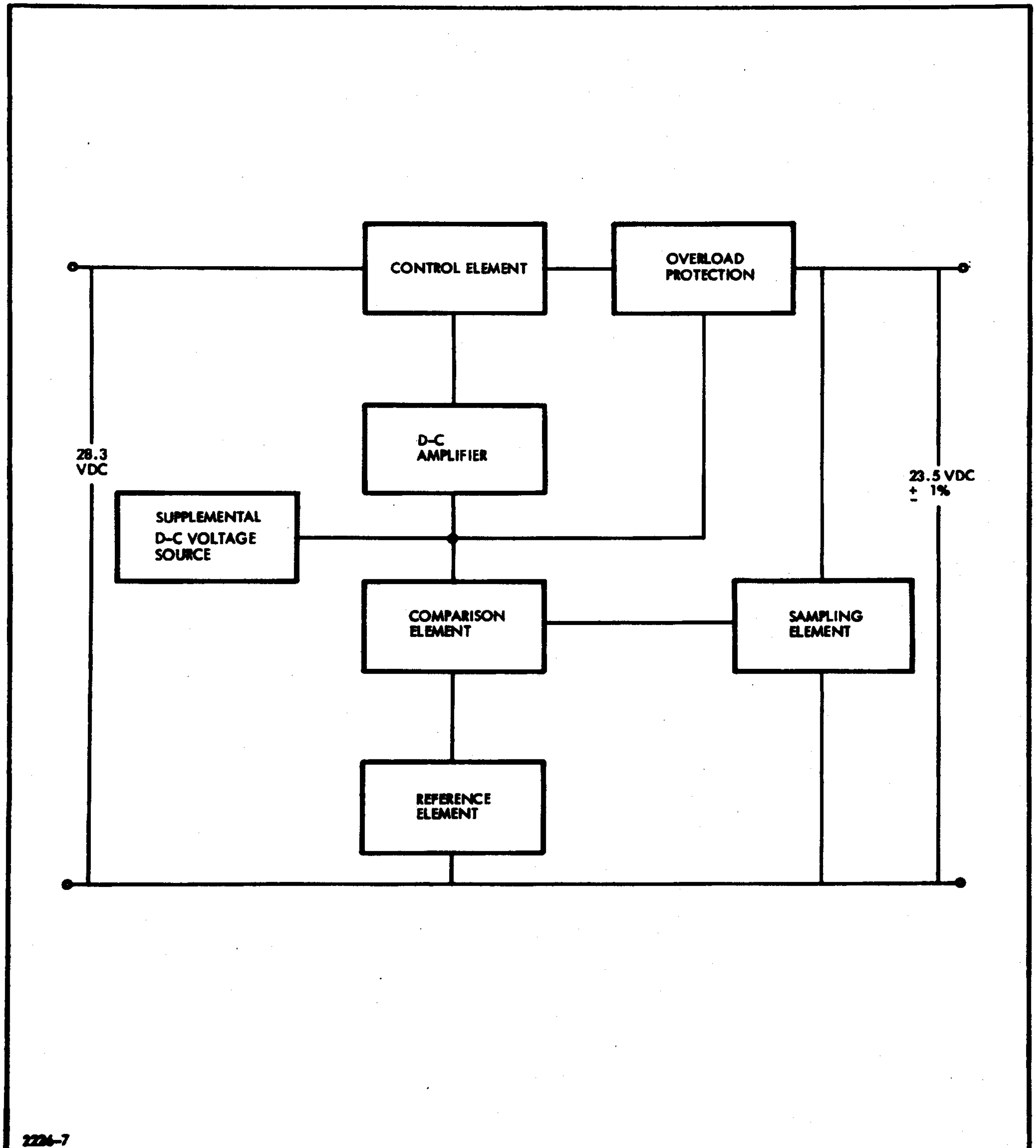


Figure 31 - Block Diagram of +23.5 Vdc Power Supply

series-regulator transistor for an overload or short-circuit condition on the output. The overload protection operates at a current of 7 to 8 amperes and recovery after overload is automatic.

The regulator is composed of seven functional elements: a sampling element, reference element, comparison element, supplemental d-c voltage source, d-c amplifier, control element, and an overload-protection circuit.

The voltage regulator, like a servoamplifier, uses an error or difference signal to correct any error in the output. The difference between a reference and a portion of the regulated output is detected and amplified by the comparison element and, if necessary, is further amplified by the d-c amplifier. The control element senses the magnitude and phase of the amplifier difference and regulates the load voltage in the proper direction to correct any voltage change.

The series control element regulates the current to the load so that the product of load current and load resistance remains equal to the required output voltage.

(c) -23.5 Vdc Regulated Power Supply

The -23.5 vdc regulated power supply is identical to the +23.5 vdc supply with the following exceptions:

1. The circuit was designed for a full-load current of 3.8 amperes
2. The primary power source for the regulator is 115 v, 2 kc, transformed down and then rectified by a full-wave bridge rectifier
3. The positive side of the output line was grounded and the return line used for the negative output voltage.

The regulator circuits are built on printed circuit cards with the exception of the control element and sensing resistors. Otherwise, being identical, the regulator circuits will operate with either primary source.

(d) +300 Vdc Power Supply

The +300 vdc power supply (Figure 32) operates from a +28.3 vdc ±2 percent source. A step-down transformer (located in the +23.5 vdc supplies) is used to supply 10-vrms, 2000-cycle power to the 300-vdc supply. The power drain on the 115-vac, 2000-cycle power is approximately 10 milliwatts. The supply is designed to deliver 30 watts of power.

The supply can be considered from an electrical viewpoint to be divided into two main sections. The first section is a simple series regulator. A transistor in series with the 28.3-vdc input is used to adjust the voltage level which is fed to the second section. The input voltage to the second section is regulated to maintain a constant (within ±1 percent) output voltage regardless of the 28.3 vdc input voltage.

The second section is a d-c to d-c converter. The converter is based on the "Jensen" circuit and as such employs two transformers. A small saturating transformer is used to set the chopping or switching frequency of the two power transistors which are used in this section. A second, nonsaturating power transformer steps the chopped voltage up to 300 volts. A full-wave bridge converts the square-wave voltage into a d-c voltage. A two-section inductance-capacitance network smooths the output and ensures low ripple on the output.

A resistor divider is used to obtain a sample of the 300-vdc output. This sample is fed back to the series regulator.

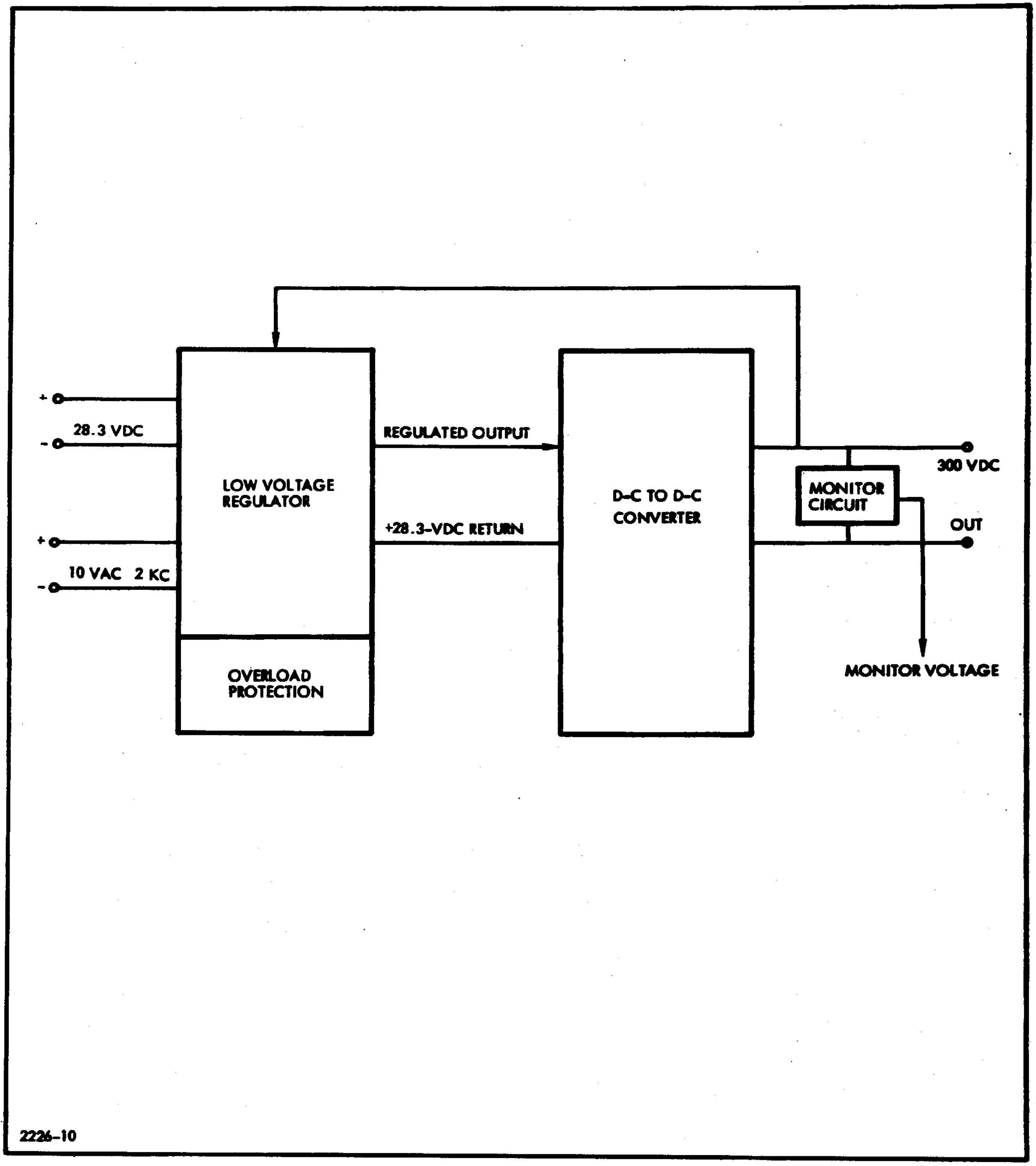


Figure 32 - Block Diagram +300 Vdc Power Supply

Semiconductor circuitry is used to control the base drive to the series regulator transistor mentioned above. The base drive is lowered if the output voltage is high and increased if the output voltage is low. In this manner it is possible to maintain a constant output voltage.

Overload protection circuitry is also employed. If the load current exceeds 120 to 160 milliamperes, a sensing circuit in the series regulator will halt the flow of base drive to the series regulator transistor. The supply is therefore protected from shorts which might accidentally be placed across its output terminals. The supply will function normally after the overload is removed.

(e) Timer Override Circuitry

The Control unit provides a means of overriding (by vehicle command) a timer-delay circuit in the Transmitter-Modulator unit of the slr (see Figure 30). When a 28-vdc signal is commanded through time-delay overload no. 2, nonlatching relay 6K3 is energized. When a 28-vdc signal is commanded through time-delay overload no. 3, nonlatching relay 6K4 is energized. The normally open contacts of the two relays form two breaks in a line connecting the time-delay overload no. 1 to an output which goes to the Transmitter-Modulator. When both relays are energized, a voltage level on the input lead is applied to the Transmitter-Modulator unit and the desired override function is accomplished. The two relays can be considered to form a three-input "and" gate.

(2) Electromagnetic Interference Considerations

Primary power from the vehicle is filtered (using Sprague rfi filters) in an rfi-tight enclosure (filter section, Figure 30) in the Control unit.

The filtering is accomplished before the primary power is distributed to other sections of the Control unit and to the other air units.

5. RECORDER

a. Mechanical Design

(1) General

The Recorder assembly (Figure 33) is composed of two major assemblies: the Recorder compartment and the film supply cassette. The Recorder compartment weighs approximately 75 pounds and consists of the basic casting, crt, transfer lens, film-transport and tension-control system, high-voltage power supply unit, and electronic-control components and their accompanying circuitry. The film supply cassette weighs approximately 24 pounds and consists of the housing casting and covers, film and spool, spool brake system and circuitry, light shield, guide roller, and a radius-sensing arm for monitoring the quantity of film remaining.

Figure 34 shows two views of the Recorder. The upper view is the unit mounted on its service stand. The lower view pictures the unit opened at the top to show the internal construction. The modular concept was selected to allow removal and/or replacement of component assemblies in a minimum time and with minimum adjustment. The film supply cassette is readily installed or removed by removing two threaded pins. The electrical connections are mated as the cassette is pivoted about the lower threaded pin. This pin also supports the weight of the cassette during handling and initial film threading. No mechanical or electrical adjustments are required with interchange of cassettes.

The electronic controls are housed in a separate package attached to the aft, right-hand side of the Recorder with electrical connectors on the upper surface. Printed circuit boards are accessible from

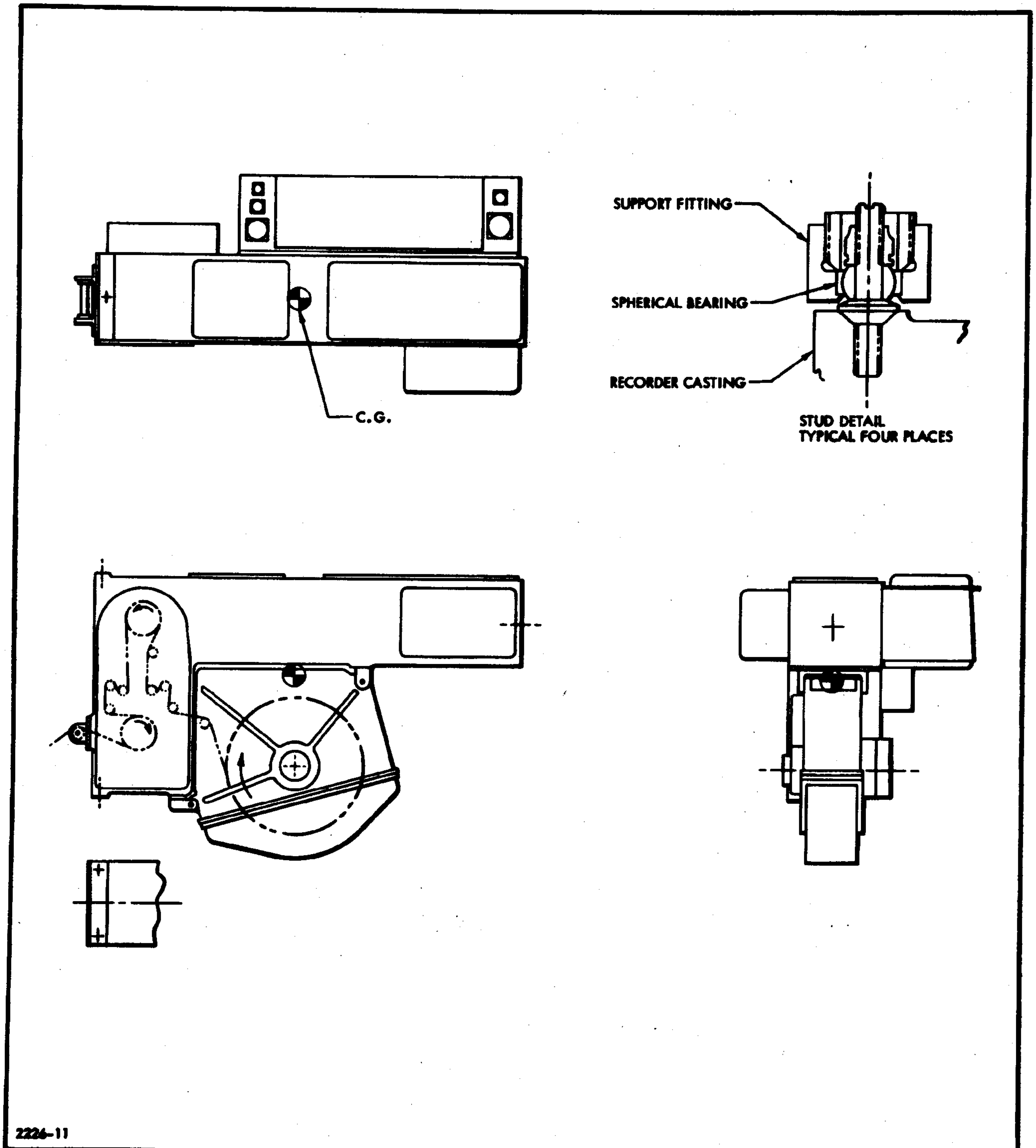


Figure 33 - General Arrangement and Mounting Stud Detail of Recorder

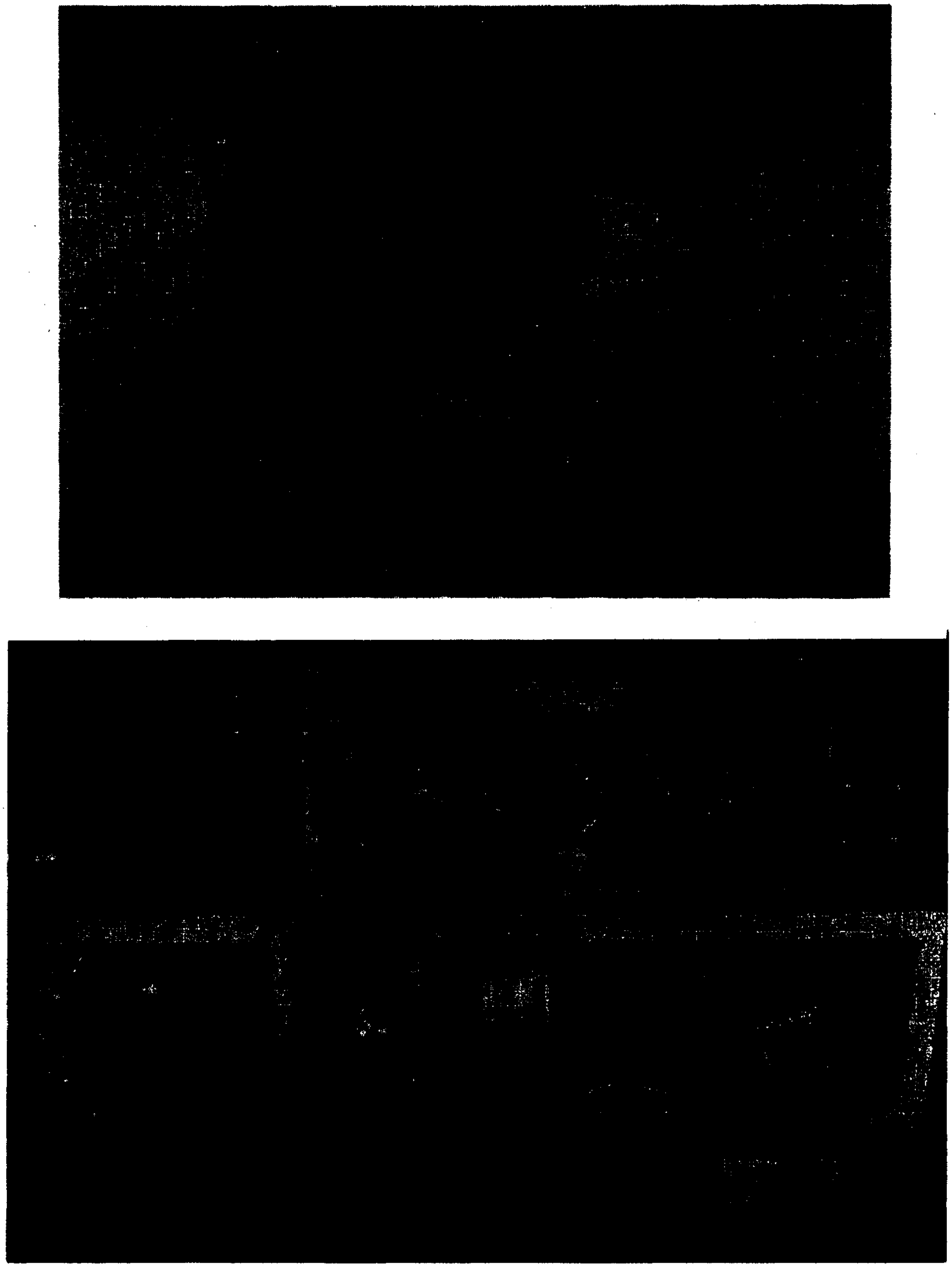

**Figure 34 - Recorder Unit**

the upper surface when the cover is removed. Two internal connectors handle all the wiring between the electronic control box and the Recorder to facilitate removal or replacement of the unit.

(2) Film Transport System

The film transport system is used to regulate accurately the speed of the film as it passes over an exposure drum and is exposed to the light from the crt through the optical system. The film transport system is depicted schematically in Figure 35. Operation of the film transport can be described in five parts: film supply, film drive, film-tension control, film transport drive, and film takeup.

(a) Film Supply

The film is stored in and supplied from the film supply cassette. Within the cassette is a film supply-spool brake assembly which contains a friction brake and a magnetic particle brake both in constant mesh with the spool shaft through a reduction gear assembly. The friction brake is applied when de-energized (recorder not operating) and released when energized (recorder operating). The magnetic particle brake is energized with the Recorder system and its braking torque regulated by a potentiometer connected to the pivot shaft of an input tension-control assembly input (refer to paragraph (c) following).

(b) Film Drive

The primary drive for the film is the metering drum. The metering drum drive (Figure 36) is powered by a hysteresis synchronous motor running at a constant 8000 rpm. An input roller drives the final friction disc through an opposed set of idler rollers. The final friction disc is keyed to the exposure metering drum which determines the film velocity (5.000 ±0.050 inches per second) of the system. The friction drive

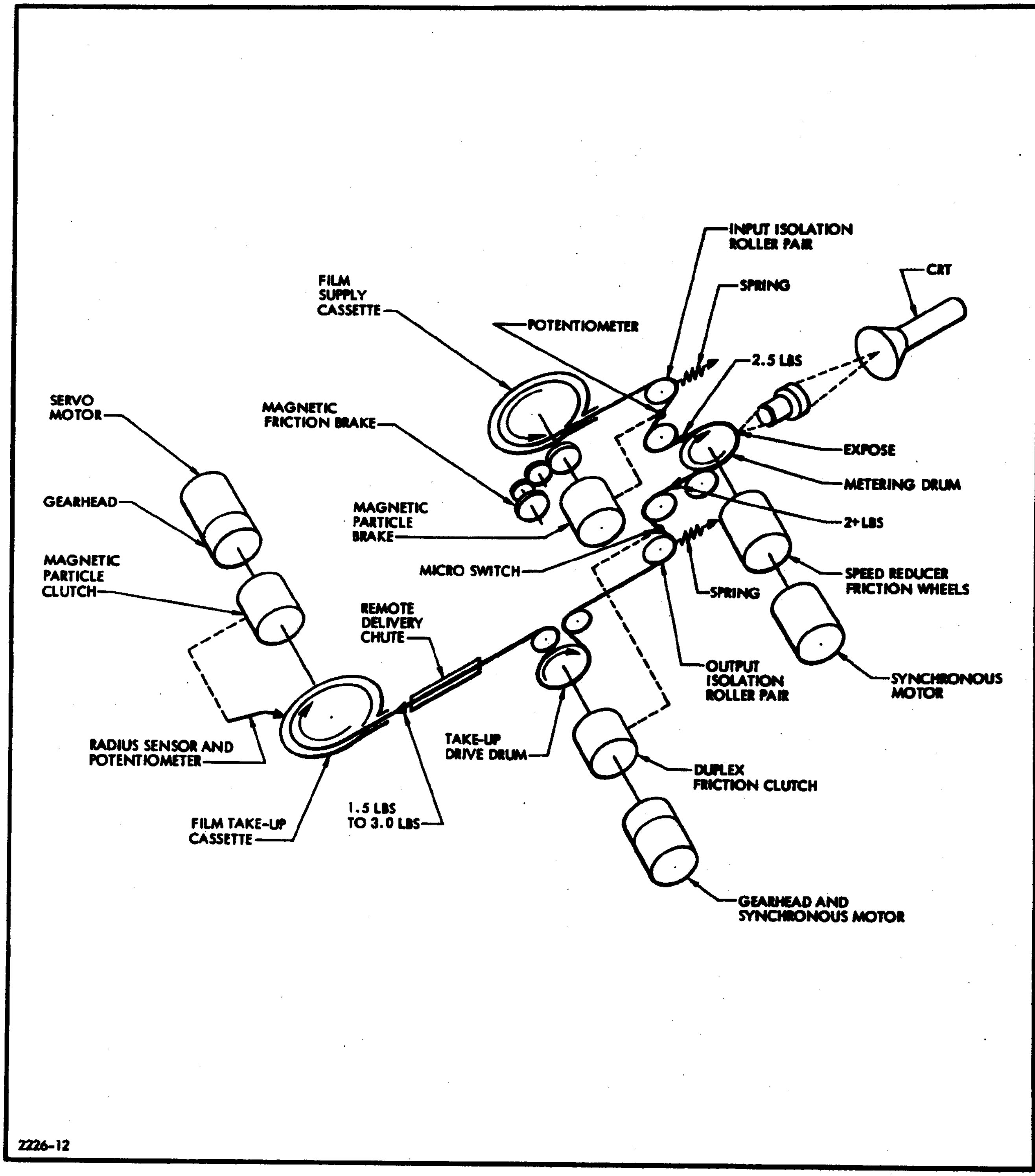


Figure 35 - Film Transport System

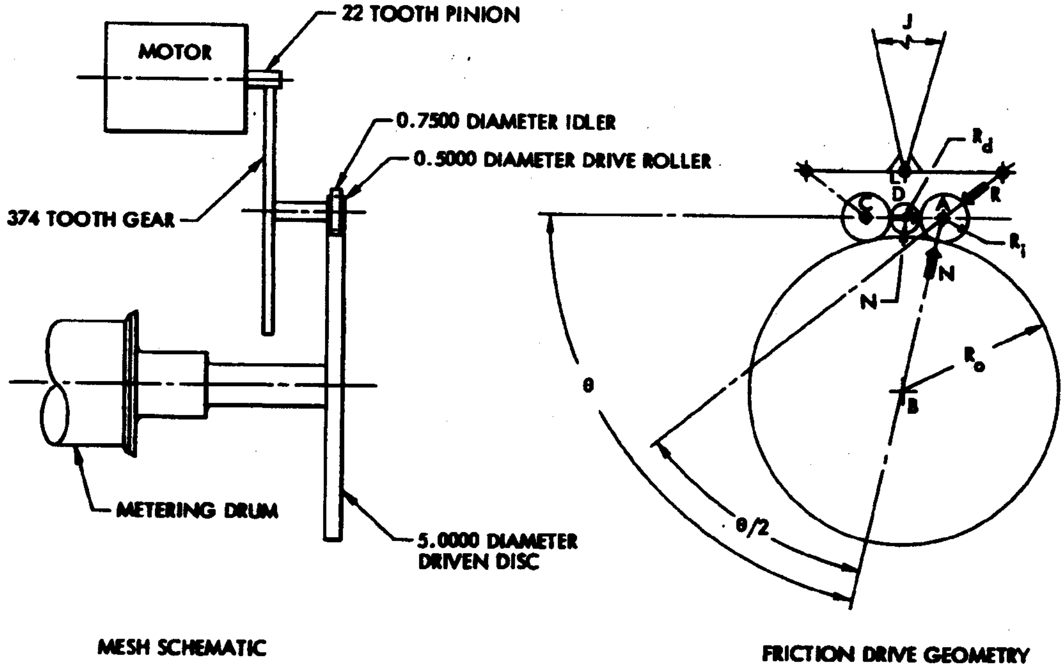


Figure 36 - Metering Drum Drive

of the final reduction was utilized to eliminate short-term velocity variances which could cause striations on the data film.

(c) Film Tension Control

Film tension is controlled (Figure 37) on both the input and output sides of the metering drum. The film tension-control assembly contains an input and an output set of balanced pivoting isolation rollers and three film guide rollers. The input set of isolation rollers (film supply spool control) activates a potentiometer connected to their pivot shaft. A preloaded pair of clock-type springs enable the isolation rollers to pivot as the film-supply tension varies and thus position the potentiometer for a compensating current to the magnetic particle brake. The output set of isolation rollers (film transport drum control) is similar to the input except that a cam is actuated by the pivot shaft to open and close a microswitch which is part of the output tension-control servo loop. The microswitch actuates a duplex friction clutch to change the film velocity as the pivoting rollers reach the limits of a predetermined angular displacement. The output tension-control servo motor tends to keep the film tension constant (2.0 pounds) on the output side of the metering drum and to isolate the film from changes of take-up tension in the film take-up mechanism.

The output-isolation roller and cam-operated switch operate in conjunction with the film-transport drum drive assembly to control the output tension.

(d) Film Transport Drive

The film transport drum drive assembly (see Figure 38) contains a hysteresis synchronous motor with an integral 40:1 ratio gearhead with a 200-rpm output. A gear on this output shaft meshes with the input gear on the duplex clutch. This clutch has two

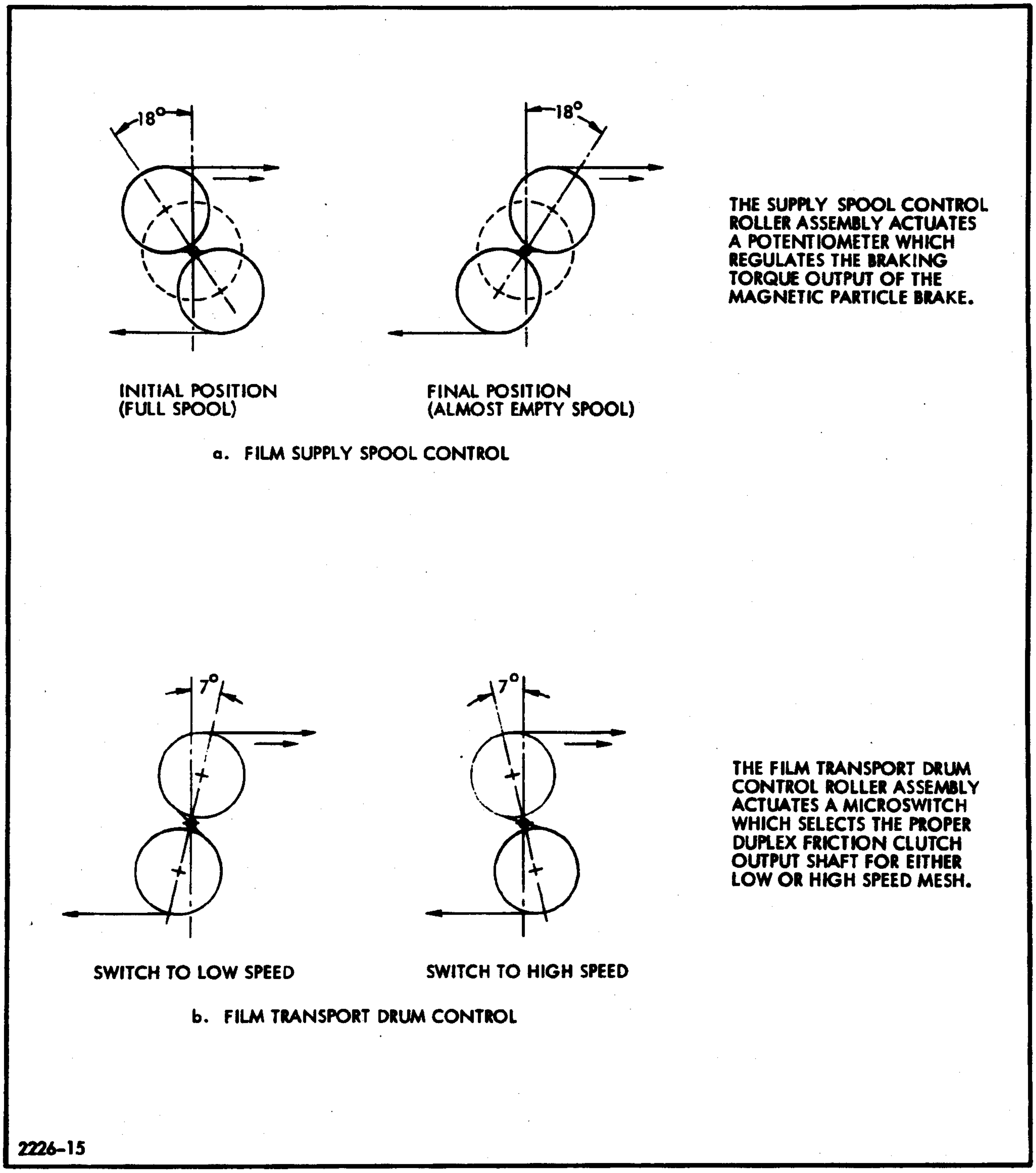


Figure 37 - Tension Control Roller Function

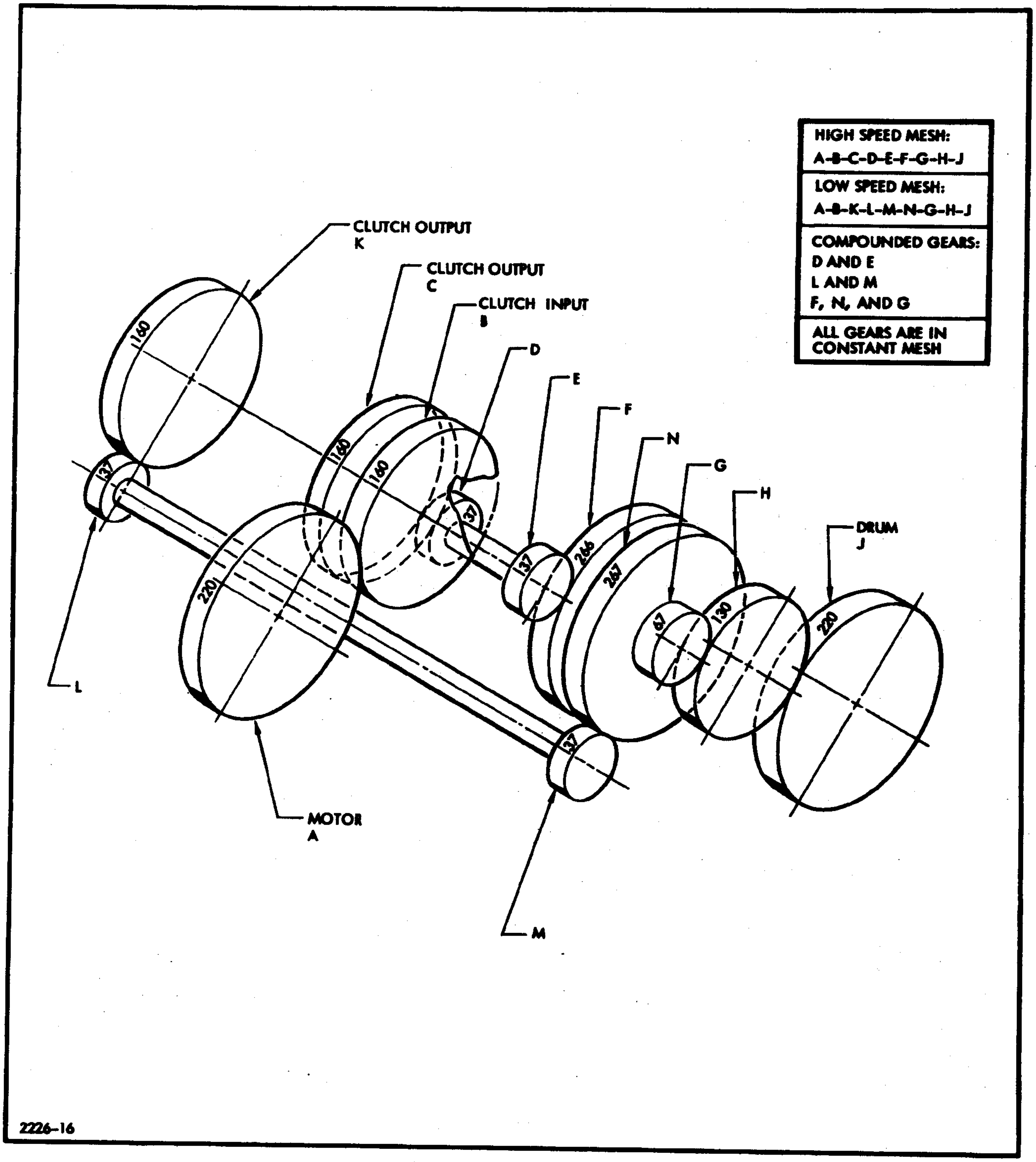


Figure 38 - Schematic of Transport Drum Drive

independent output gears meshing with 1:1 compounded gears. These gears are in constant mesh with their respective bull gear, one of which has 266 teeth and the other 267 teeth. This one-tooth difference creates a 0.375-percent change in the nominal film velocity to prevent a long-term accumulation or shortening of the film between the exposure metering drum and transport drum for proper isolation roller operation. The two bull gears are compounded on the same shaft with an output pinion gear which meshes with an idler gear which in turn meshes with the transport drum drive gear. As the duplex clutch is energized or de-energized by the microswitch on the output isolation roller, the power flow is directed through the appropriate gear train to increase or decrease the transport drum velocity. The idle gear train remains in mesh and free-wheels in the same direction as it does when it functions as the power train.

(e) Film Takeup

The recoverable capsule which contains the film take-up mechanism used in the flight equipment is not part of the KP-II side-looking radar. However, the slr ground-based operating equipment (GBOE) is supplied with a take-up cassette which provides a similar function and will be described here.

The ground-based film take-up cassette (Figure 39) utilizes many of the film-supply cassette parts. However, it is powered by a servo motor gearhead unit coupled directly to a magnetic particle clutch. The clutch output shaft is connected to the spool shaft through a 3.5:1 reduction gear assembly. The clutch output torque is regulated by a potentiometer which is actuated by a radius-sensing arm following the outer layer of the spooled film.

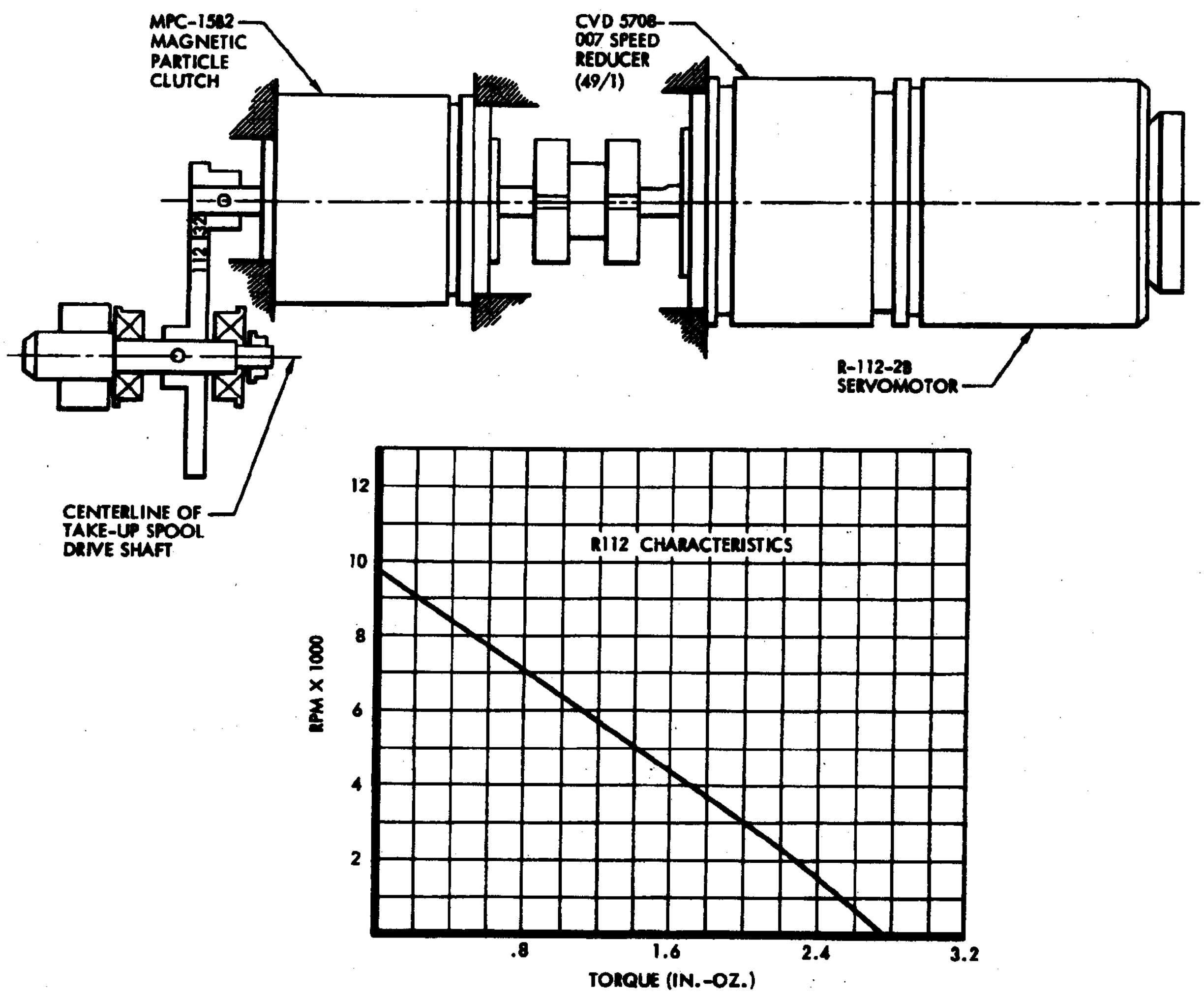


Figure 39 - Film Take-Up Cassette Drive System

The Recorder and take-up cassette for the GBOE units are mounted on a welded, aluminum-alloy service stand which incorporates castering wheels and positioning pedestals. This stand is also used for testing and calibration of the flight Recorders.

(3) Stress and Vibration

(a) Stress

The basic structure of the Recorder is a magnesium casting. This type of structure was selected because of the requirements for minimum weight, the need for dimensional stability and high local stiffening, and the requirement for light tightness.

Magnesium AZ91C-T6 was selected as the casting alloy because of its superior strength-to-weight ratio, inherent internal damping, and light weight.

The entire Recorder is mounted on four studs which have a tapered shoulder (see Figure 33). This shoulder mates with a countersunk hole in the recorder casting (1) to eliminate the possibility of having threads in direct shear and (2) to take out part of the bearing loads with a shoulder couple. The aft support has integrally-cast stiffeners to transfer the load from the extreme fibers of the section to the central boss where the mounting stud is located.

(b) Vibration

As vibrations and vibration-deflections within the unit were prime factors in the operation of the unit, it was necessary to test fully this structure in a rigid test fixture. The test fixture is a large magnesium casting roughly in the shape of a bent I-beam. The primary consideration of this fixture was a very low deflection at the expected loadings and as high a natural frequency as practical.

## b. Electrical Design

### (1) Operation

The operation of the electronic portion of the Recorder will be described by breaking it down into five major divisions: ramp generator, deflection amplifier, focus and intensity circuits, video and vertical-position amplifiers, and magnetic brake amplifier.

#### (a) Ramp Generator

The ramp generator (Figure 40) produces a linear voltage ramp which is proportional to the slant range to the target. The accuracy and stability which is required of the output wave form is provided by a stable, high-gain, d-c amplifier-integrator and controlled bias current.

The sweep trigger causes the bistable multivibrator (flip-flop) to open the switch across integrating capacitor $C_1$ in the feedback circuit of $A_1$, which is a three-stage, high-gain d-c amplifier (gain approximately 50,000). This allows the capacitor to charge through R1 and a stable and precise charging current is developed by the bias supply. An internal r-c feedback loop within the amplifier $A_1$ serves to further stabilize and maintain linearity of the wave form.

#### (b) Deflection Amplifier

The rising linear output from the ramp generator is fed to the deflection amplifier $A_2$. This amplifier is a stable, high-gain, d-c feedback amplifier that provides deflection signals to the crt yoke. Nonlinear feedback is provided so that the amplifier gain may be varied as the crt spot is deflected from the center of the tube, thereby compensating for the nonlinearity introduced because of the flat face of the crt. The nonlinear feedback network which produces the so-called "Flat-Face Correction" is

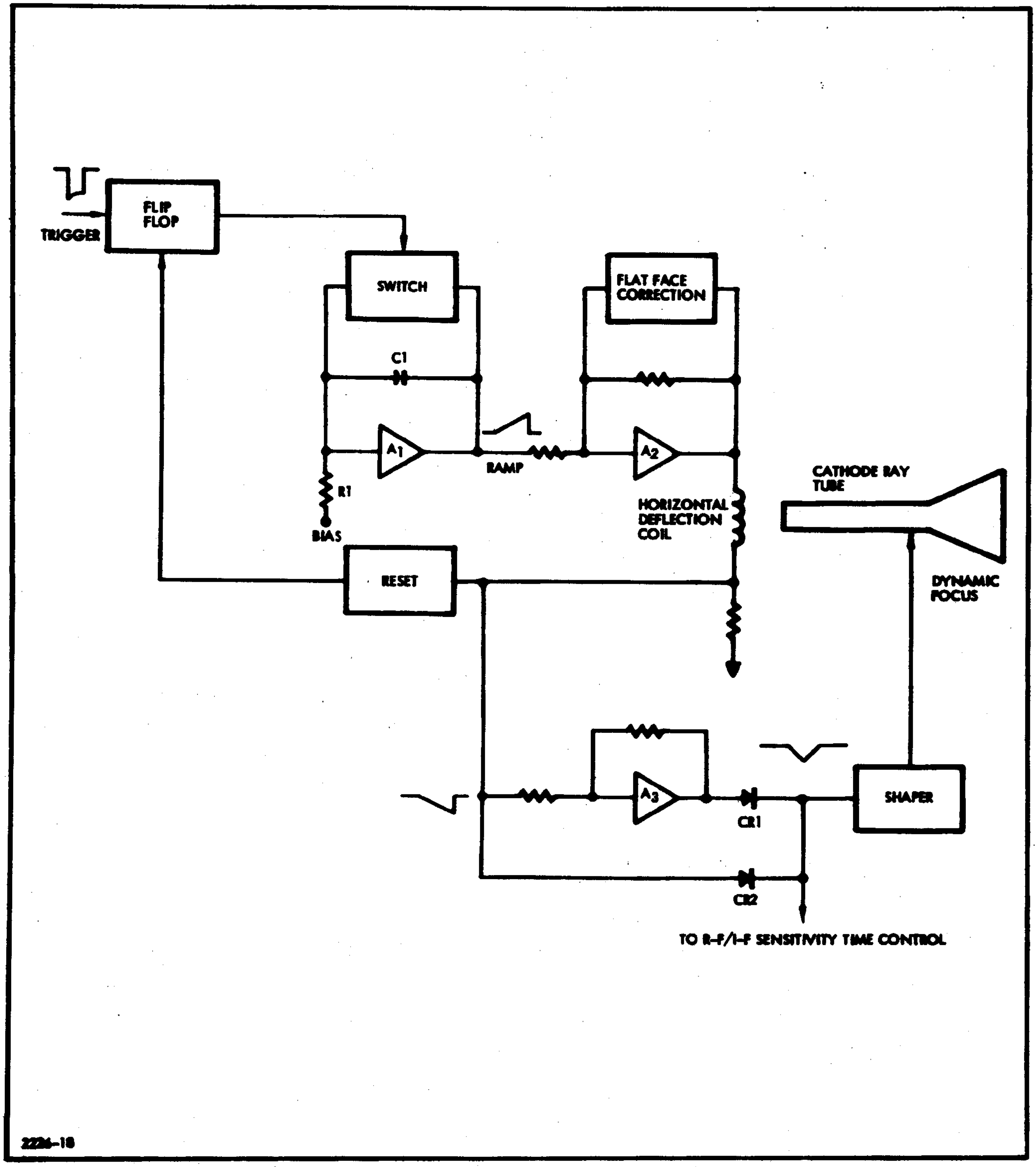


Figure 40 - Recorder Sweep Circuits

a symmetrical one using diodes (eight) and resistors to provide a linear sweep throughout the entire range. The deflection-amplifier output is used to reset the bistable multivibrator thereby cutting off the sweep and preparing the ramp generator for the next sweep cycle.

(c) Focus and Intensity Circuits

The Recorder crt focus and intensity unit is comprised of two separate functional circuits which provide dynamic focus and a crt intensity gate.

The crt exhibits spot defocusing at the sweep extremities caused by the flat-plane display surface and resulting beam-path length differences. This defocusing effect is eliminated by generating a dynamic focus signal which has a parabolic wave shape and feeding it to the focus anode of the crt.

The required focus control signal must be symmetrical about the sweep center and is derived from the deflection current wave form.

As the deflection signal is symmetrical about zero, the negative portion is passed through diode CR1 and inverted by amplifier $A_3$. The positive portion is passed through diode CR2 and added to the inverted signal to provide the V-shaped signal. This signal is used in the R-F/I-F unit as a stc signal. This V-shaped signal is also fed to a biased diode circuit which gives a parabolic shape to the slopes of the V. The parabolic V-shaped wave form is in turn applied to the two-kilovolt focus anode voltage source to compensate for the defocusing at the extreme portions of the sweep.

The crt display is held blanked off at all times except during a deflection sweep. The deflection drive signal generates a voltage gate. This voltage gate signal is fed to the crt cathode, unblanking the crt during the sweep time and intensifying the sweep to the desired viewing level.

(d) Video Amplifier

The video amplifier, which has a 10-kc to 12-mc 3-db band width, accepts the video output from the Reference Computer and linearly amplifies up to outputs of 6 volts peak-to-peak. For output signals greater than this value, limiting is done by a diode bridge which reduces the gain of the amplifier and prevents excessive swing of the crt grid. The gains in the system, however, are chosen to allow most of the limiting to be done by the data film rather than by this video circuit.

(e) Magnetic Brake Amplifier

The magnetic brake amplifier assists in maintaining a constant film tension as the film is passed through the input isolation roller assembly. This is achieved by using a d-c feedback amplifier whose load is the magnetic particle brake coil and whose input is approximately proportional to brake tension.. This input is from the potentiometer which is mechanically coupled to the isolation-roller assembly so that as the tension is increased, the current is decreased in the brake coil, thereby decreasing the drag and compensating for the change in tension.

## SECTION VIII - VOLTAGE BREAKDOWN, POTTING, AND PRESSURIZATION

### 1. GENERAL

Initial design-phase assumptions were (1) that the radar units would be operating at pressures below $10^{-6}$ mm Hg, and (2) hermetic sealing and potting (or alternately pressurization) would not be required to prevent high-voltage breakdown.

Subsequent investigations indicated the possibility that higher pressures might be encountered in the confined space within the Agena because of outgassing materials. As complete data were not yet available for the actual pressure, it was necessary to design the equipment to operate at higher pressures. Accordingly, the specification was changed to cover the range from $10^{-1}$ to $10^{-8}$ mm Hg.

### 2. EARLY TEST RESULTS

Tests were conducted at pressures ranging from 2 mm Hg to $10^{-4}$ mm Hg on each of the radar system units. These tests showed that many design changes would be required to ensure proper operation at the higher pressure limit of the specification. Ionization occurred in some of the r-f driver stages of the varacter frequency multiplier at pressures of 2 mm Hg and at voltages as low as 50 volts. This caused severe circuit loading and reduced the output to near zero. Figure 41(a) is a frequency multiplier which was tested. Figure 41(b) shows the same multiplier operating in the darkened interior of the altitude chamber. The Transmitter-Modulator at 2 mm Hg pressure also tended to break down at very low input voltages. Figure 41(c) is the Transmitter-Modulator operating in the altitude chamber. For this test, the high-voltage power supply voltage was reduced from the nominal 4300 volts to 500 volts dc. The photograph shows the corona pattern around the hydrogen thyratron.

In the following paragraphs, the design of each of the five radar units as influenced by the voltage breakdown problem, will be discussed.

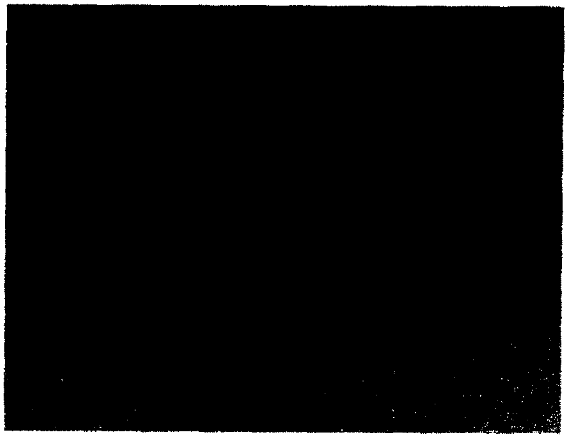

(A) FREQUENCY MULTIPLIER

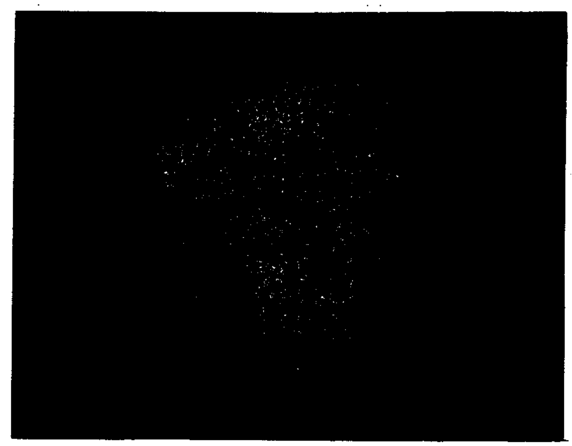

(B) FREQUENCY MULTIPLIER OPERATING IN ALTITUDE CHAMBER

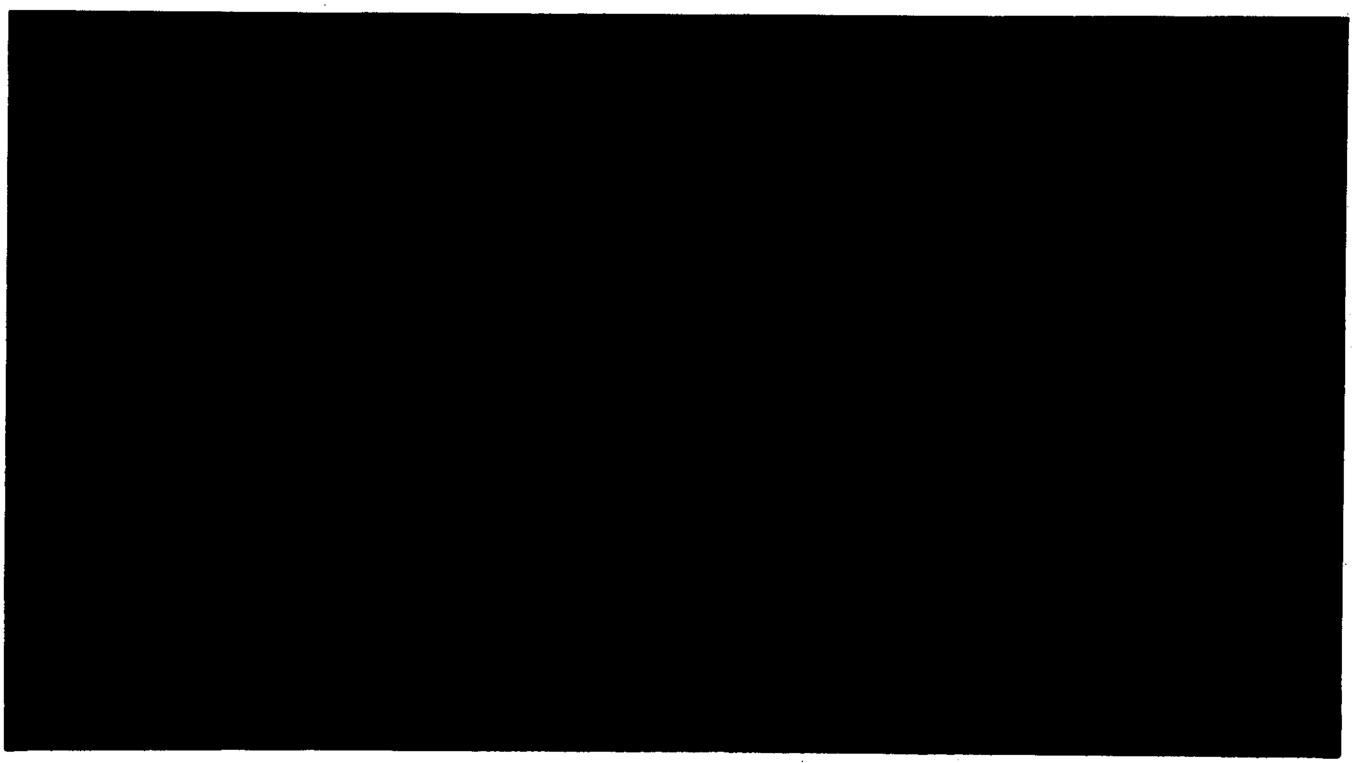

(C) TRANSMITTER-MODULATOR OPERATING AT ALTITUDE

**Figure 41 – Examples of Voltage Breakdown at Altitude**

## 3. TRANSMITTER-MODULATOR

### a. Potting versus Pressurization

Because of the very high pulsed voltage involved in the Transmitter-Modulator (up to 30 kv), it was decided that two design approaches would be investigated. The first of these approaches made use of a pressurized container in which the entire Transmitter-Modulator unit would be mounted. Figure 42 shows a mock-up of the pressure container which was fabricated.

The second approach used various potting techniques to totally encapsulate all exposed high voltage areas. This method was finally adopted and the pressurized container development was discontinued.

### b. Initial Potting Investigation

First potting attempts utilized RTV 211 silicon rubber encapsulation for all high-voltage components with interconnecting leads integrally potted. The other end of the lead was soldered to an exposed terminal and then protected by a slip-on boot which was potted in place. This arrangement solved the high-voltage breakdown problem at the higher pressure limit of the specification but a glow discharge was still present. It was felt that this glow discharge might eventually deteriorate the potting compound and might also result in r-f interference to the radar or to other subsystems in the satellite.

For complete suppression of corona in this unit, it was found necessary to provide (1) grounded shields potted in place around all interconnecting leads, and (2) shields around the potted high-voltage components. The leads were terminated on the components by means of high-voltage connectors. These leads were in turn inserted into the connectors and potted in place.

### c. Final Potting Configuration

(1) General

Extensive study and experimentation was required before final potting processes, materials, and configuration could be established. It was

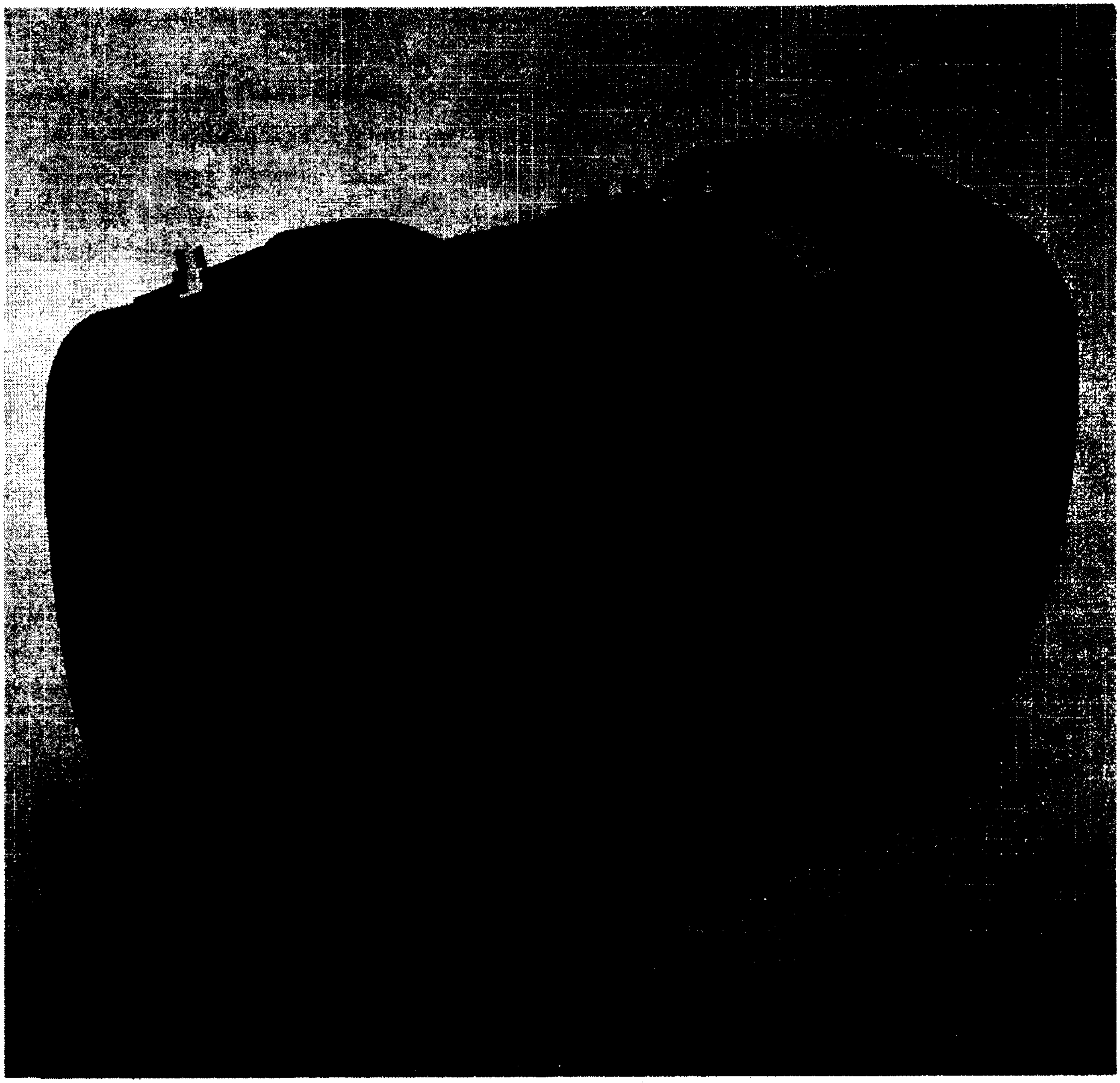

Figure 42 - Transmitter-Modulator Pressurized Container Mockup

found that extreme care was necessary to eliminate voids in the potted components. Special procedures were followed to provide for:

1. Adequate cleaning (sand blasting and vapor degreasing) of all parts prior to potting
2. Proper application of primer material
3. Proper mixing and multiple degassing of potting materials
4. Correct temperatures for cure cycles.

Additionally, the choice of mechanical configuration of the metal shield surrounding the component is an important factor in the elimination of voids.

(2) Potted Components

The diode assembly (used as the charging diode and inverse diode) required several design changes before high voltage breakdown could be eliminated. The problems were eliminated by redesign of the metal container to avoid entrapment of air bubbles around high-voltage terminals. The potting compound was changed from RTV 211 to a four-part Scotchcast epoxy compound. This diode assembly is pictured in Figure 43(a) along with a typical shielded and potted lead.

The grid and plate choke configurations were changed to allow for proper venting of air bubbles during the pumping operation. These assemblies are pictured in Figures 43(b) and 43(d).

The potting of the hydrogen thyratron was extremely difficult because of the high temperatures (550 degrees F) involved. For this application Sylgard 183 was used because of its high temperature characteristics. The originally designed round metal container for the thyratron ruptured because of thermal expansion of the potting material. This problem was eliminated by use of a square can with a flexible braid shield over the open top to allow for expansion of the potting material. (This thyratron assembly is shown in Figure 43(c).)

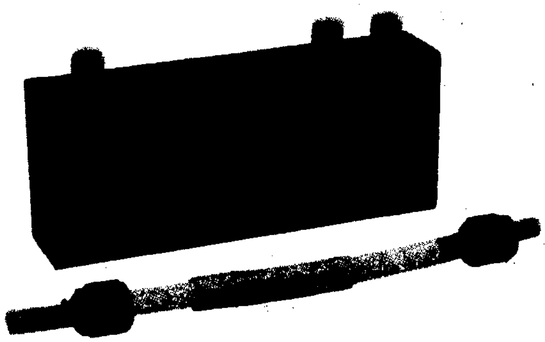

(A) DIODE ASSEMBLY AND LEAD

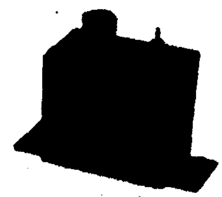

(B) GRID CHOKE ASSEMBLY

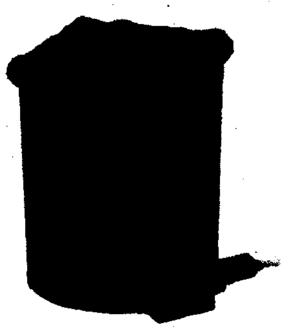

(C) POTTED THYRATRON ASSEMBLY

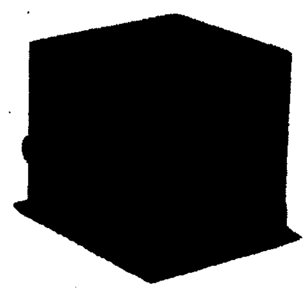

(D) POTTED THYRATRON PLATE CHOKE

**Figure 43 - Metal Shielded Potted Components**

(3) Circuit Board Coating

To prevent accidental short circuiting and corona discharge, the circuit boards are coated with 3M5072 Scotchcast material to a minimum coating thickness of 0.050 inch. Interconnecting wires from circuit boards are integrally sealed into the board coating.

(4) Pulse Components

The pulse transformer, pulse forming network (pfn), and charging choke are hermetically sealed, oil filled components. Each of these components uses a bellows to allow for thermal expansion of the oil. These components are potted with epoxy sand. This is silica sand with epoxy coating around the individual granules. Heat causes the granules to join together, forming a porous solid into which the oil can be introduced. The epoxy sand serves two functions: it reduces the oil expansion problem, since less oil is required to fill the unit, and it provides mechanical support for interconnecting leads and other parts. Additional potting is required around the high-voltage terminal of the pulse transformer to prevent voltage breakdown.

(5) Klystron Potting

High voltage breakdown around the cathode of the klystron presented a severe problem late in the program. It was found that the vendor had used a coating of silicon grease around the cathode high-voltage terminal during initial testing of the tube. After the testing was completed, the terminal was improperly cleaned and potted by the vendor. The thin layer of grease which remained after cleaning prevented the potting from adhering to the terminal and subsequently caused a failure.

Figure 44 shows the potting removed from the klystron cathode to expose the failed section. To correct the problem, all klystrons were stripped, thoroughly recleaned (using a degreaser and an abrasive detergent and water) and repotted.

4. R-F/I-F UNIT

This unit and the other units of the radar system make use of techniques similar to those used in the Transmitter-Modulator. Four sections of the R-F/I-F unit required special consideration because of the high altitude environment:

1. The 2000-vdc power supply which provides the high voltage to the various elements of the twt was potted to prevent electrical breakdown by arcing and corona.

[redacted]

Figure 44 - Voltage Breakdown at Klystron Cathode

2. The high-voltage divider which distributes the 2000 volts to the various elements of the twt was also potted to prevent electrical breakdown by arcing and corona. Figure 45 shows the assembly ready for potting.

3. The end of the twt where the leads enter the tube envelope were vacuum potted.

4. The frequency multiplier had to be potted in a certain portion of the r-f circuits. This problem was discussed in paragraph 2:. Early Test Results. Potting with a closed-cell foam reduced the tendency to ionization, without adding a great deal of dielectric material and allowing the circuits to be retuned with the potting material present. The potting also solved a vibration problem by providing better support for the component parts. A potted frequency multiplier is shown in Figure 46.

5. RECORDER UNIT

The Recorder unit was given special consideration in the following areas:

1. The high-voltage supply which contained voltages of 10 kv and 2 kv was potted with an epoxy compound.

2. The high-voltage leads to the crt were potted at the points of connection to the tube with RTV 501 silicon rubber compound.

3. All other points having voltages above 200 volts were potted. These included terminal strips, circuit boards, and connectors.

6. REFERENCE COMPUTER AND CONTROL UNITS

Since these units do not contain voltages above 300 volts the usual methods were used for coating of circuit boards, terminal strips, etc. Humiseal was used on all of the terminal boards as protection against accidental shorting.

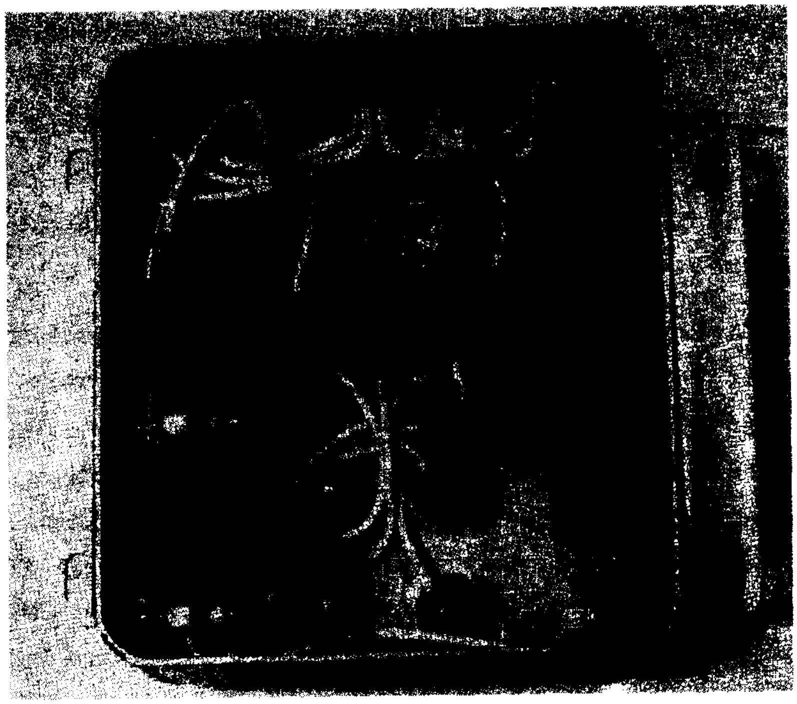

Figure 45 - Voltage Divider Assembly

[redacted]

Figure 46 - Foam-Potted Frequency Multiplier

## SECTION IX - RELIABILITY STUDIES

### 1. GENERAL APPROACH

As mentioned in Section I: Introduction, the KP-II radar is an adaptation of the AN/UPQ-102 radar. As the development period for redesign of the AN/UPQ-102 radar to the KP-II requirements was limited, steps were taken to achieve the highest practical reliability consistent with the Agena program schedule. Included were the following procedures:

1. Inherent reliability was developed by adequate derating and circuit review during the design phase
2. Sources for the electrical piece parts were restricted to vendors known for their high quality levels
3. The Reliability Group coordinated with the Quality Control Department to ensure that any observed deficiencies were corrected.

### 2. RELIABILITY PROGRAM FUNCTIONS

#### a. Reliability Analysis and Prediction

During the design study phase the reliability of system configuration was computed based on estimated parts population and average failure rates applicable for the environment. The mean-time-between-failures (mtbf) goals for the radar system and for the individual system units are shown in Table XVI.

After completion of the design phase, the final mtbf was calculated based on actual parts population and actual stress levels for these parts population and actual stress levels for these parts. Results of this are also summarized in Table XVI. Mechanical items are included in the mtbf calculation.

TABLE XVI - MEAN-TIME-BETWEEN-FAILURES CALCULATIONS

| Radar unit | MTBF goal (hours) | Final MTBF prediction (hours) |
|---|---|---|
| Transmitter-Modulator | 555 | 841 |
| RF-IF | 752 | 609 |
| Reference Computer | 833 | 717 |
| Control | 1250 | 1985 |
| Recorder | 604 | 724 |
| System | 150 | 164 |

It will be noted that the prediction exceeded the mtbf goal for several of the individual units and the over-all system. This prediction is conservative for the following reasons:

1. The prediction was based on a 212 degree F environment for all units mounted in the barrel section. An environment of 140 degrees F was assumed for the Recorder which was mounted in the conical section. Flight data show that the actual box temperatures were considerably cooler than those assumed for the prediction.

2. The signal conditioning circuitry is included in this prediction and the system would continue to operate properly even if the signal conditioners failed. The signal conditioning circuitry was designed so that a failure could not reflect a malfunction in the circuitry being monitored.

Reliability (or probability of success) is defined as

$$R = \exp\left(-\frac{t}{mtbf}\right) \tag{89}$$

where t is the mission operating time. For small values of t, Equation (89) can be simplified to

$$R = 1 - \frac{t}{mtbf} \quad . \tag{90}$$

The probability of success can be calculated using the system mtbf of 164 hours and an average operating period of 2.25 minutes. Based on these values the probability of at least one successful operating period is 0.9998.

## b. Component Part Engineering

During the study phase derating schedules were given to design engineering for all component parts used in the system. Special parts were selected as required.

Environmental considerations for finishes and materials were closely coordinated with LMSC to eliminate those materials which might degrade performance. Such materials as cadmium and zinc chromate were eliminated wherever possible. Mechanical parts requiring lubrication were lubricated with Apiezon greases.

During development considerable effort was expended to eliminate high-voltage breakdowns. Three primary problem areas were:

1. The high-voltage components and leads in the Transmitter-Modulator circuitry
2. The traveling wave tube and power supply in R-F/I-F unit
3. The cathode ray tube and power supply in the Recorder unit.

The potting methods which were developed satisfactorily solved these problems.

(1) Derating Information

Recommended types and derating schedules for high-usage parts are given in the Goodyear Aerospace Corporation AAP 17051: Component Parts Handbook. These derated stress levels are equal to approximately 80 percent of the military specification ratings for a 212-degree F environment. These stress levels are consistent with those used by LMSC in space applications.

(2) Component Selection

(a) Tantalum Capacitors and Semiconductors

Tantalum capacitors and semiconductors as a category have higher failure rates than the other component parts used in the system. Consequently, the special considerations described below were used to upgrade the reliability of these parts.

Tantalum capacitors having hermetically sealed construction were used throughout the system. Also, for additional reliability improvement, a current limiting resistance was used in series with all dry-tantalum capacitors.

Semiconductors were given X-ray testing and 250-hour high-temperature storage tests when these tests would improve the reliability. Only units which passed the X-ray test were given the high-temperature storage tests. After the high-temperature tests, the following criteria were used as a basis for rejections:

1. 100 percent increase in reverse leakage
2. Beta changes greater than -10 percent or +20 percent
3. Instability.

The X-ray rejection rate varied from 0 to 100 percent. The rejection rate for electrical characteristics after high-temperature storage test ranged from 0 to 100 percent. The average rejection rate was approximately 18 percent in each category.

(b) Relays

To upgrade reliability, all relays for use in the KP-II radar system were purchased with the following special test requirements:

1. 5000 cycles operational burn-in at -85 degrees F with no misses allowed
2. 5000 cycles operational burn-in at 257 degrees F with no misses allowed
3. Helium leak rate approximately $1 \times 10^{-8}$ cc/sec depending on the specific relay type.

(c) Connectors

Connectors selected for the system include Deutsch DTK series and Bendix PT-SE series for the external connectors. Module connectors internal to the system are Cannon DM series. The finish for connectors and other hardware was selected to avoid cadmium plating whenever possible.

c. Stress Analysis

Stress analysis was performed on every circuit to determine that all electrical stresses were within the derating limits established by the components engineer. During these calculations the following conditions were considered:

1. Power supply excursions
2. Initial tolerance and long-term drift
3. Ambient temperature.

Before schematics could be released for production they were reviewed by a Goodyear Aerospace Design Review Board. A member of the Reliability Group attended these meetings and approved the circuit for electrical stress.

Any parts having a stress level higher than that allowed by the derating schedules were changed before the drawing was approved for release.

d. Failure Reporting

Failed parts were forwarded to the Reliability Group. These parts were tested to determine if there was a failure and, if so, whether it resulted from improper application or a circuit deficiency. The necessary follow-up action was taken.

Vendor follow-up was taken to correct an observed deficiency in a purchased part. Reliability improvements on the AN/APQ-102 radar program were incorporated into the KP-II equipment where applicable.

e. Program Controls

The reliability engineer assured the effectiveness of the program functions by signature approval of the following:

1. Parts lists and purchase requisitions
2. Schematics and assembly drawings
3. Engineering Orders changing a released drawing
4. Specification control drawings
5. Vendor and subcontractor data.

## 3. RELIABILITY PERFORMANCE

The confidence level in an mtbf calculation based on only one system would be low and almost without statistical significance. Therefore, no attempt will be made to establish a demonstrated mtbf for the flight system. This discussion will be concerned primarily with evaluating information from the field and the steps taken by Goodyear Aerospace to ensure a high degree of confidence that the systems will operate properly during flight.

a. System Operating Times

Table XVII tabulates by unit the operating time after delivery to LMSC.

TABLE XVII - SYSTEM OPERATING HISTORY BY UNIT

| Unit | Serial number | Total hours of operation | Time in vacuum (hours)* | | |
|---|---|---|---|---|---|
| | | | Soak | Warm-up and pre-operate | Operate |
| Transmitter-Modulator | 300-4 | 282 | 48 | 6 hours 11 min | 1 hour 37 min |
| RF-IF | 400-5 | 231 | 162 hours 25 min | 5 hours 6 min | 7 hours 21 min |
| Reference Computer | 500-3 | 508 | 121 | 4 hours 52min | 2 hours 13 min |
| Control | 600-3 | 245 | 152 | 6 hours 3 min | 2 hours 44min |
| Recorder | 700-3 | 358 | 165 | 6 hours 58 min | 2 hours 46 min |

*Data prior to flight. Times shown include only operation after last significant change to the unit configuration.

The total hours operation shown in Table XVII demonstrate that system performance is not degraded by several hundred hours of operating time. All units had also operated in vacuum for several times the total flight operating period.

(1) Discussion by Unit

(a) Transmitter-Modulator (A300-4)

The soak time for the Transmitter-Modulator is considerably less than any other units. Potting difficulties with the high-voltage parts (diodes and klystron) and pulse transformer failures resulted in several changes to the unit configuration. The tabulated times for this unit are the times after the last pulse transformer replacement. Table XVII listed 48 hours soak time on this unit. However, most components in the unit had 136 hours soak time, 10 hours warm-up and pre-operate, and 3 hours and 41 minutes operation in vacuum.

To ensure configuration control on the pulse transformers, an engineer was sent to the vendor's plant to inspect the units before they were sealed. X-ray examination was utilized for receiving inspection to determine the bellows position.

(b) RF-IF (A400-5)

This unit was used in all system tests conducted at the LMSC facility. No failure occurred in the unit; however, intermittent malfunctions were observed on the high-voltage and power-output conditioned signals. These malfunctions consisted of a single transient of short duration.

On December 8, 1964, this unit was received at Goodyear Aerospace and extensive vacuum testing was done. The unit received 17 hours and 25 minutes vacuum soak time plus 4 hours and 37 minutes of operate time. The equipment was being cycled on and off with various duty cycles. No transients occurred during the first 2 hours and 43 minutes of operation. After a 10 hour and 37 minute soak between operating periods, 8 transients occurred during the first 21 minutes of warm-up and operation. Generally these transients were observed in both the power-output and high-voltage conditioned signals. There were no more malfunctions during another 1 hour and 33 minutes of operating time. These data indicate that the malfunction may be temperature dependent. However, no cause for the malfunctions was determined. It was believed that this intermittent transient condition would not jeopardize the radar performance.

(c) Reference Computer (A500-3)

This unit also was used in all system tests. Minor resistance value changes were made in three modules shortly after delivery. The single side band module had to be realigned after 443 hours of operation because of system grounding changes.

(d) Control (A600-3)

This unit was used in all system tests. The rfi filters in the 400-cycle power leads for this unit were replaced because of oil leaks. The oil leaks produced a slight change in the filter capacitance. This resulted in power factor changes in the 400-cycle inverter which supplies power to the radar system. The power factor changes in turn caused the output voltage to vary. This voltage variation caused the crt in the Recorder to defocus.

(e) Recorder (A700-3)

The rfi filters in the 400-cycle power leads for this box were also removed to eliminate possible interaction with the 400-cycle inverter. The filters removed from this and the Control unit were tested and found to be within electrical specifications.

A failure occurred in the rfi filter on the +300 volt line. This failure resulted from overheating of the terminals when the filter was soldered into the circuit. A squeak developed in the film supply spool and a new spindle and bearing were installed. The meter drum drive assembly was exchanged a number of times to determine the optimum unit drive assembly for the first flight.

**b. Conclusions**

It is believed that X-ray inspection contributed significantly to controlling the quality of semiconductors. X-ray inspection was a valuable method of mechanical configuration control of larger components such as the high-voltage diode assemblies and high-voltage pulse transformers.

Extensive testing in vacuum proved to be an effective way to build confidence in the system's electrical performance capability. This testing did not degrade the performance capability since there are no limited-life components in the system.

During the flight, the equipment demonstrated the ability to operate properly after several hundred hours of preflight testing. This is an excellent indication of long service life for the equipment.

# APPENDIX I

## CHRONOLOGY OF DEVELOPMENT HISTORY

This page intentionally left blank.

## 1963

### January

Work started on program on January 15.

### February

First system block diagram drawn up.
Power and temperature studies begun.
Design concept of film drive established.

### March

Prf, slant range, and depression angle selected.
Modulator design parameters established.
System test points and telemetry signals selected.

### April

Effort concentrated on system interconnections, control circuitry, and parts specifications.

### May

Circuit development 90 percent completed on Reference Computer.
Peak of engineering manpower reached.

### June

Structural mock-up of R-F/I-F unit completed.
Engineering model of Transmitter-Modulator begun.

### July

Final revised system specifications and work statement distributed.
First set of Transmitter-Modulator pulse components received.
Tests of structural Transmitter-Modulator revealed excessive vibration.
Reference Computer and Control units engineering models started.

## 1963

### August

Major emphasis placed on preparation of qualification and acceptance test documents.
Vibration problem encountered on Reference Computer printed circuit boards.
Potting versus pressurization studies authorized for Transmitter-Modulator.

### September

Transmitter-Modulator redesigned for center-of-gravity mounting using vibration isolators.
Traveling wave tube power supply (2 kv) experienced voltage breakdown at low pressure.
R-F/I-F and Control units engineering models completed

### October

Diagonal mounting using vibration isolators selected for R-F/I-F unit following extensive tests.
Reference Computer and Control unit qualification units completed.

### November

First system tester and maintenance testers completed.
Varactor multiplier experienced high-voltage breakdown at low pressure.
Problems of high-voltage breakdown increased in Transmitter-Modulator; first successful operation achieved at 2,000 microns pressure.

### December

R-F/I-F unit successfully tested with combined acceleration and vibration Control unit. R-F/I-F unit and Recorder passed low-level vibration tests. Decision reached to fly unpressurized, shock-mounted Transmitter-Modulator. First radar system design approval tests started. Grounding problems encountered and solved.

The balance of the program history which discusses the testing phase is shown in Appendix I of Volume II.